Berichte
zur Polar-
und Meeresforschung

593
2009

Reports
on Polar and Marine Research

The Campaign MELTEX with Research Aircraft "POLAR 5" in the Arctic in 2008

Edited by
Gerit Birnbaum, Wolfgang Dierking, Jörg Hartmann, Christof Lüpkes, André Ehrlich, Thomas Garbrecht, and Manuel Sellmann

HELMHOLTZ GEMEINSCHAFT

ALFRED-WEGENER-INSTITUT FÜR
POLAR- UND MEERESFORSCHUNG
In der Helmholtz-Gemeinschaft
D-27570 BREMERHAVEN
Bundesrepublik Deutschland

ISSN 1866-3192

Hinweis

Die Berichte zur Polar- und Meeresforschung werden vom Alfred-Wegener-Institut für Polar-und Meeresforschung in Bremerhaven* in unregelmäßiger Abfolge herausgegeben.

Sie enthalten Beschreibungen und Ergebnisse der vom Institut (AWI) oder mit seiner Unterstützung durchgeführten Forschungsarbeiten in den Polargebieten und in den Meeren.

Es werden veröffentlicht:

— Expeditionsberichte (inkl. Stationslisten und Routenkarten)
— Expeditionsergebnisse (inkl. Dissertationen)
— wissenschaftliche Ergebnisse der Antarktis-Stationen und anderer Forschungs-Stationen des AWI
— Berichte wissenschaftlicher Tagungen

Die Beiträge geben nicht notwendigerweise die Auffassung des Instituts wieder.

Notice

The Reports on Polar and Marine Research are issued by the Alfred Wegener Institute for Polar and Marine Research in Bremerhaven*, Federal Republic of Germany. They appear in irregular intervals.

They contain descriptions and results of investigations in polar regions and in the seas either conducted by the Institute (AWI) or with its support.

The following items are published:

— expedition reports (incl. station lists and route maps)
— expedition results (incl. Ph.D. theses)
— scientific results of the Antarctic stations and of other AWI research stations
— reports on scientific meetings

The papers contained in the Reports do not necessarily reflect the opinion of the Institute.

The „Berichte zur Polar- und Meeresforschung” continue the former „Berichte zur Polarforschung”

* Anschrift / Address
Alfred-Wegener-Institut
Für Polar- und Meeresforschung
D-27570 Bremerhaven
Germany
www.awi.de

Editor in charge:
Dr. Horst Bornemann

Assistant editor:
Birgit Chiaventone

Die "Berichte zur Polar- und Meeresforschung" (ISSN 1866-3192) werden ab 2008 ausschließlich elektronisch als Open-Access-Publikation herausgegeben (URL: http://epic.awi.de).

Please cite or link this item using the identifier
hdl:10013/epic.32677 or http://hdl.handle.net/10013/epic.32677

The Campaign MELTEX with Research Aircraft "POLAR 5" in the Arctic in 2008

Edited by
Gerit Birnbaum, Wolfgang Dierking, Jörg Hartmann, Christof Lüpkes, André Ehrlich, Thomas Garbrecht, and Manuel Sellmann

Please cite or link this item using the identifier hdl:10013/epic.32677

ISSN 1866-3192

Contents

Summary

The scientific aircraft campaign MELTEX (Impact of melt ponds on energy and momentum fluxes between atmosphere and sea ice) was a joint project conducted by the Alfred Wegener Institute for Polar and Marine Research (AWI), the Institute for Atmospheric Physics (IPA) at the University of Mainz, and Environment Canada (EC). It is a contribution to the EU funded project DAMOCLES and to the International Polar Year 2007/2008.

Melt ponds at the surface of Arctic sea ice usually form from end of May to end of August. They have a strong impact on the energy exchange between atmosphere, sea ice, and ocean. The most important effect is the enhancement of absorption of solar radiation due to the considerably lower albedo of melt ponds than that of the surrounding snow/ice. The goal of the project MELTEX is to improve the quantitative understanding of the impact of melt ponds on radiation, heat, moisture, and momentum fluxes over Arctic sea ice.

In that phase of the melt season, when melt ponds begin to form, the description of the temporal evolution of pond fraction and albedo in sea ice and climate models is particularly erroneous. Therefore, the campaign took place in late spring / early summer. From 9 May to 8 June 2008, we operated in the Canadian Arctic, mainly over the southern Beaufort Sea with Inuvik as airbase for POLAR 5. For a measurement flight over rough multi-year ice north of Ellesmere Island POLAR 5 was transferred to Eureka from 22 to 24 May. Overall, 12 measurement flights were performed.

Zusammenfassung

Die wissenschaftliche Flugzeugmesskampagne MELTEX (Einfluss von Schmelztümpeln auf Energie- und Impulsflüsse zwischen Atmosphäre und Meereis) war ein gemeinsames Projekt des Alfred-Wegener-Instituts für Polar- und Meeresforschung (AWI), des Instituts für Atmosphärenphysik (IPA) der Universität Mainz und von Environment Canada (EC). Sie stellt einen Beitrag zum EU-Projekt DAMOCLES und zum internationalen Polarjahr 2007/2008 dar.

Schmelztümpel an der Oberfläche arktischen Meereises bilden sich gewöhnlich von Ende Mai bis Ende August. Sie haben einen starken Einfluss auf den Energieaustausch zwischen Atmosphäre, Meereis und Ozean. Der bedeutendste Effekt ist die Erhöhung der Absorption von Solarstrahlung auf Grund ihrer erheblich niedrigeren Albedo gegenüber der des umgebenden Schnees/Eises. Das Ziel des Projektes MELTEX ist eine Verbesserung des quantitativen Verständnisses des Einflusses von Schmelztümpeln auf Strahlungs-, Wärme-, Feuchte- sowie Impulsflüsse über arktischem Meereis.

Insbesondere in der Phase der Schmelzsaison, in der Schmelztümpel anfangen, sich zu bilden, wird die zeitliche Entwicklung des Schmelztümpelbedeckungsgrades und der Albedo in Meereis- und Klimamodellen nur sehr grob erfasst. Deshalb fand die Kampagne im Spätfrühling/Frühsommer statt. Vom 09. Mai bis 08. Juni 2008 operierten wir in der kanadischen Arktis, hauptsächlich über der südlichen Beaufort See mit Inuvik als Basis für POLAR 5. Für einen Messflug über rauhem mehrjährigen Eis nördlich von Ellesmere Island wurde POLAR 5 vom 22. bis 24. Mai 2008 nach Eureka überführt. Insgesamt wurden 12 Messflüge durchgeführt.

1 Scientific Objectives

According to the IPCC Fourth Assessment Report (IPCC, 2007) there are still significant differences in the predicted Arctic summer sea ice extent during the next decades among several state-of-the-art global and regional climate models, whereas the winter sea ice extent is predicted relatively consistently.

Atmospheric boundary layer processes and surface characteristics like albedo play an important role in the energy exchange between atmosphere and sea ice covered oceans. Their parameterization strongly influences the results of climate simulations in polar regions (e.g., Rinke et al., 2006, Tjernström et al., 2005). Therefore, the main goal of the aircraft campaign MELTEX was to study atmosphere - sea ice interactions and particularly radiation characteristics of sea ice in the first phase of the melt season in the Arctic, when melt ponds that considerably enhance absorption of solar radiation, begin to form.

During Arctic summer, major changes in the sea ice cover are mainly caused by near-surface melting. Wherever the surface topography allows lateral motion, the meltwater will seek the lowest elevation, that is, either it will drain into the ocean through cracks, or it will collect on the ice floes in melt ponds. Surficial meltwater can move over distances ranging from several meters up to hundreds of meters along topographic structures (Fetterer and Untersteiner, 1998). Hence pond fraction depends significantly on sea ice surface topography (Eicken et al., 2004).
Pond coverage typically varies between 5% and 50% depending on sea ice type (Tschudi et al., 2001). The largest mean pond fractions are found on first-year undeformed ice. Second- and multi-year ice often show pond structures already formed in previous melting seasons. Heavily deformed multi-year ice usually exhibits the lowest pond fractions. On multi-year ice, pond coverage usually reaches its maximum value in July. Especially first-year floes covered with ponds by more than 50% frequently melt completely in the course of the summer (Fetterer and Untersteiner, 1998).

With values varying between 0.2 and 0.5 melt ponds have a considerably lower albedo than the surrounding ice/snow with values between 0.6 and 0.9 (Perovich et al., 1998). Curry et al. (2001) and Kølzow (2007) validated several sea ice albedo schemes of different complexity employed in global and regional climate models against albedo observations in the Arctic, e.g., obtained during the Surface Heat Budget of the Arctic Ocean (SHEBA) field experiment (Uttal et al., 2002). None of the evaluated schemes appeared to be appropriate for simulating the full annual albedo cycle. A common deficiency was a too high albedo in summer due to an underestimation of the effect of albedo decrease caused by melt ponds. More complex schemes, typically calculating melt pond fraction and melt pond albedo as function of surface temperature, performed better in summer. However, they gave a too low albedo during the transition from spring to summer, particularly immediately after the onset of snowmelt. The reason for this deficiency is that surface temperature-dependent schemes overestimate melt pond fraction in the initial phase of the melt season.

Most radiation schemes in regional and global climate models need area-averaged albedo values as input parameter for grid cells with horizontal extensions of several kilometers up to some hundreds of kilometers. However, present albedo parameterizations for melt pond covered sea ice are mainly based only on small-scale observations at drifting stations. Therefore, MELTEX was performed as a larger-scale approach for investigating area-averaged albedo and pond fraction by utilizing airborne measurements.

Recently, new satellites were launched carrying radar systems: ALOS, TerraSAR-X, and Radarsat-2. Therefore, a further main objective of MELTEX was to employ optical scanner systems, aerial photography, and hand-held photo cameras to collect data for the interpretation of such satellite radar imagery acquired over the same sea ice region as overflown by POLAR 5. Important questions to be answered were: What is the influence of melting conditions on ice type discrimination in radar images? How well can we determine the timing of melt onset using radar images? Is it possible to detect melt ponds in the high-resolution imagery?

To summarize, MELTEX aimed

- to determine pond fraction and broadband as well as spectral surface albedo of melt-pond covered sea ice,
- to investigate momentum and heat transport in the atmospheric boundary layer over melting sea ice,
- to collect data that can be used to improve algorithms for the retrieval of sea ice parameters such as melt pond fraction from satellite measurements.

In contrast to most of the previous airborne projects on the investigation of melt ponds the comprehensive instrumentation of the BASLER BT-67 type aircraft POLAR 5 allows both, the measurement of surface horizontal structure and radiative fluxes, and the derivation of basic meteorological quantities, turbulent fluxes, surface temperature and surface topography. Temp-like flight patterns, for example, give information on the vertical structure of the atmospheric boundary layer. Hence vertical heat transport in the atmospheric boundary layer towards the surface during events of warm-air advection from land over sea ice could be studied during MELTEX, a process decisive for the onset of melt pond formation in late spring.

2 Instrumentation and Observational Procedures

2.1 Aircraft Instrumentation

MELTEX was the first meteorological campaign performed with the new polar aircraft of the Alfred Wegener Institute, POLAR 5. The aircraft was mainly instrumented with well proven devices that had been used successfully by AWI on POLAR 2 and POLAR 4 in previous campaigns. In addition, the Spectral Modular Airborne Radiation measurement sysTem (SMART)-albedometer (Ehrlich et al., 2008) operated by IPA, a new meteorological nose boom, a UV/VIS- and IR-line scanner, a digital photo camera, and the Composition and Photodissociative Flux Measurements (CPFM)-pod (McElroy, 1995) operated by EC were employed.

measurement	instrument
position	GPS, INS
height	radar altimeter, laser altimeter, pressure transducer
pressure	Rosemount absolute pressure transducer
airspeed	Rosemount differential pressure transducer
wind vector	nose boom, GPS, INS
temperature	Pt100
humidity	Lyman-alpha, dew point mirror, Vaisala humicap, CR-2
turbulence	nose boom turbulence probe (5-hole probe)
broadband short-wave radiation	Eppley pyranometer (up and down)
broadband long-wave radiation	Eppley pyrgeometer (up and down)
spectral short-wave radiation	SMART-albedometer
surface temperature	KT15 radiation thermometer, IR-line scanner
sea ice topography	two laser altimeters
sea ice concentration, melt pond concentration	UV/VIS-line scanner, digital photo and video camera
composition and photo-dissociative flux measurements	CPFM-pod

Table 2.1: Aircraft instruments operated on POLAR 5 on all flights.

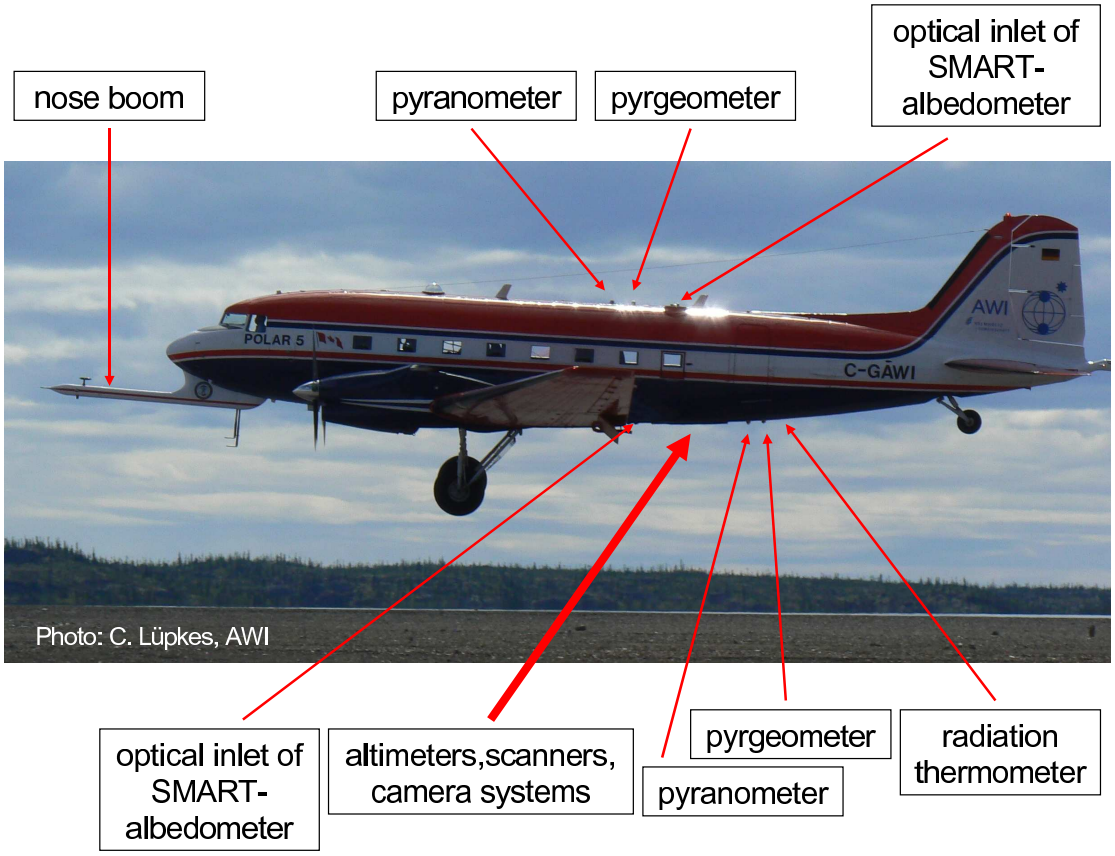

Figure 2.1: Instrumentation of POLAR 5.

Table 2.1 lists all instruments installed onboard POLAR 5 during MELTEX, and Fig. 2.1 shows, where they were mounted.
The meteorological basic instrumentation was generally running well, but some data of the nose boom were lost caused by icing problems, which have to be fixed in future.
The broadband radiation instruments, the pyrano- and pyrgeometers, were running very reliably. After solving some initial problems with the levelling unit, the SMART-albedometer was run with active horizontal stabilization.
All three instruments used for the investigation of the horizontal optical structure of the sea ice cover were working well; the UV/VIS-line scanner, the digital photo camera, and the digital video camera.
Caused by a serious technical problem, the data of the IR-line scanner cannot be analyzed in a meaningful way. The radiation thermometer, in contrast, was running well, allowing us to derive surface temperature at least along the line of the flight track.
The CPFM-pod for Composition and Photodissociative Flux Measurements was working autonomously all the time. It was mounted at POLAR 5 as a tail boom.

2.2 Sea Ice Buoys

To monitor the temporal evolution of sea ice surface properties like melt ponds during the campaign we intended to continuously follow the drift of a certain sea ice area marked by an array of position transmitting sea ice buoys. In the Arctic, positions of buoys of the International Arctic Buoy Program (IABP) are freely available via http://iabp.apl.washington.edu/. However, the number of IABP-buoys in the southern Beaufort Sea was very limited in spring 2008. Only the IABP-buoy with ARGOS-ID 5303 was located in our selected measurement region; actually, quite far north between 73°N and 74°N.
To mark a north-south section for repeated flights between the pack-ice and the thinner and broken first-year ice near the coastal polynya, we decided to deploy a further sea ice buoy at about 71°N. Figure 2.2 shows this buoy with ARGOS-ID 28832 right after its deployment during the first measurement flight on 11 May 2008. This ICEXAIR-type sea ice buoy worked very reliably. During MELTEX is was positioned on the ice floe shown in Fig. 2.2. After melting of the floe it was afloat in open water and was finally destroyed in the Chukchi Sea in November 2008.
Figure 2.3 shows the entire drift track of ARGOS-buoy 28832. This figure also indicates the drift tracks of the two ARGOS-buoys 5303 and 28832 used during the MELTEX measurement period. The two thin black lines in Fig. 2.3 connect the two positions on 12 May 2008 and on 07 June 2008, respectively.

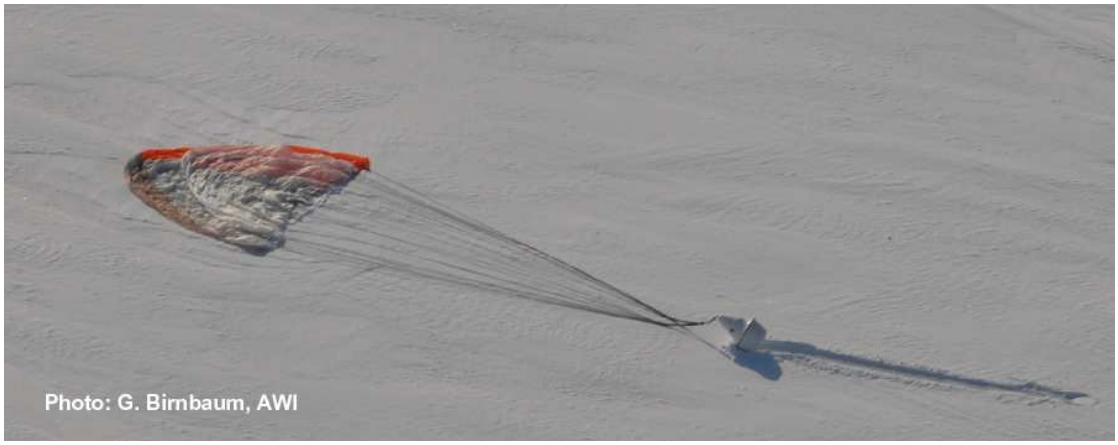

Figure 2.2: Sea ice buoy with ARGOS-ID number 28832 right after its deployment on 11 May 2008.

2.3 Measurement Inventory

This section summarizes data sets collected during the campaign in addition to the aircraft data. First, satellite derived sea ice concentration maps, operational weather forecast products and satellite images are described. Finally, a catalogue of the flight missions is given.

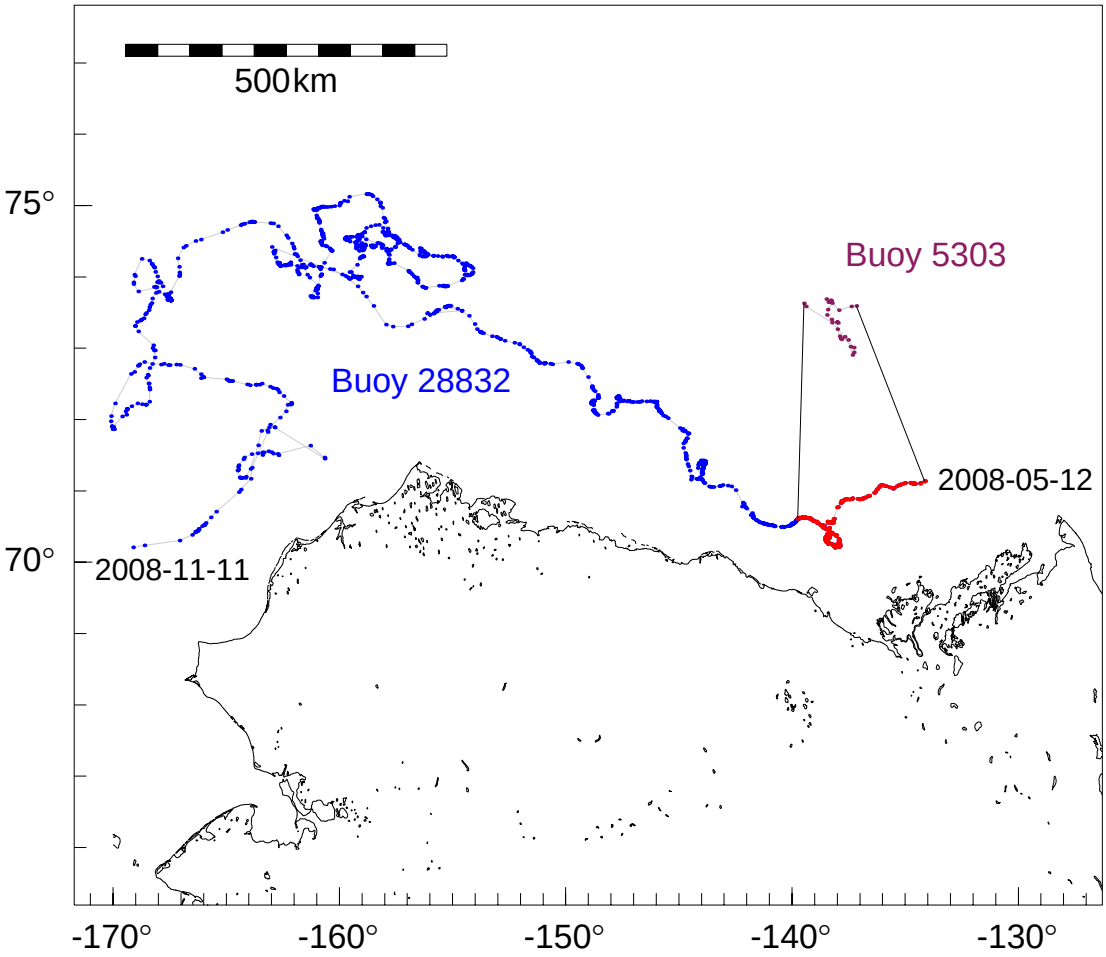

Figure 2.3: Drift track of buoy with ARGOS-ID 28832 from the day after its deployment, 12 May 2008, to its disintegration on 11 November 2008. The red part of the track covers the MELTEX time period from 12 May to 07 June 2008, the day of the last measurement flight. The violet dots indicate the drift track of IABP-buoy with ARGOS-ID 5303 from 12 May to 07 June 2008.

2.3.1 Sea Ice Concentration Maps

Daily sea ice concentration maps for the Beaufort Sea and also for our second measurement region north of Ellesmere Island were obtained from Prof. L. Kaleschke (Center for Marine and Atmospheric Research, Institute of Oceanography, University of Hamburg). The sea ice concentration data have been derived from the AMSR-E passive microwave radiometer.

Figure 2.4 compares the ice concentration on the first measurement day, 11 May 2008, with the concentration on the last measurement day, 07 June 2008. It is clearly visible that the Amundsen Gulf (70-71°N, 118-125°W) and the Cape Bathurst Polynya west of it opened very rapidly during the MELTEX campaign. South of the Cape Bathurst Polynya, which is essentially a coastal polynya, a narrow band of fast ice remained along the coast till the end of MELTEX.

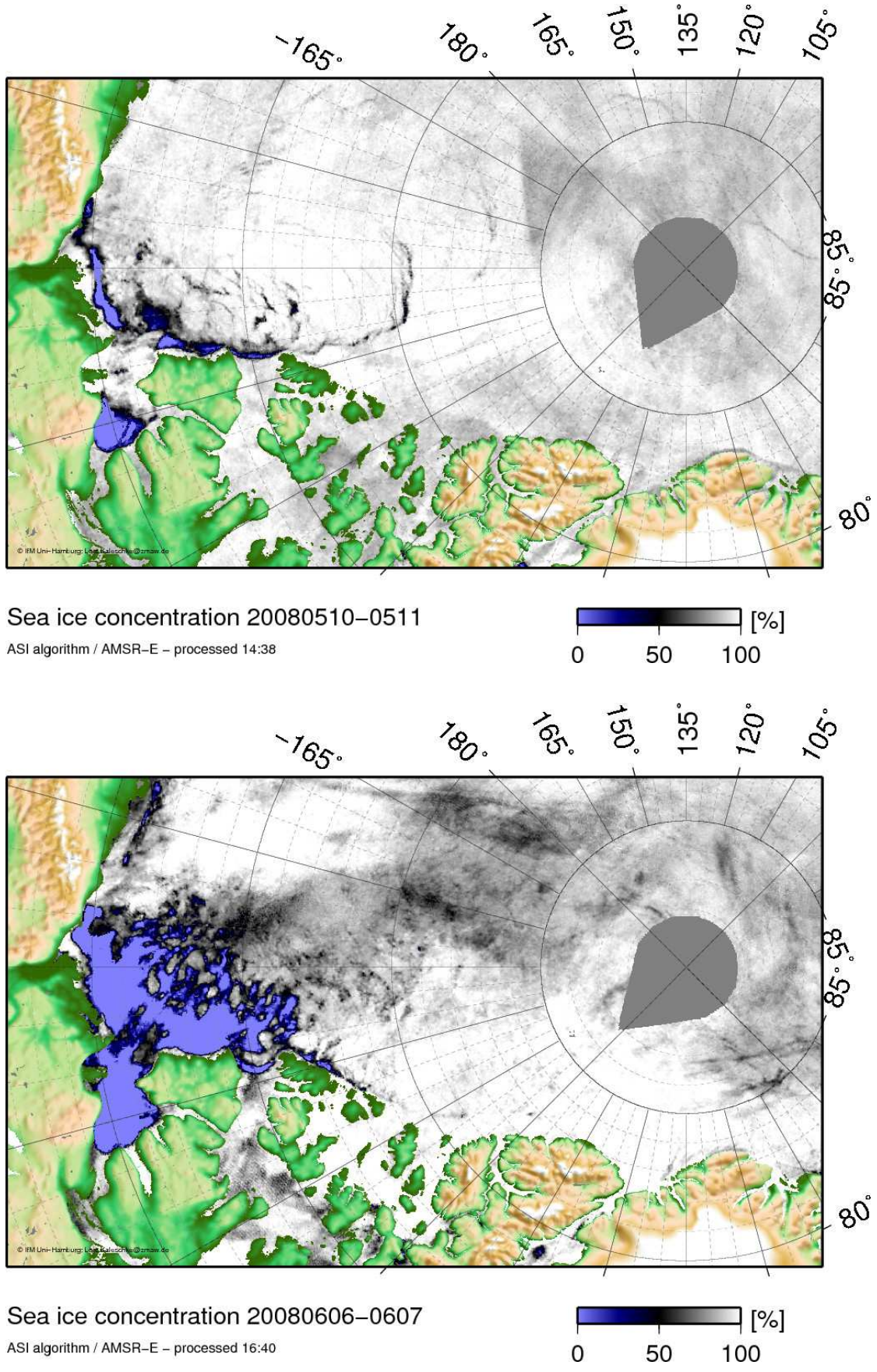

Figure 2.4: Satellite derived sea ice concentration on 11 May (upper) and 07 June 2008 (lower panel) at 00 UTC.

2.3.2 Operational Weather Forecast Maps and Satellite Images

Operational weather forecast maps based on the Global Forecast System (GFS-) Model were obtained daily via http://www.wetterzentrale.de. In addition, we used various forecast products provided by the Meteorological Service of Canada, e.g., the Marine Wind Prognosis. With respect to operational satellite images we used AVHRR images in the visible and infrared range provided by Environment Canada on special web-sites for Logistical Support Products for Field Operations within the International Polar Year.

2.3.3 Flight Missions

This section presents a catalogue of all measurement flights during MELTEX.

The aircraft missions can be characterized as follows:

- **buoydrop**: Deployment of ICEXAIR-type sea ice buoy
- **ABL/surface measurements**: Horizontal flight legs of several tens of km up to 300 km length were flown at low and/or medium level to record surface structure, surface temperature, meteorological basic quantities, and radiative as well as turbulent fluxes. The hight of the lowest flight level was about 100 ft. The horizontal legs were interrupted by temp-like ascents and descents to measure the vertical structure of the atmospheric boundary layer (ABL).
- **turbulence**: This type of mission was performed during off-ice flow conditions, when cold air was advected into southerly directions from pack-ice towards land. Horizontal flight legs of several tens of km up to 300 km length were flown parallel to the wind direction at different hight levels to measure turbulent fluxes in the ABL, and to derive drag coefficients.
- **warm-air advection**: This type of mission was performed during on-ice flow conditions, when air heated over land was advected into northerly directions towards the pack-ice. Horizontal flight legs of different length interrupted by temp-like ascents and descents were flown parallel to the wind direction at different hight levels in the ABL to investigate the turbulent transport of heat over the ice-covered ocean.
- **satellite remote sensing**: Horizontal flight legs of different length were flown at low levels and at 1000 ft or 2000 ft in areas covered by scenes of radar satellites like TerraSAR-X and Radarsat-2.
- **fast ice**: ABL/surface measurements were performed over fast ice.

Table 2.2 gives a brief listing of the measurement flights.

date	**code**	**missions**	**calibration**
11 May	a	buoydrop ABL/surface measurements	
14 May	b	ABL/surface measurements	yes
17 May	c	ABL/surface measurements	
19 May	d	turbulence ABL/surface measurements	
23 May	e	turbulence ABL/surface measurements	yes
26 May	f	warm-air advection ABL/surface measurements	yes
29 May	g	ABL/surface measurements remote sensing	
02 June	h	ABL/surface measurements	
03 June	i	ABL/surface measurements remote sensing	
04 June	j	warm-air advection ABL/surface measurements	
06 June	k	fast ice ABL/surface measurements warm-air advection	
07 June	l	ABL/surface measurements remote sensing	

Table 2.2: Flight missions of POLAR 5 during the MELTEX field campaign.
The table lists: **date** of flight; **code** assigned to each day for use in the nomenclature of flight legs; **mission** main goals; **calibration** pattern flown for radiation measurements.

All flight missions, except the one on 23 May 2008, were performed over the southern Beaufort Sea with Inuvik (68°22'N, 133°44'W) as airbase for POLAR 5. The town Inuvik is situated in the delta of the Mackenzie River about 100 km south of the coastline. During all missions, the transfer flights over land were mostly carried out at an altitude of about 10.000 ft. After reaching the coastline, we usually passed a band of fast ice before reaching the Cape Bathurst Polynya. North of this coastal polynya, we entered into our measurement region over the drifting sea ice in the southern Beaufort Sea.
For a measurement flight over rough multi-year ice north of Ellesmere Island POLAR 5 was transferred to Eureka (79°59'N, 85°57'W), where we performed a measurement flight on 23 May 2008.

In the following, each flight day is described in more detail by summarizing its main goals and by giving a short description of the weather and ice situation. Figures show 3D- and 2D-plots of the flight pattern also included in satellite images of the measurement region.

11 May 2008

Main goals of the flight

- Deployment of a sea ice buoy (ARGOS-ID 28832),
- assessment of sea ice conditions on a north-south section over the southern Beaufort Sea prior to the melting period,
- boundary-layer and surface measurements on a section between buoy-28832 and buoy-5303.

Weather and ice situation

While a strong low pressure system was situated over the Aleutian Islands, the pressure gradients around Inuvik and over the southern Beaufort Sea were weak. Stratus clouds were present over land and sea ice.
All lakes and rivers between Inuvik and the coast were ice-covered, the land was snow-covered. The band of fast ice along the coast showed no indications of melting. Ice-free parts of the Cape Bathurst Polynya could be clearly recognized between the fast ice belt and the drift ice. There were no visible indications for surface melting on drift ice. Ice surface temperatures were partly below -10°C.

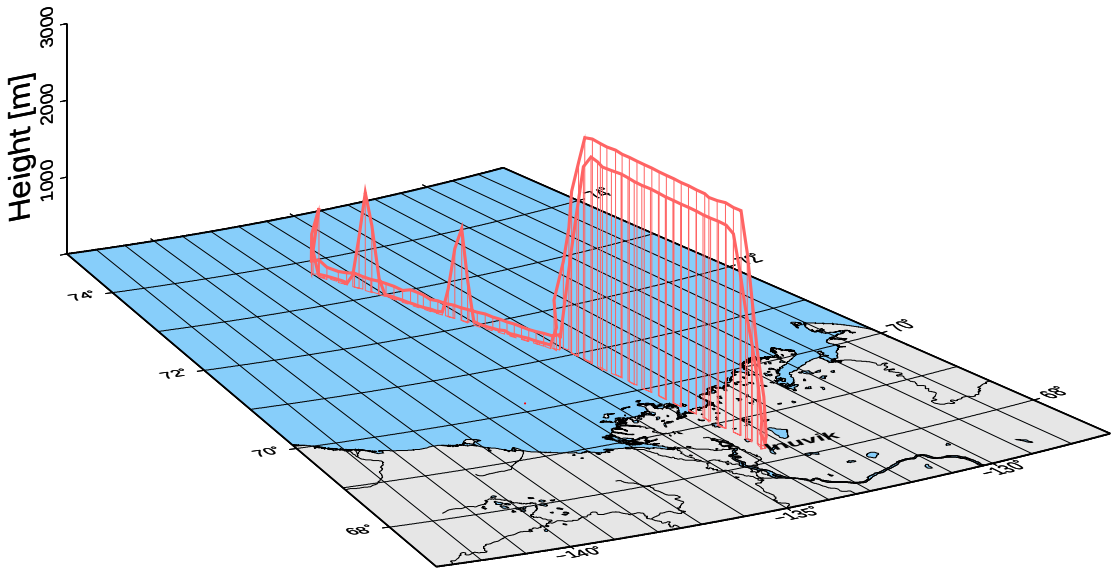

Figure 2.5: 3D-illustration of the pattern flown from Inuvik over the southern Beaufort Sea on 11 May 2008.

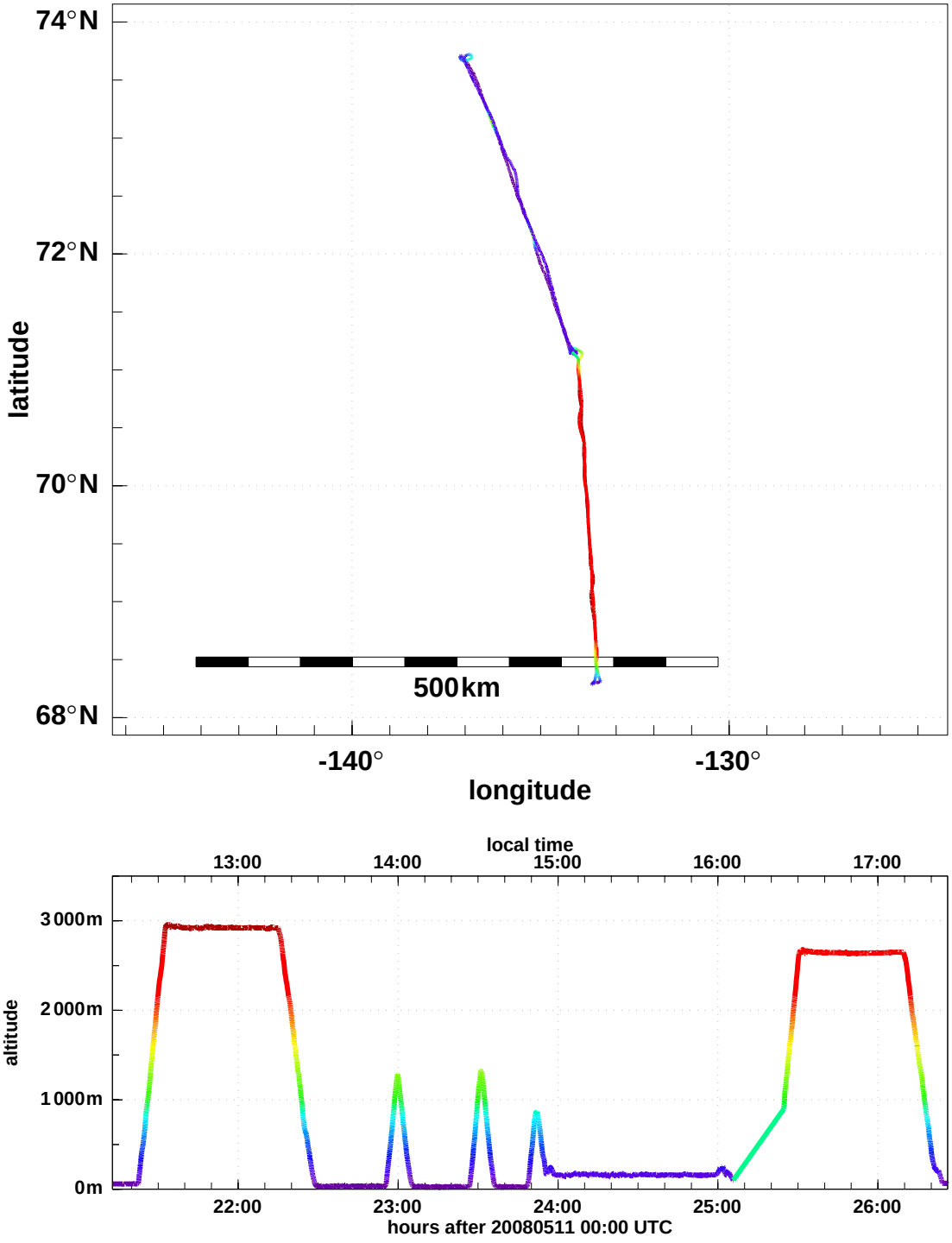

Figure 2.6: Horizontal projection of flight path (upper panel) and flight altitude as function of time (lower panel) for the mission on 11 May 2008. Violet (red) lines indicate low (high) level flight sections.

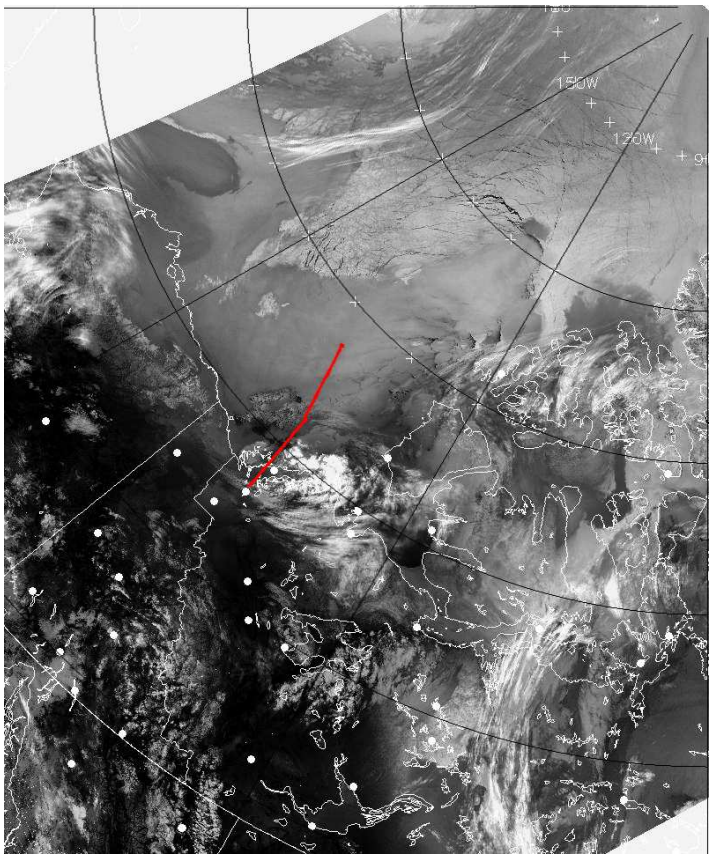

Figure 2.7: AVHRR satellite image in the infrared range on 11 May 2008, 11:33 UTC. The flight path is marked in red.

14 May 2008

Main goals of the flight

- Square-like flight pattern to calibrate radiation instruments,
- boundary-layer and surface measurements on a section between buoy-28832 and buoy-5303.

Weather and ice situation

A strong low pressure system was moving from the Aleutian Islands to Alaska. On its eastern side, it caused advection of warm air with south-easterly flow from land over the Beaufort Sea. This synoptic situation lasted for some days. While clear-sky conditions were met over land, stratus clouds dominated over the coastal polynya and the sea ice. The ice surface temperatures were significantly higher than during the first flight, they had partly increased up to -1°C. From time to time darker patches were observed along pressure ridges, they looked like wet snow or bare ice.

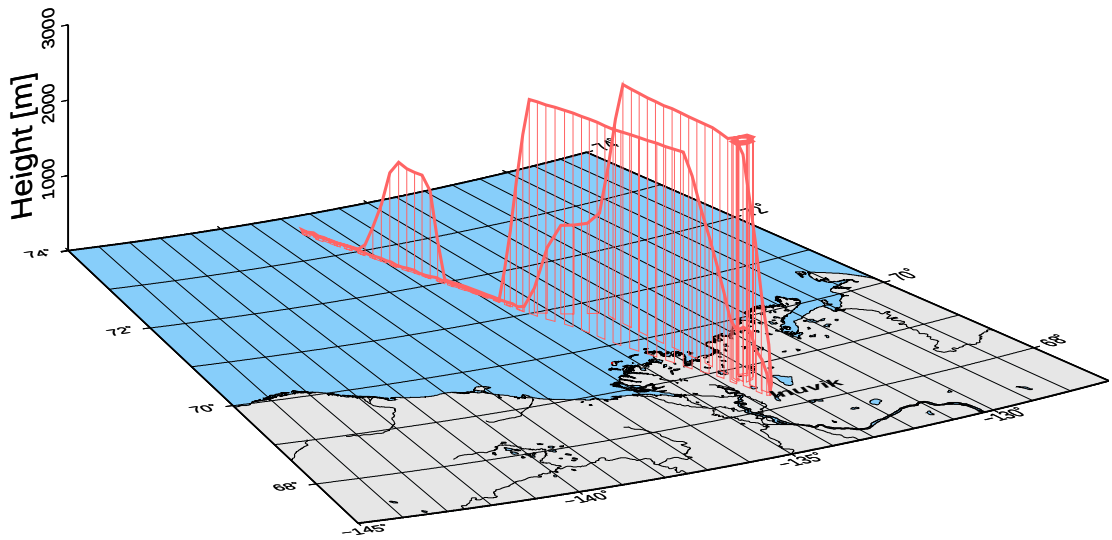

Figure 2.8: 3D-illustration of the pattern flown from Inuvik over the southern Beaufort Sea on 14 May 2008.

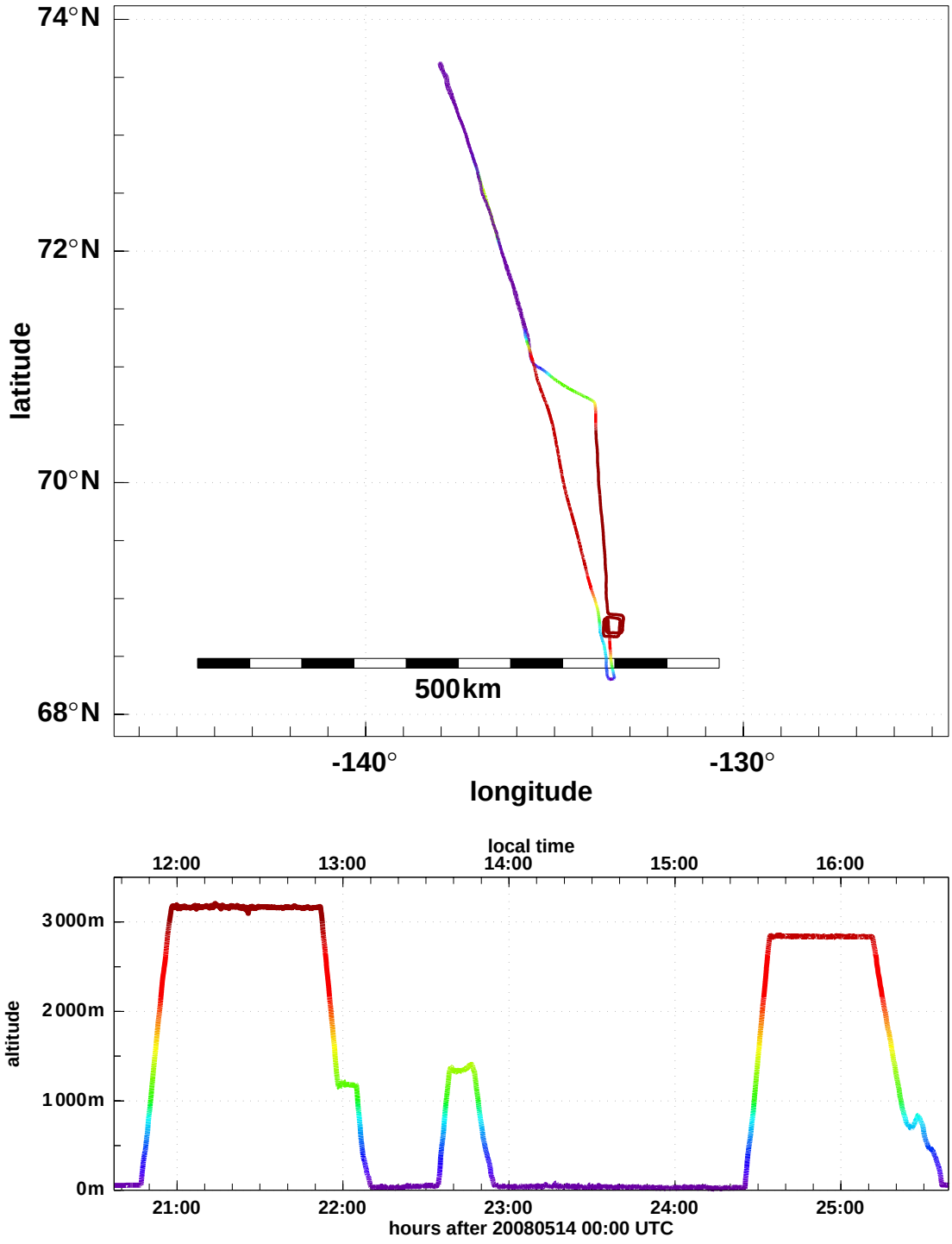

Figure 2.9: Horizontal projection of flight path (upper panel) and flight altitude as function of time (lower panel) for the mission on 14 May 2008. Violet (red) lines indicate low (high) level flight sections.

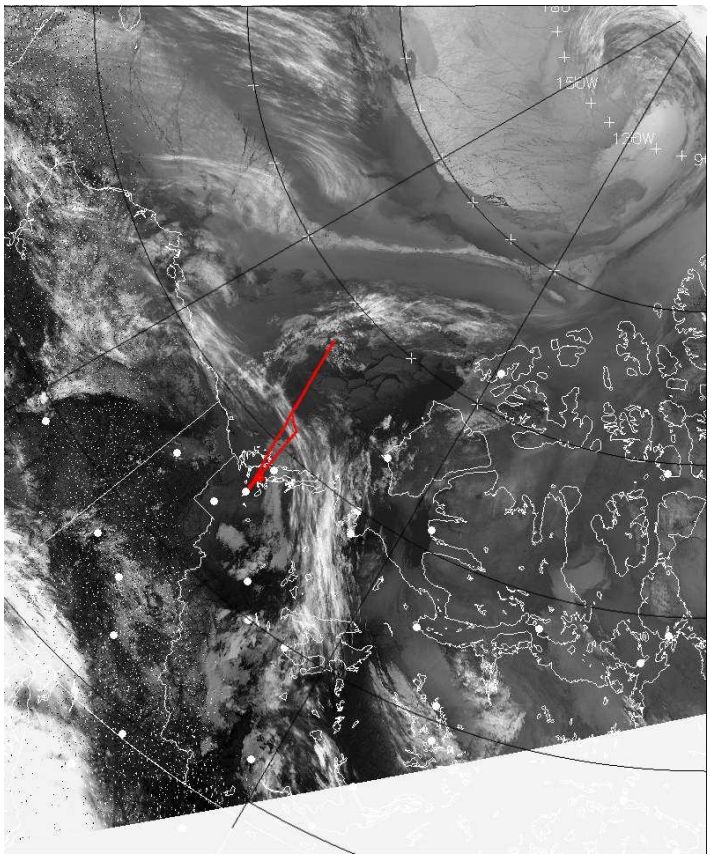

Figure 2.10: AVHRR satellite image in the infrared range on 14 May 2008, 12:46 UTC. The flight path is marked in red.

17 May 2008

Main goals of the flight

- Boundary-layer and surface measurements on two north-south oriented sections over drifting sea ice, first, between buoy-28832 and buoy-5303, and second, between buoy-5303 and buoy-22203.

Weather and ice situation

Weak high pressure with partly clear-sky conditions over sea ice prevailed in the measurement region. Air temperatures were again considerably higher than during the very first flight.
Sea ice showed no clear signs of large-scale melting, however, darker snow-free patches, mostly along pressure ridges, were visible again, especially in the southern part of the two north-south sections.

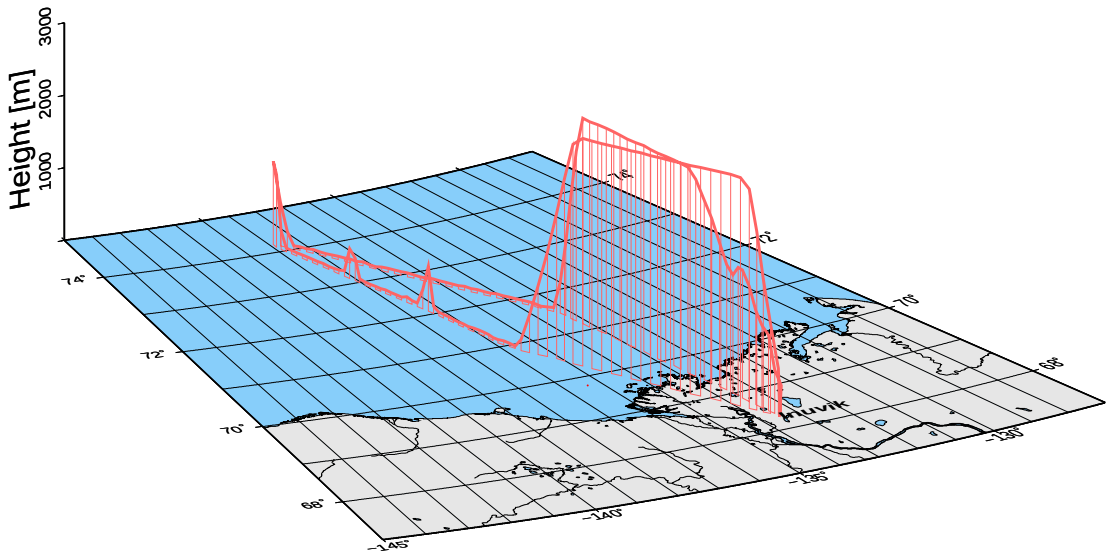

Figure 2.11: 3D-illustration of the pattern flown from Inuvik over the southern Beaufort Sea on 17 May 2008.

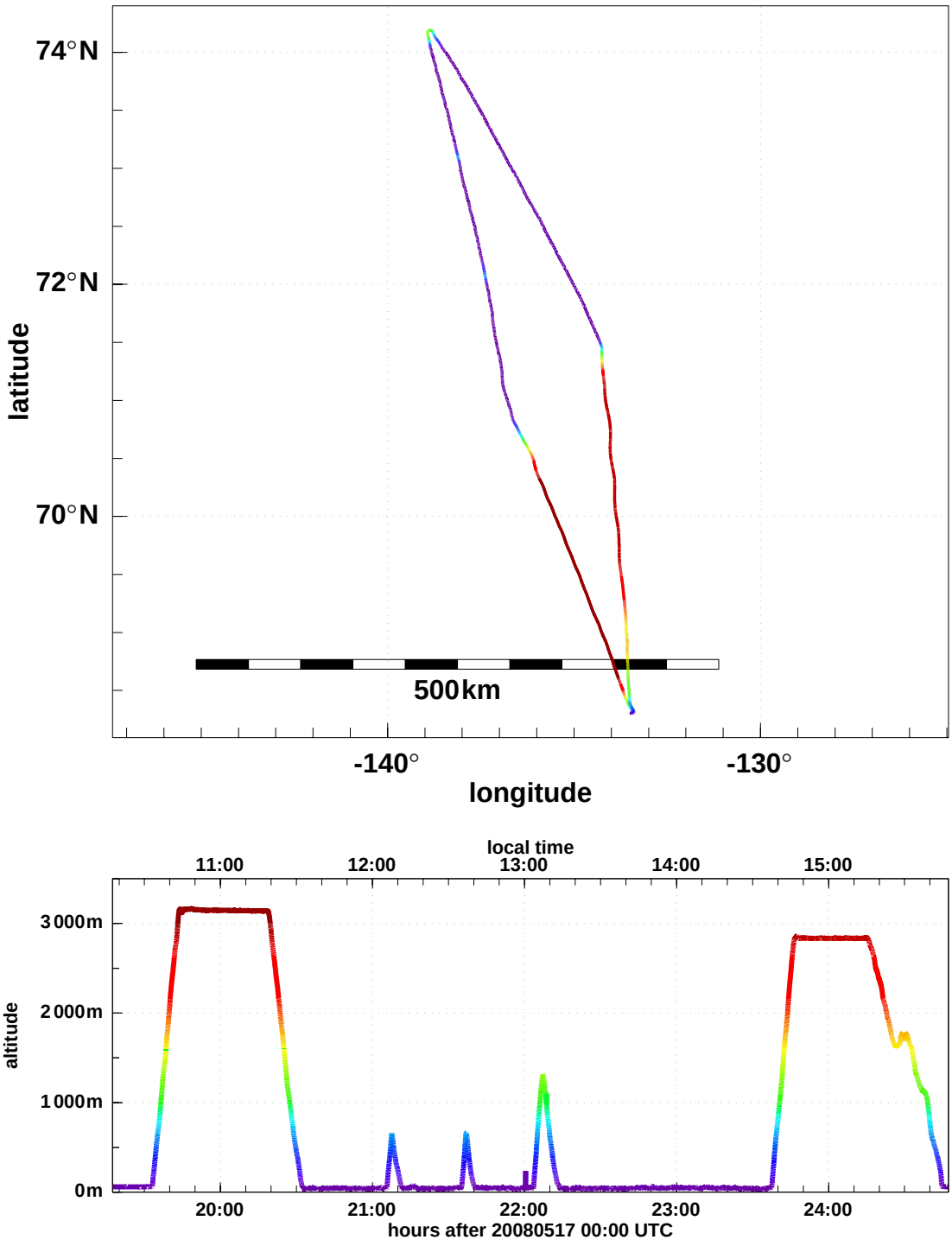

Figure 2.12: Horizontal projection of flight path (upper panel) and flight altitude as function of time (lower panel) for the mission on 17 May 2008. Violet (red) lines indicate low (high) level flight sections.

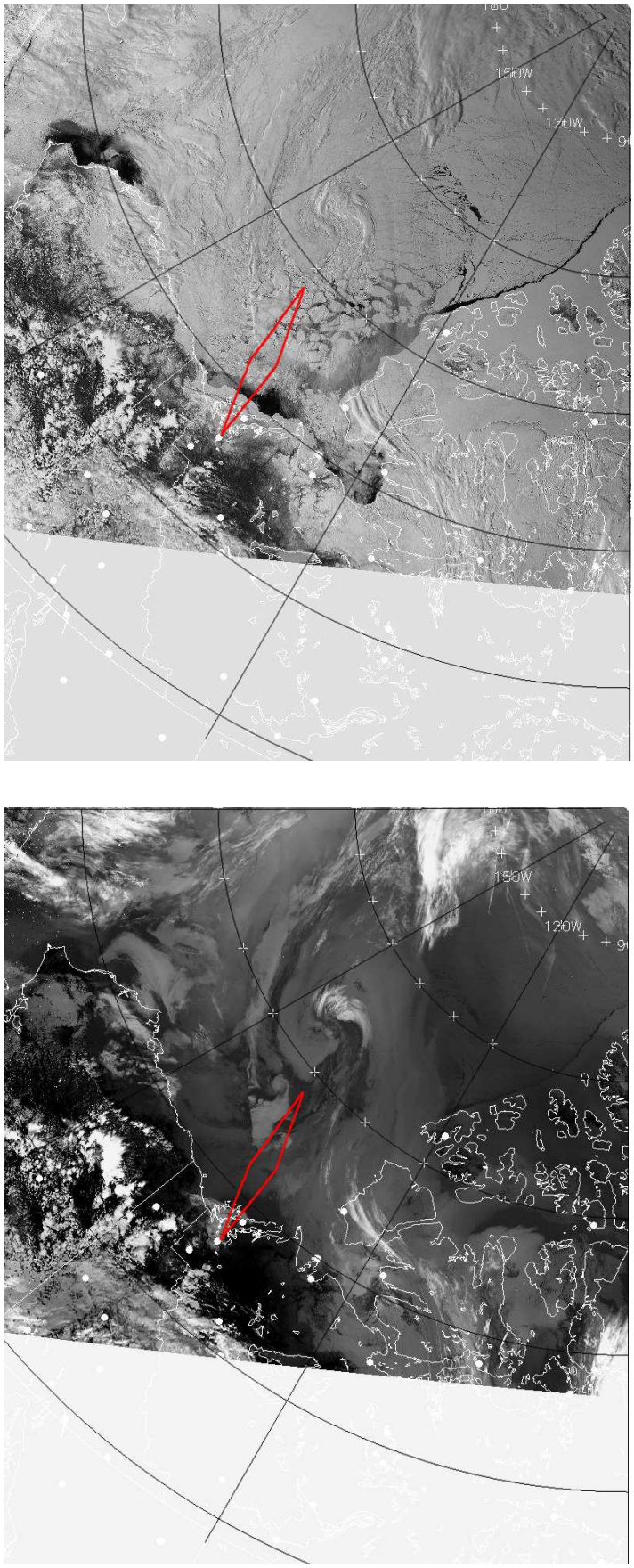

Figure 2.13: AVHRR satellite image in the visible (upper) and infrared (lower panel) range on 17 May 2008, 22:06 UTC. The flight path is marked in red.

19 May 2008

Main goals of the flight

- Boundary-layer and especially turbulence measurements as well as surface measurements with a flight pattern parallel to the near-surface wind,
- temps to record boundary-layer variability over changing ice conditions,
- stack of horizontal legs to measure the height dependence of drag coefficients over sea ice,
- start of systematic measurements on a section over fast ice north of the Mackenzie Delta.

Weather and ice situation

A low pressure system situated over Victoria Island caused a northerly flow. Near-surface air temperature basically varied between -5°C and -4°C, whereas sea ice surface temperature was between -2.0°C and -0.8°C and sea surface temperature was about -0.8°C. Hence a slightly unstable stratification existed over the sea ice region.
The dominant type of sea ice changed from nilas (south) to first- and finally second-year ice with numerous ridges (north). There, over a very large floe, a stack of horizontal legs was flown. During the entire flight many leads were observed with widths of up to several kilometers.

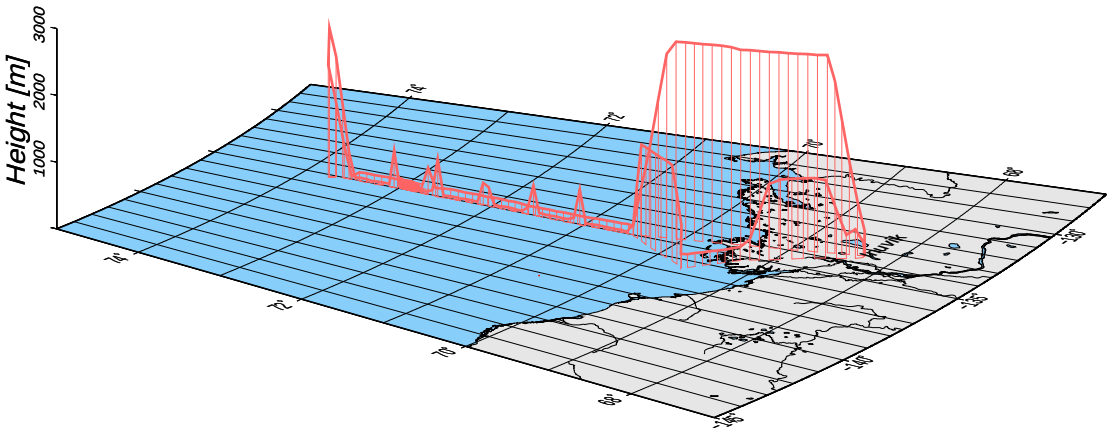

Figure 2.14: 3D-illustration of the pattern flown from Inuvik over the southern Beaufort Sea on 19 May 2008.

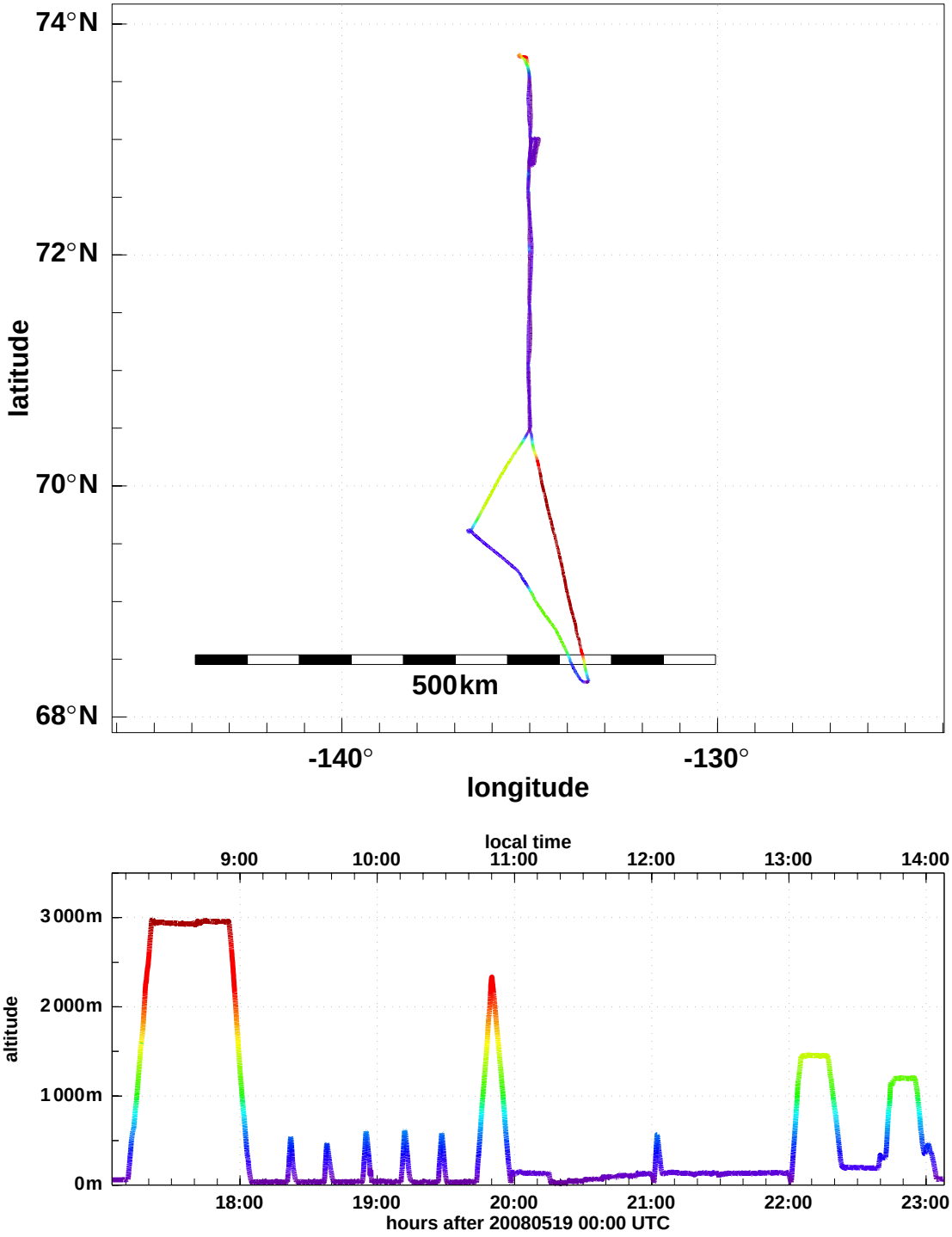

Figure 2.15: Horizontal projection of flight path (upper panel) and flight altitude as function of time (lower panel) for the mission on 19 May 2008. Violet (red) lines indicate low (high) level flight sections.

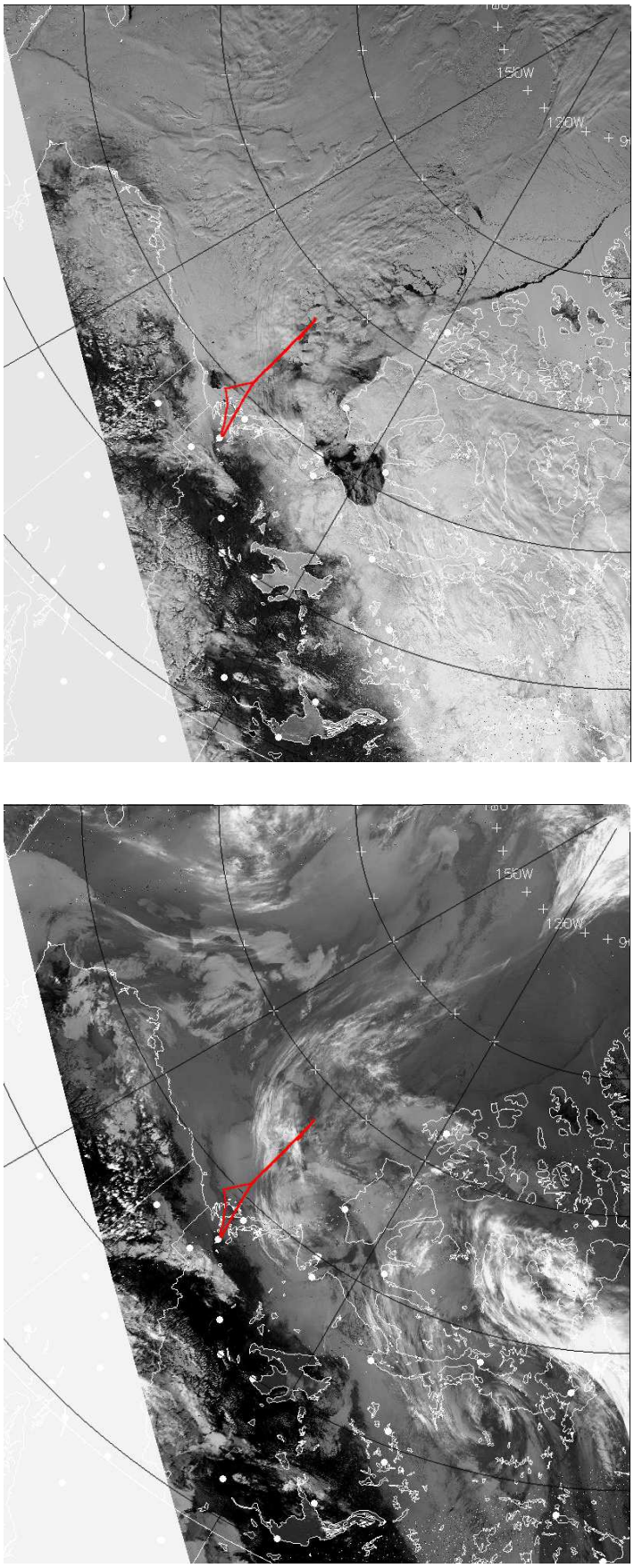

Figure 2.16: AVHRR satellite image in the visible (upper) and infrared (lower panel) range on 19 May 2008, 18:33 UTC. The flight path is marked in red.

23 May 2008

Main goals of the flight

- Boundary-layer, turbulence, and surface measurements over rough multi-year ice north of Ellesmere Island,
- Square-like flight pattern to calibrate radiation instruments.

Weather and ice situation

The flight was performed in a region with weak pressure gradients south-east of a large, but weak low pressure system with its core at about 85°N moving eastward. North west of a line between (82°N, 100°W) and (83°N, 90°W) thin fog occured, which, however, made surface and turbulence measurements impossible. Hence the flight had to be performed south of this line, where we met clear-sky conditions.
All fjords and lakes between Eureka and the north coast of Ellesmere Island were covered by ice and snow. At the north coast, a band of non-moving sea ice was present, which was separated from drifting sea ice by a small polynya. Avoiding the fog mentioned above we mainly operated over the non-moving ice close to the coast. Altough this band consisted of thick multi-year ice, the ice was less rough than we had expected it to be in the shear and convergence zones north of Ellesmere Island. Fig. 2.20 shows a typical horizontal distribution of sea ice topography for a flight section of 1500 m length over the non-moving sea ice. Fig. 2.21 shows a picture taken on this section.

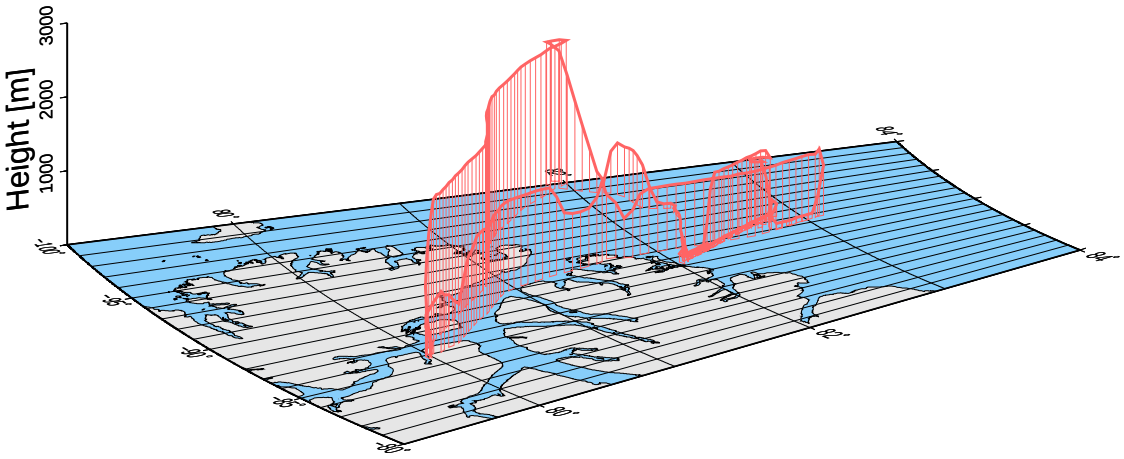

Figure 2.17: 3D-illustration of the pattern flown from Eureka over the Arctic Ocean on 23 May 2008.

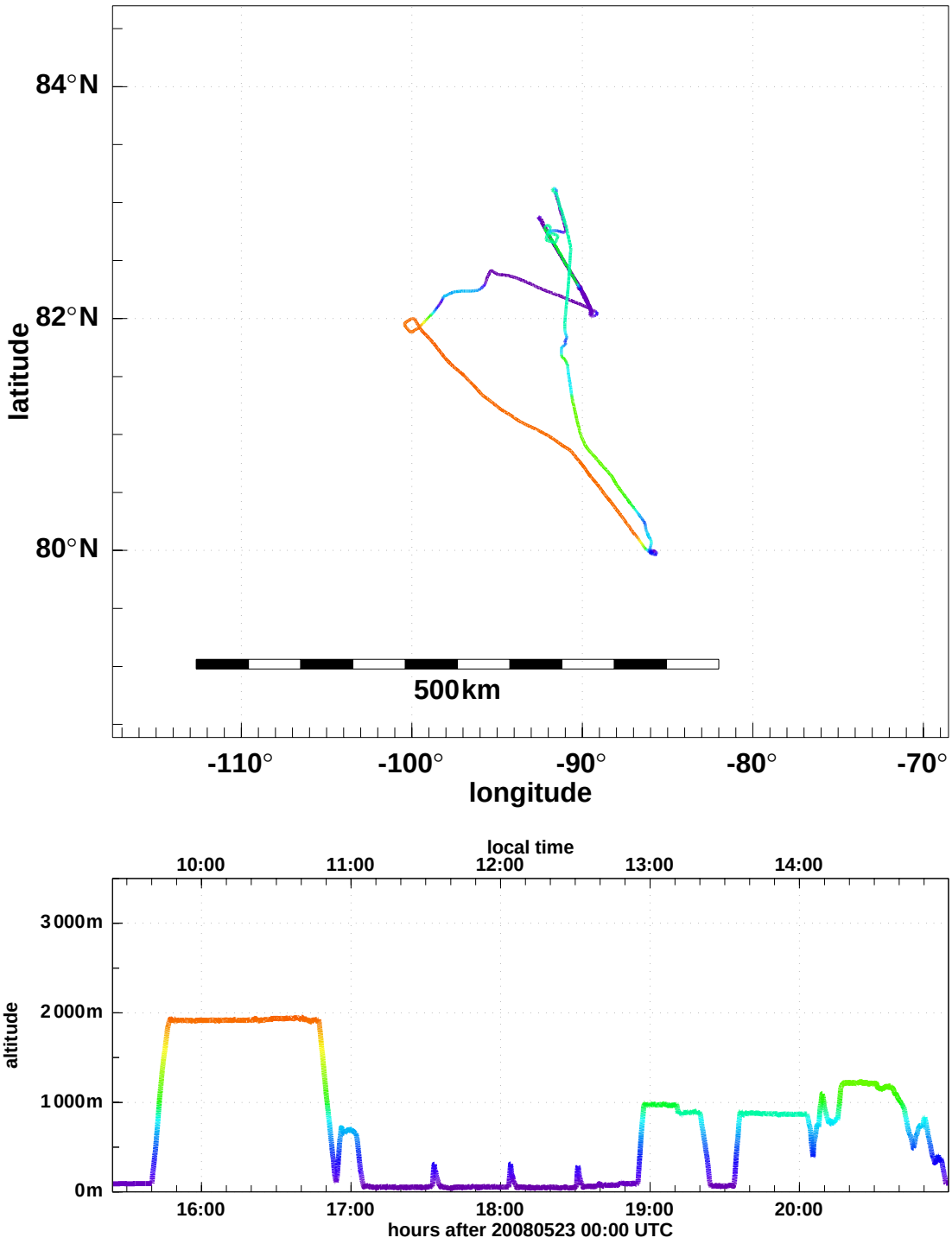

Figure 2.18: Horizontal projection of flight path (upper panel) and flight altitude as function of time (lower panel) for the mission on 23 May 2008. Violet (red) lines indicate low (high) level flight sections.

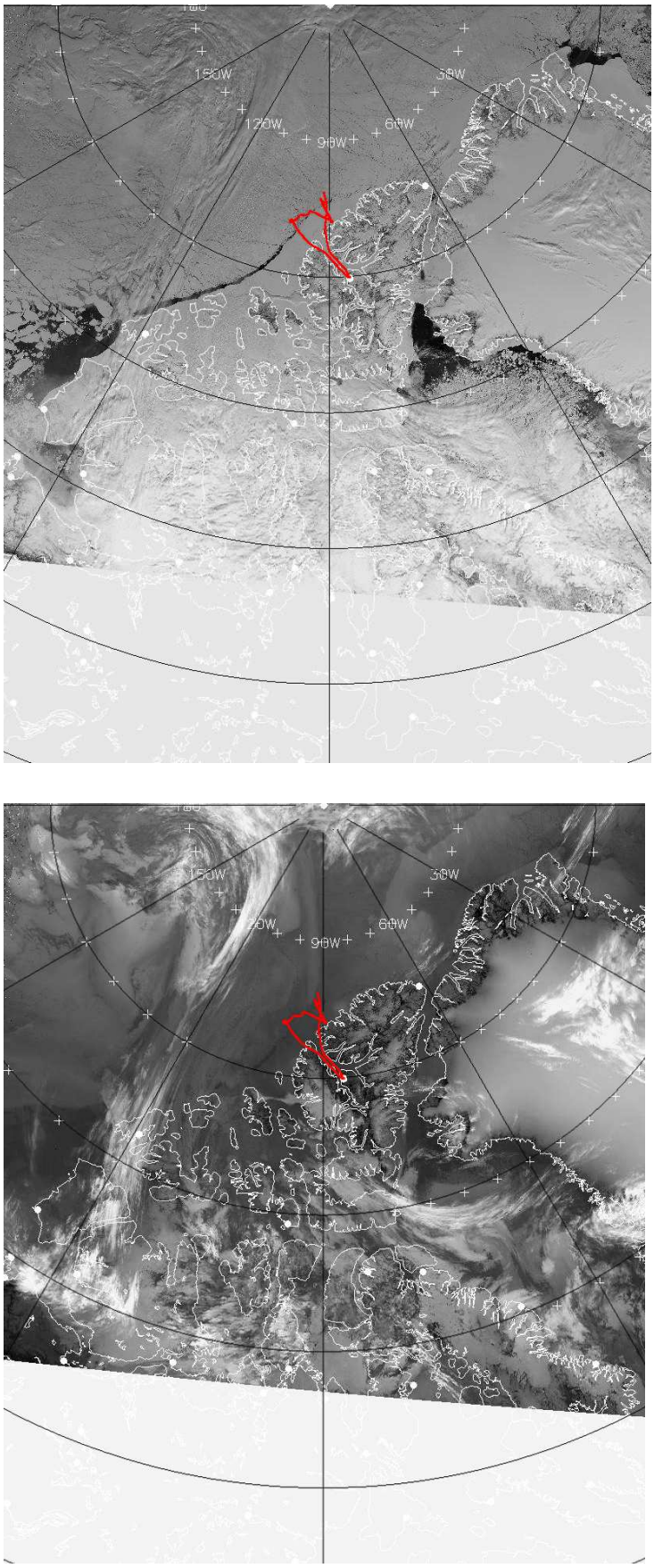

Figure 2.19: AVHRR satellite image in the visible (upper) and infrared (lower panel) range on 23 May 2008, 17:18 UTC. The flight path is marked in red.

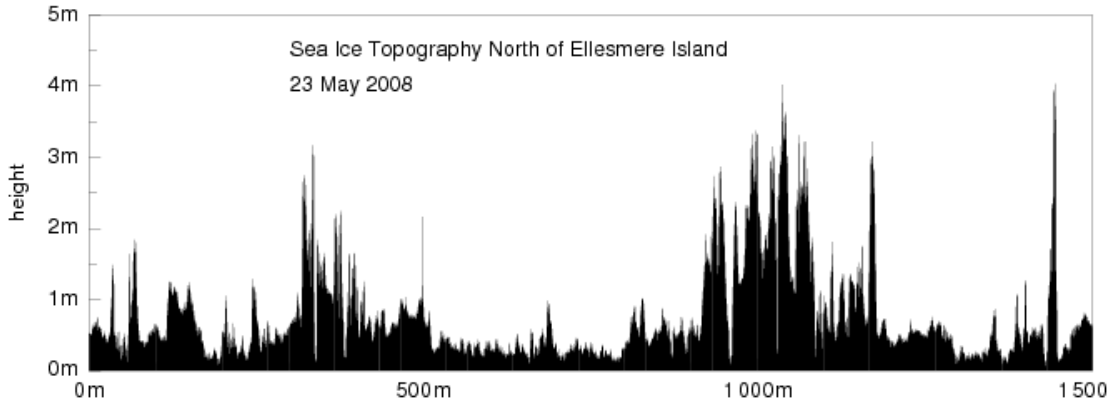

Figure 2.20: Horizontal distribution of sea ice topography for a flight section of 1500 m length over sea ice north of Ellesmere Island on 23 May 2008.

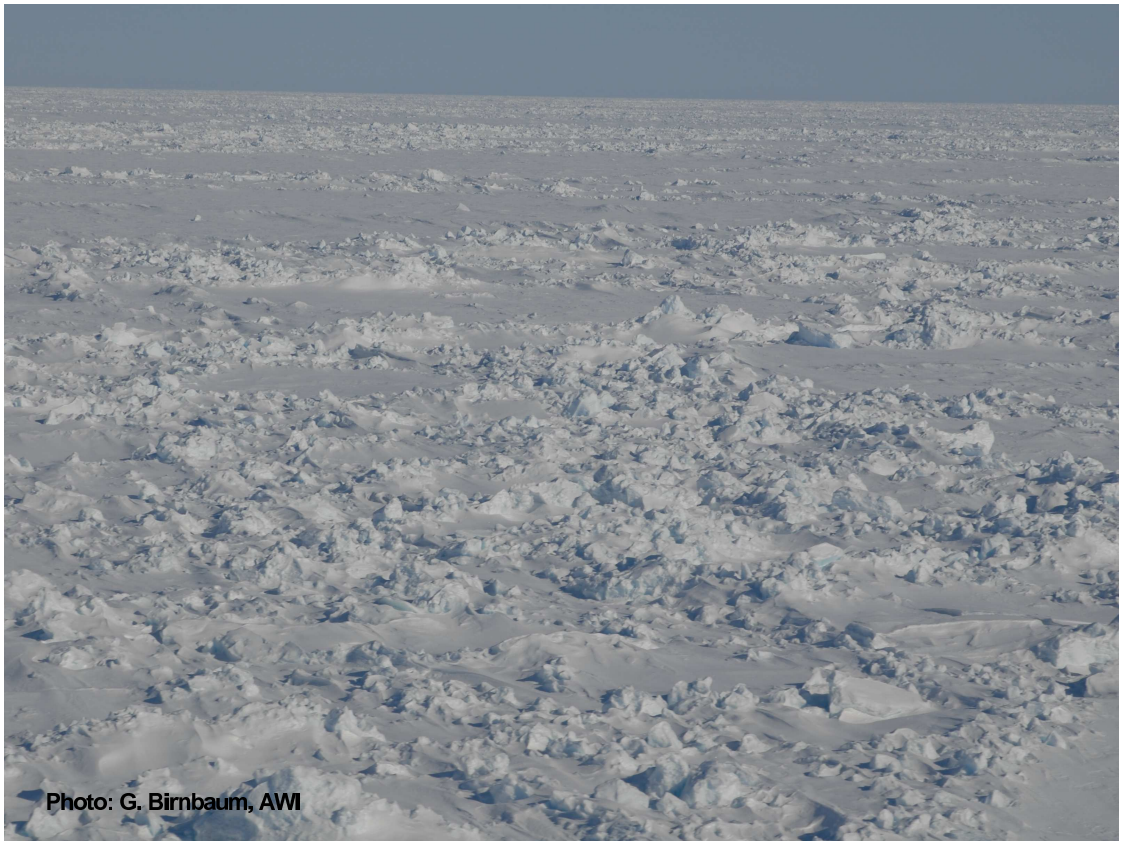

Figure 2.21: Sea ice north of Ellesmere Island on 23 May 2008. The picture was taken at an altitude of appr. 50 m with a hand-held camera.

26 May 2008

Main goals of the flight

- Boundary-layer and surface measurements on a section from fast ice via buoy-28832 to a position at (70°20'N, 141°00'W) to investigate boundary-layer processes linked to warm-air advection,
- square-like flight pattern to calibrate radiation instruments.

Weather and ice situation

On the previous three days strong advection of warm air from southerly directions had dominated. Air temperatures increased up to 23°C in Inuvik. However, the situation changed, and on the day of the flight a strong low moved from the coastal region north of Alaska towards Banks Island. This caused a weak westerly flow over sea ice in near-coastal regions, and the flight was performed quasi-parallel to this flow direction.
For the first time during the campaign, an early stage of melt pond development on drifting sea ice could be clearly observed.

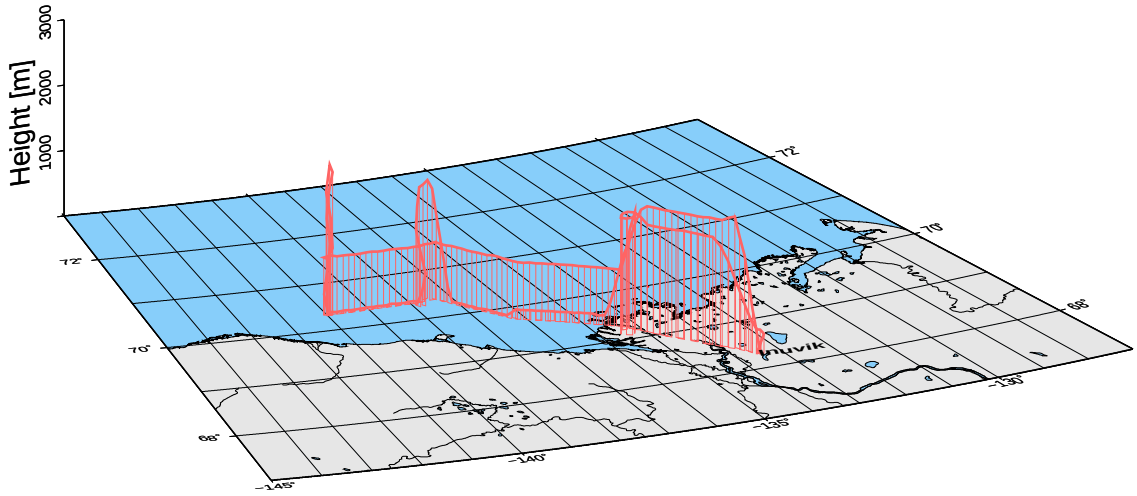

Figure 2.22: 3D-illustration of the pattern flown from Inuvik over the southern Beaufort Sea on 26 May 2008.

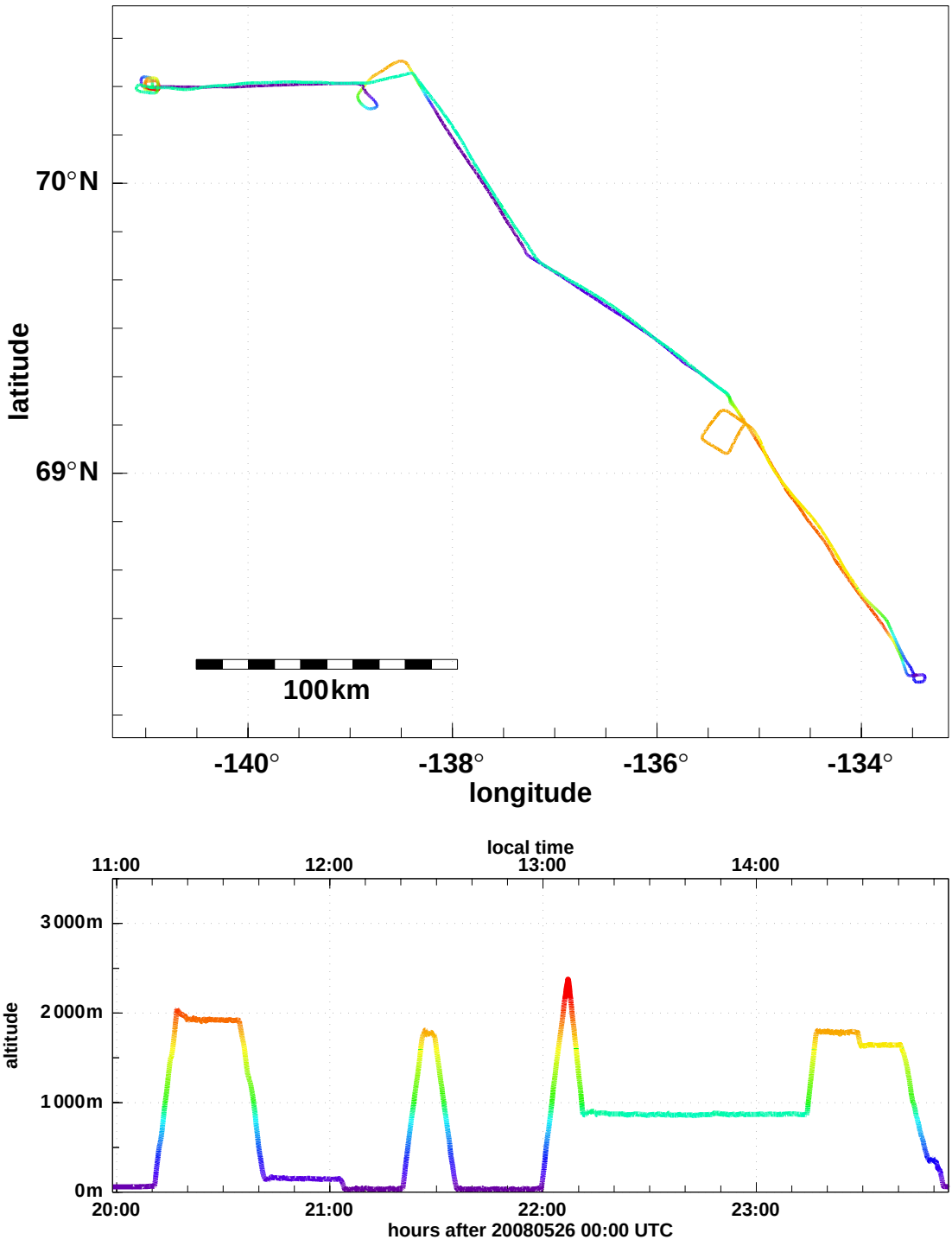

Figure 2.23: Horizontal projection of flight path (upper panel) and flight altitude as function of time (lower panel) for the mission on 26 May 2008. Violet (red) lines indicate low (high) level flight sections.

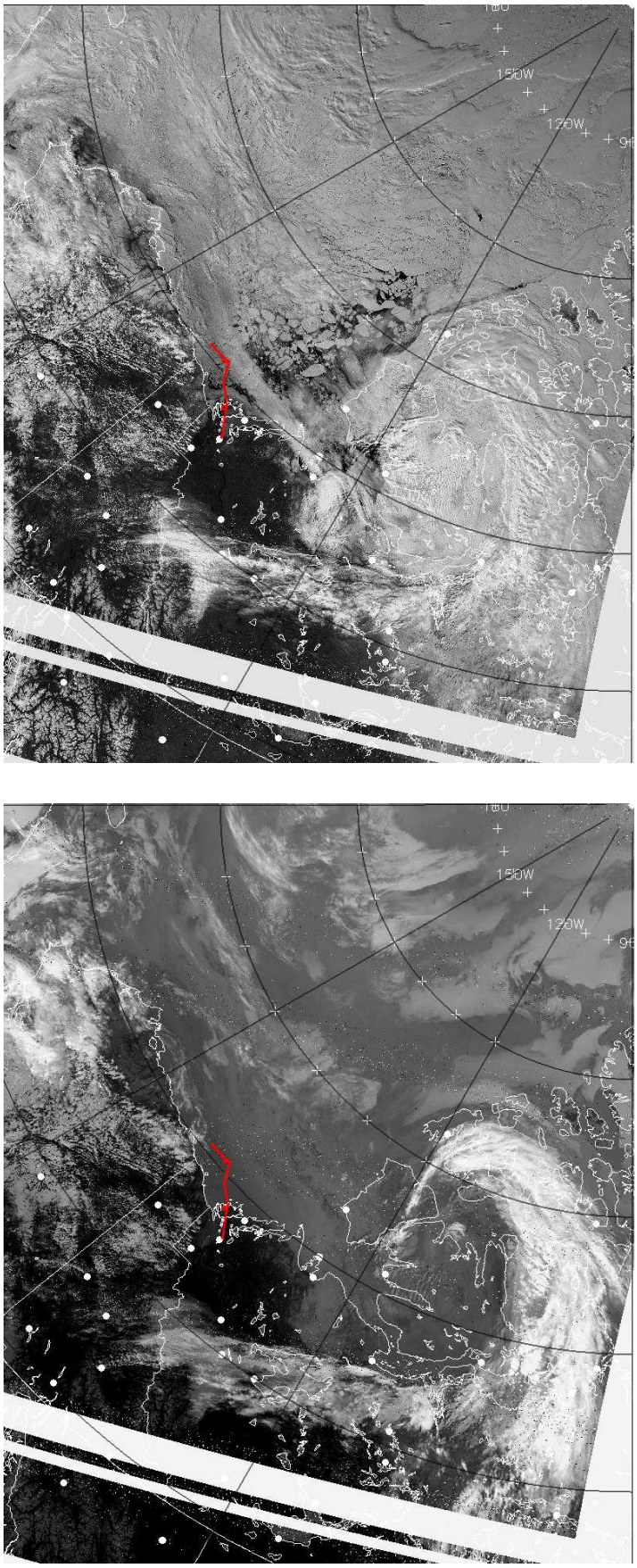

Figure 2.24: AVHRR satellite image in the visible (upper) and infrared (lower panel) range on 26 May 2008, 20:44 UTC. The flight path is marked in red.

29 May 2008

Main goals of the flight

- Determination of sea ice structure in a region covered by two scenes of the satellite TerraSAR-X,
- boundary-layer and surface measurements on a section from buoy-5303 via buoy-28832 to the fast ice.

Weather and ice situation

Under the influence of a strong low pressure system rather bad weather conditions with icing were met during the whole flight.
Melt ponds were mostly refrozen, at least at the surface, caused by cold-air flow over the southern Beaufort Sea during the last days.

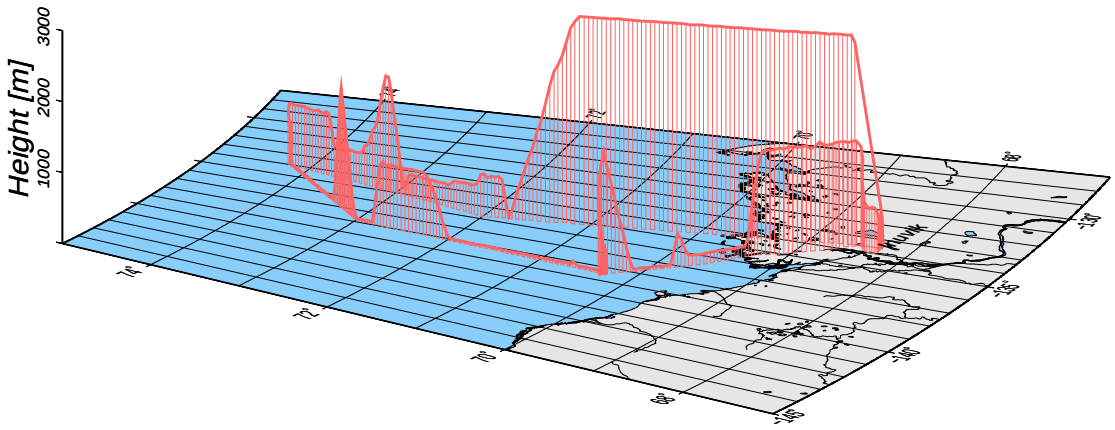

Figure 2.25: 3D-illustration of the pattern flown from Inuvik over the southern Beaufort Sea on 29 May 2008.

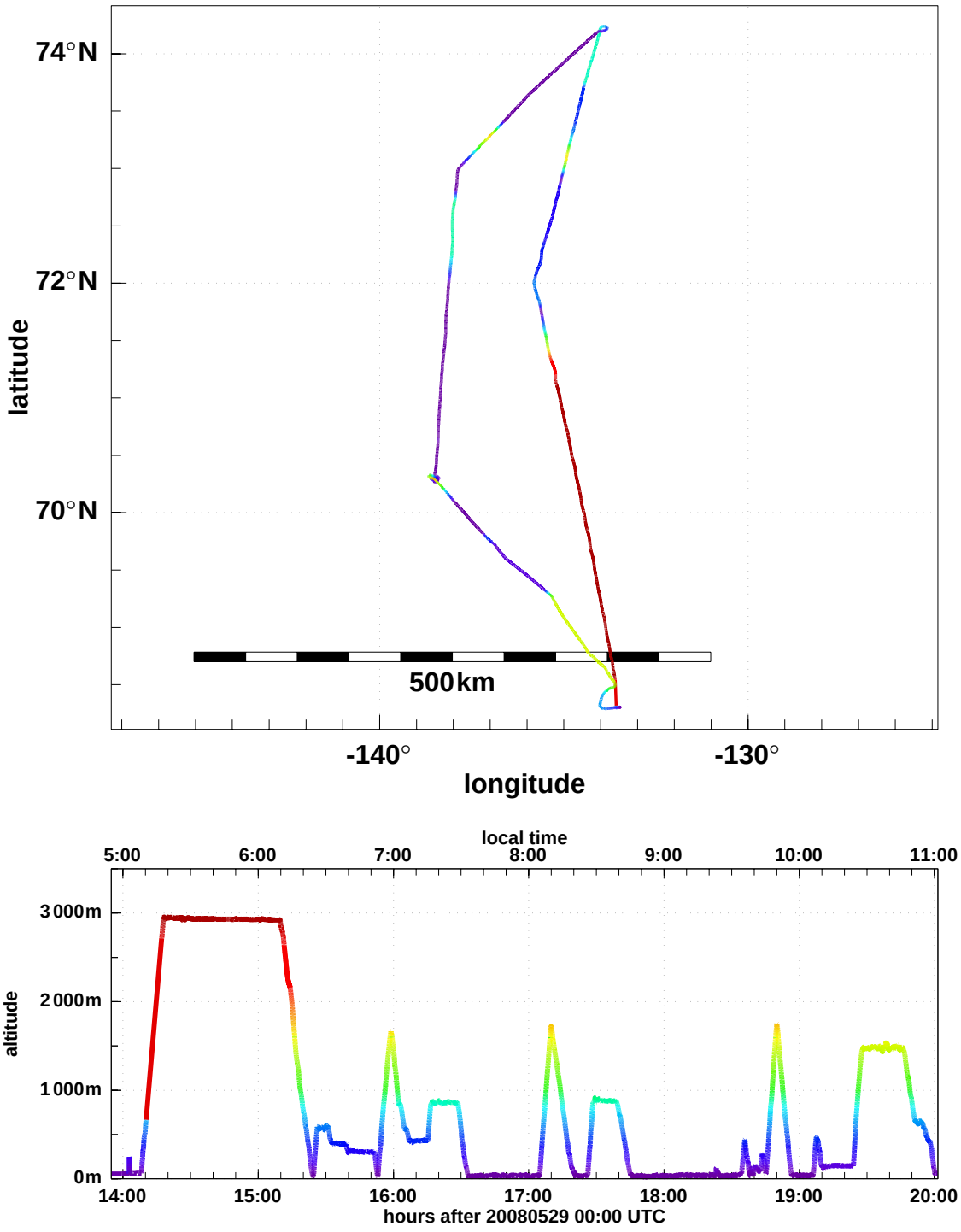

Figure 2.26: Horizontal projection of flight path (upper panel) and flight altitude as function of time (lower panel) for the mission on 29 May 2008. Violet (red) lines indicate low (high) level flight sections.

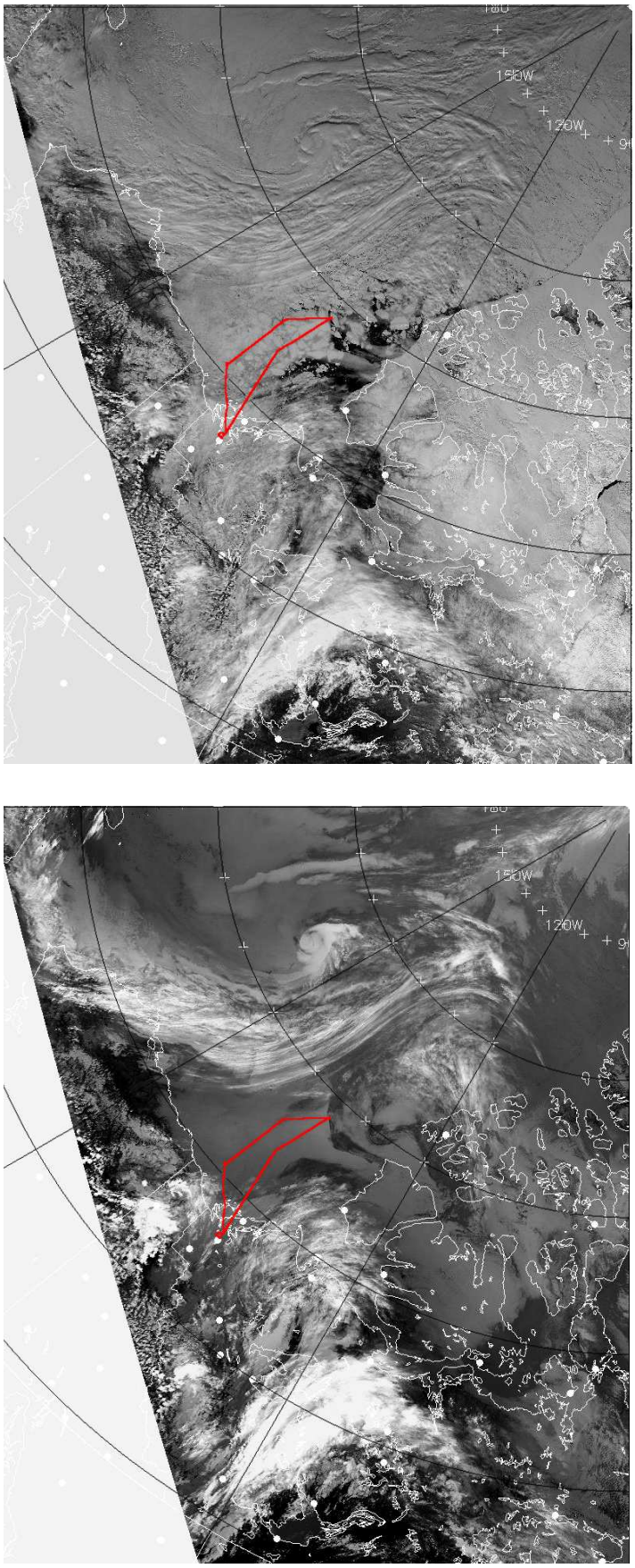

Figure 2.27: AVHRR satellite image in the visible (upper) and infrared (lower panel) range on 29 May 2008, 18:29 UTC. The flight path is marked in red.

02 June 2008

Main goals of the flight

- Boundary-layer and surface measurements over the fast ice section north west of the Mackenzie Delta and over a region of drifting sea ice further to the north west including the buoy-28832 region,
- determination of the boundary-layer structure.

Weather and ice situation

During the last days a low pressure system moved from Alaska over the southern Beaufort Sea towards Banks Island. A second low pressure system formed at the coast of Alaska. Between both lows a north-westerly flow existed. At the day of the flight the conditions were changing from the colder period to the advection of warm air from land.
The flight was performed into north-westerly direction over the fast ice section in the Mackenzie Delta to the buoy-28832 region. There we decided to continue into north-westerly direction, because north of buoy-28832 a cloud layer existed.
The sea ice was still covered by refrozen melt ponds, and a thin layer of fresh snow covered the ice.

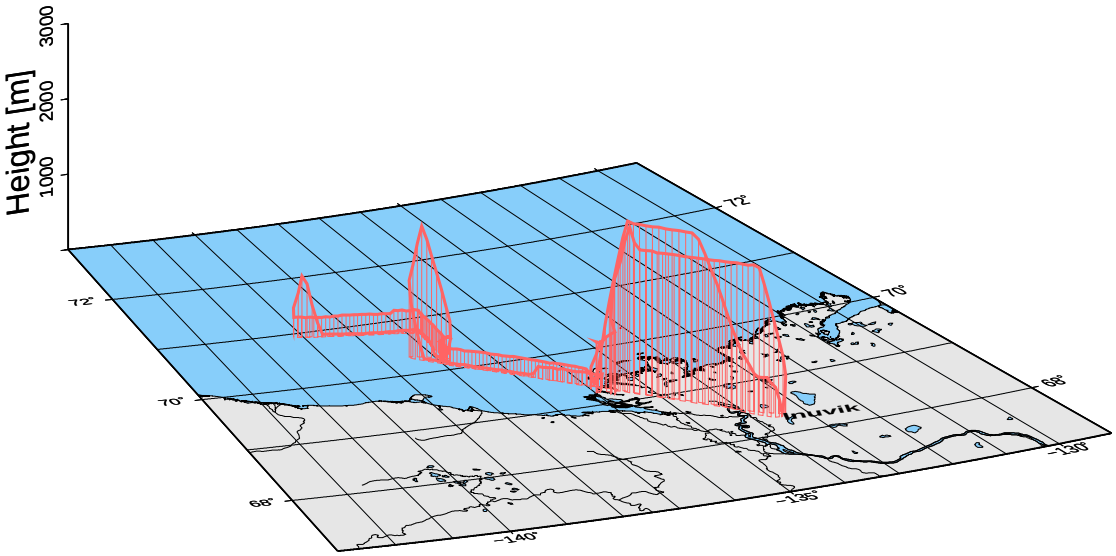

Figure 2.28: 3D-illustration of the pattern flown from Inuvik over the southern Beaufort Sea on 02 June 2008.

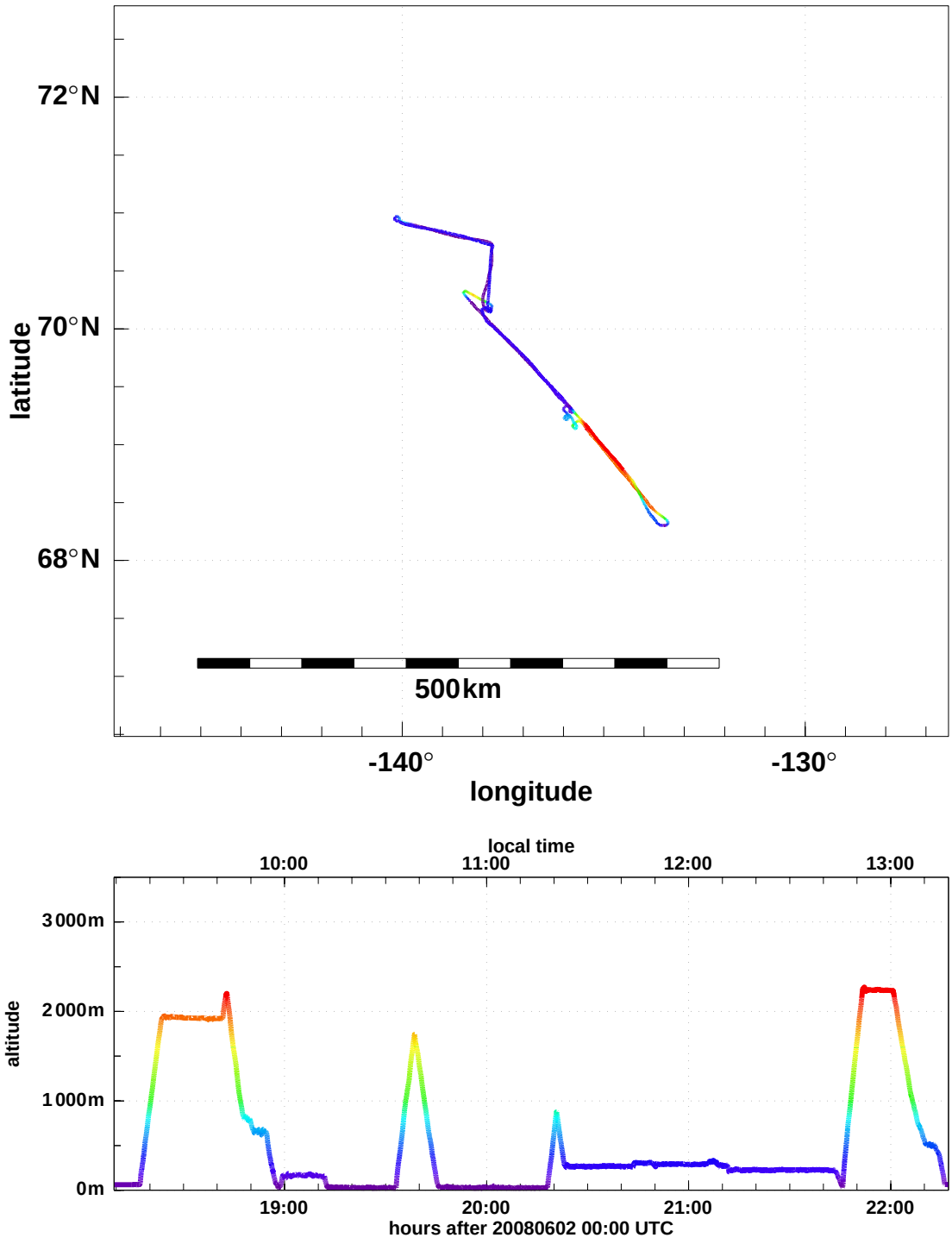

Figure 2.29: Horizontal projection of flight path (upper panel) and flight altitude as function of time (lower panel) for the mission on 02 June 2008. Violet (red) lines indicate low (high) level flight sections.

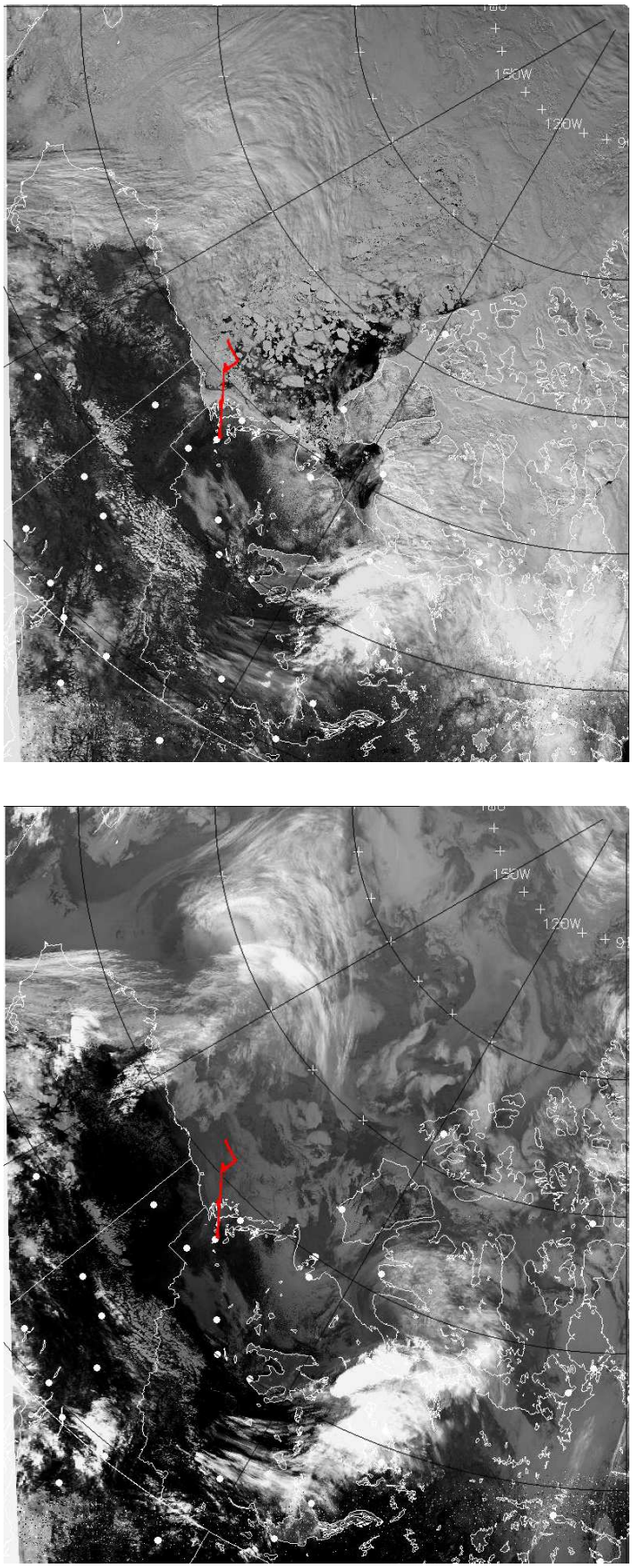

Figure 2.30: AVHRR satellite image in the visible (upper) and infrared (lower panel) range on 02 June 2008, 19:31 UTC. The flight path is marked in red.

03 June 2008

Main goals of the flight

- Determination of sea ice structure over a region covered by scenes of the satellites TerraSAR-X and Radarsat-2,
- boundary-layer and surface measurements on a flight section from buoy-5303 via buoy-28832 to the fast ice.

Weather and ice situation

Advection of warm air from south-easterly directions occurred during the whole day. However, surficial melting and formation of melt ponds north of 71°N progressed very slowly. Open melt ponds were mainly found only south of 71°N.

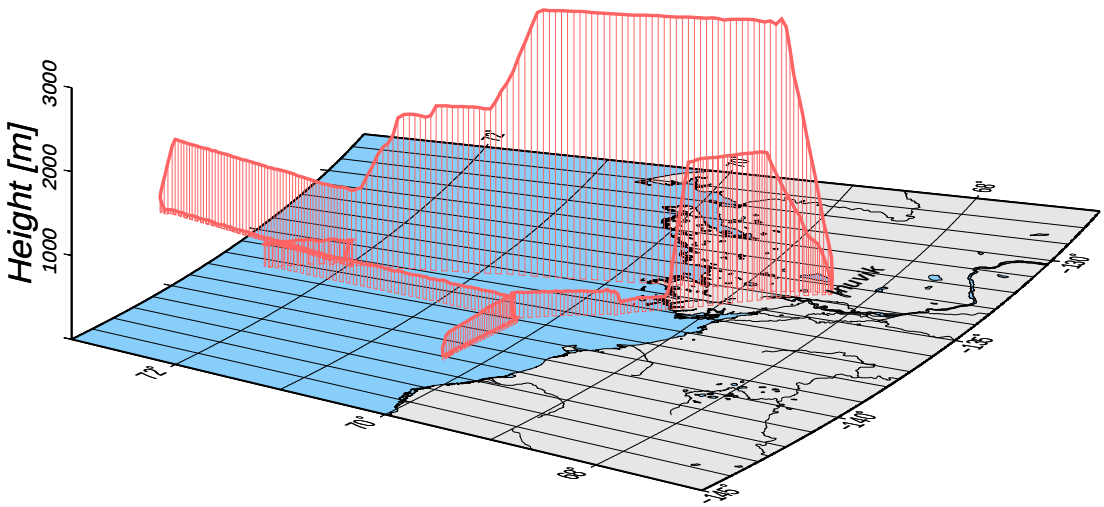

Figure 2.31: 3D-illustration of the pattern flown from Inuvik over the southern Beaufort Sea on 03 June 2008.

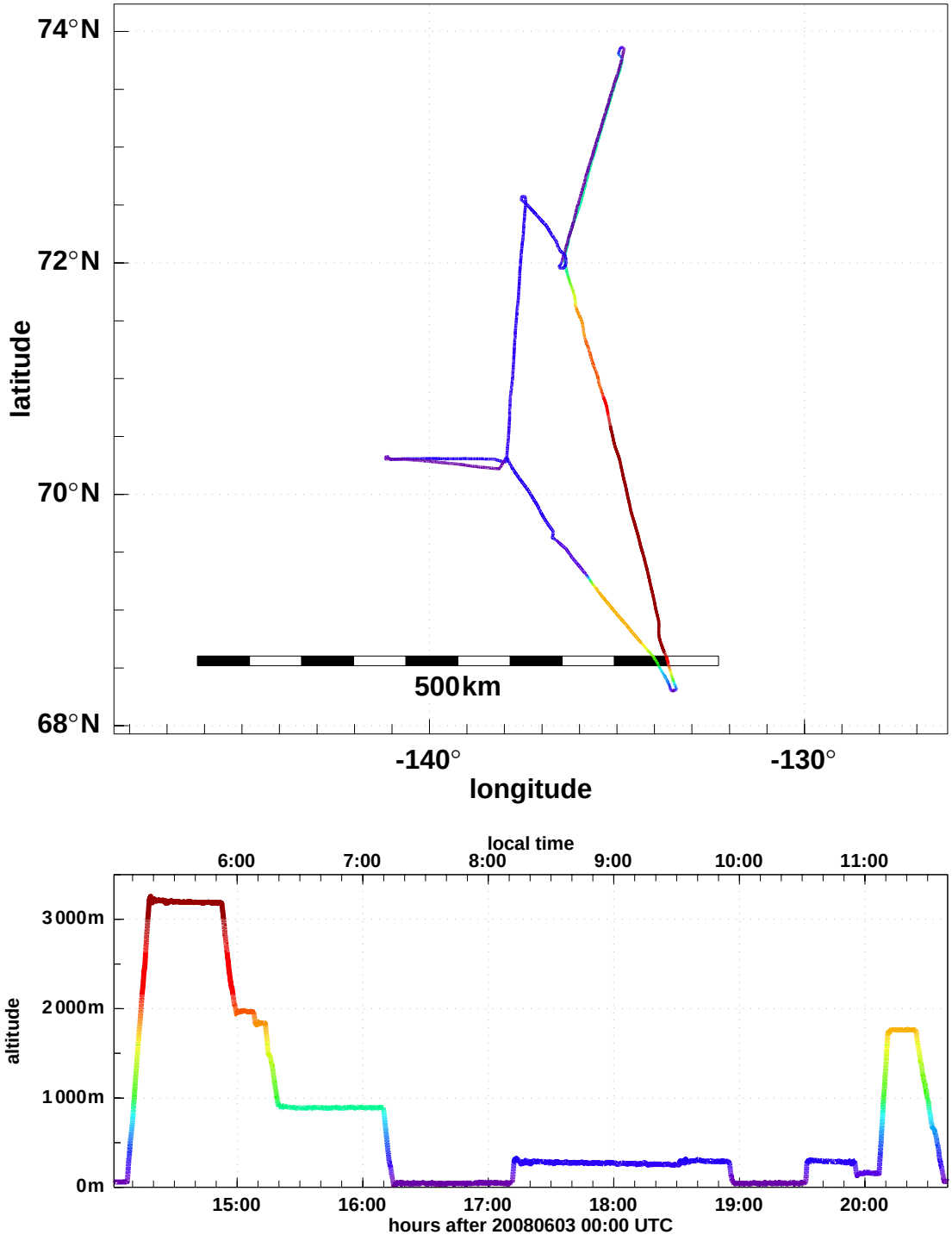

Figure 2.32: Horizontal projection of flight path (upper panel) and flight altitude as function of time (lower panel) for the mission on 03 June 2008. Violet (red) lines indicate low (high) level flight sections.

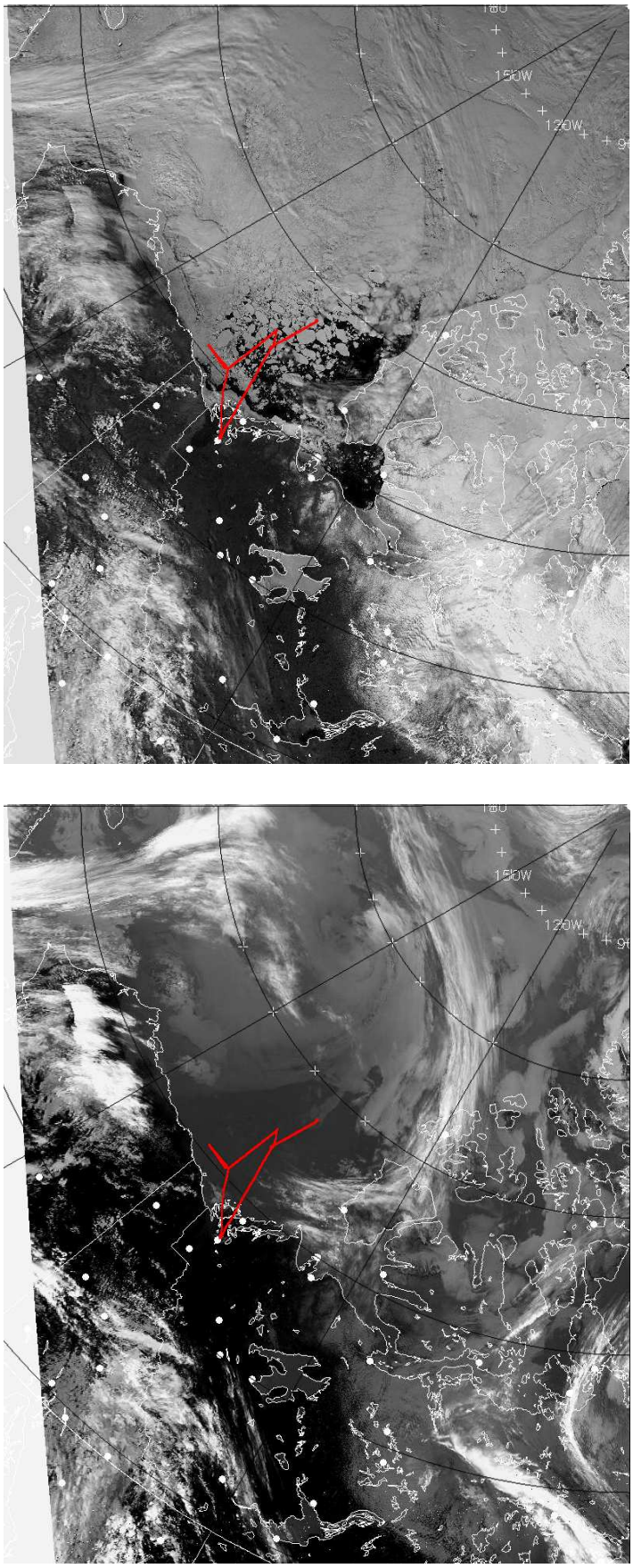

Figure 2.33: AVHRR satellite image in the visible (upper) and infrared (lower panel) range on 03 June 2008, 19:17 UTC. The flight path is marked in red.

04 June 2008

Main goals of the flight

- Flight pattern parallel to the wind with boundary-layer and surface measurements during strong warm-air advection,
- measurement of turbulent fluxes near the surface and below the inversion to investigate the heat transport in the boundary-layer over the ice,
- attempt to determine the influence of entrainment by flux measurements at the capping inversion level.

Weather and ice situation

A low pressure system with its center at (80°N, 150°W) and a high pressure system with its core between Banks and Ellesmere Island caused a strong south-easterly flow over the Canadian part of the Beaufort Sea. Almost clear-sky conditions were present.
The snow on sea ice had either melted away or was very wet. The number of melt ponds was significantly larger compared to previous days. Especially, west of 141°W many well-developed ponds were observed.

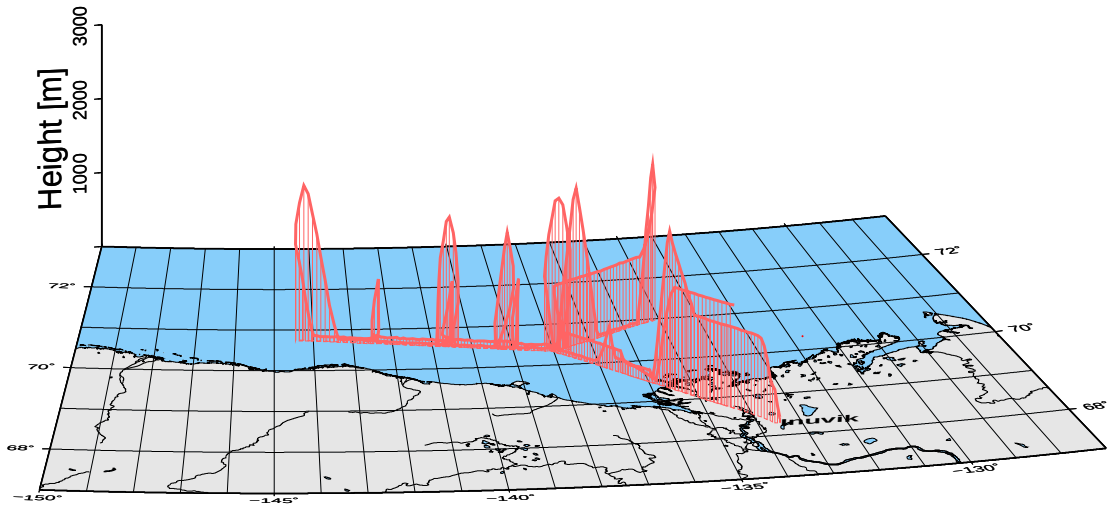

Figure 2.34: 3D-illustration of the pattern flown from Inuvik over the southern Beaufort Sea on 04 June 2008.

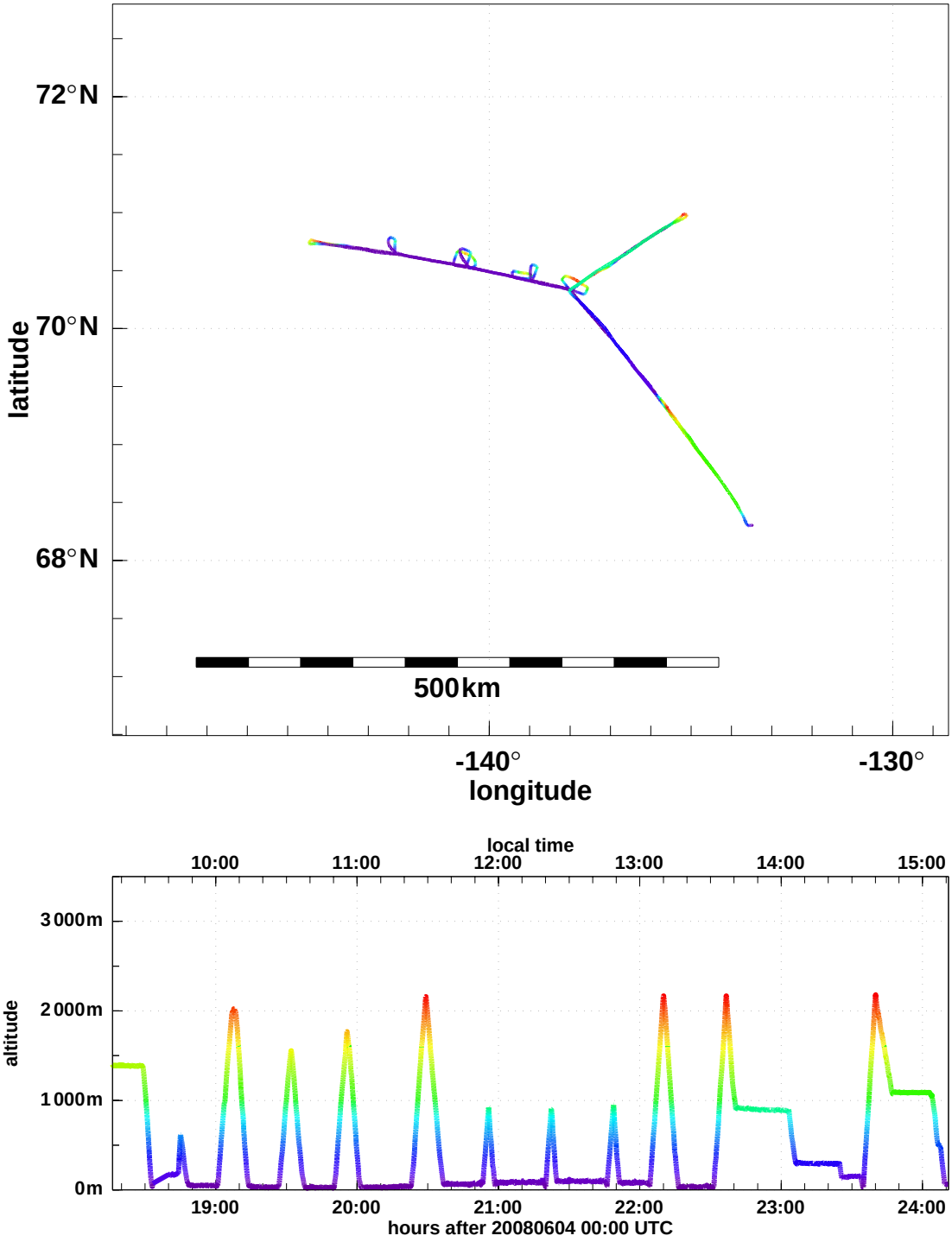

Figure 2.35: Horizontal projection of flight path (upper panel) and flight altitude as function of time (lower panel) for the mission on 04 June 2008. Violet (red) lines indicate low (high) level flight sections.

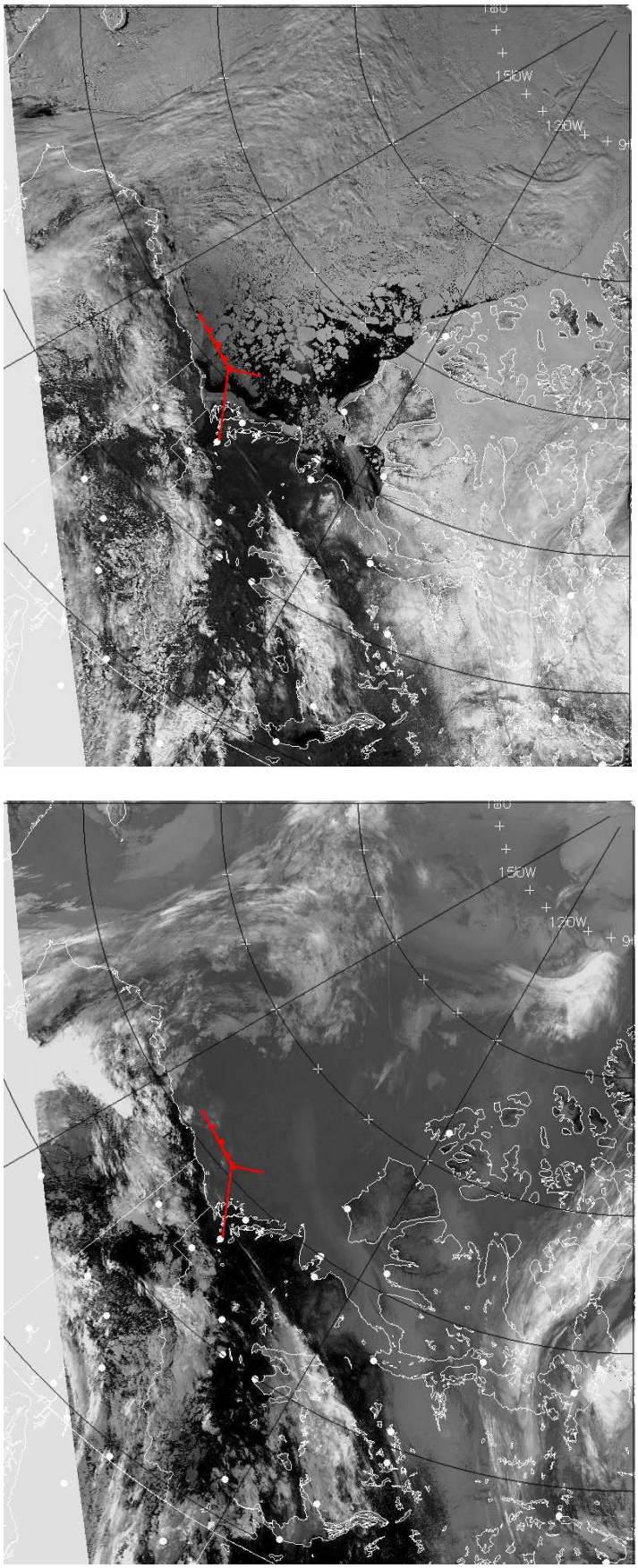

Figure 2.36: AVHRR satellite image in the visible (upper) and infrared (lower panel) range on 04 June 2008, 19:09 UTC. The flight path is marked in red.

06 June 2008

Main goals of the flight

- Boundary-layer and surface measurements over fast ice of Darnley and Franklin Bay situated west of the Amundsen Gulf,
- boundary-layer pattern to investigate the effect of the advection of warm-air from land over pond-covered ice.

This flight was performed as a contribution to the Canadian IPY-CFL project.

Weather and ice situation

A high pressure system over the eastern Beaufort Sea still caused easterly flow, hence, warm-air advection was still present as on previous days. Over Darnley and Franklin Bay, clear-sky conditions were met, over land, a cumulus cloud layer formed.
Darnley and Franklin Bay were still covered by fast ice (see Fig. 2.40), which was, however, nearly completely covered by well-developed melt pond. These ponds (see Fig. 2.41) appeared to be much larger than the ponds observed over drift ice.

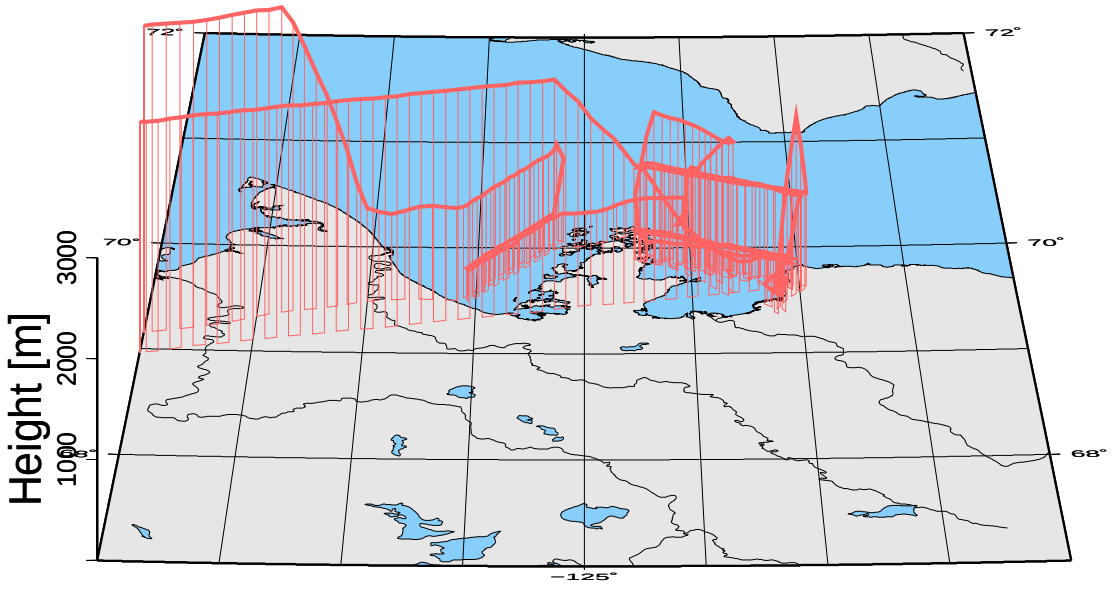

Figure 2.37: 3D-illustration of the pattern flown from Inuvik over the southern Beaufort Sea on 06 June 2008.

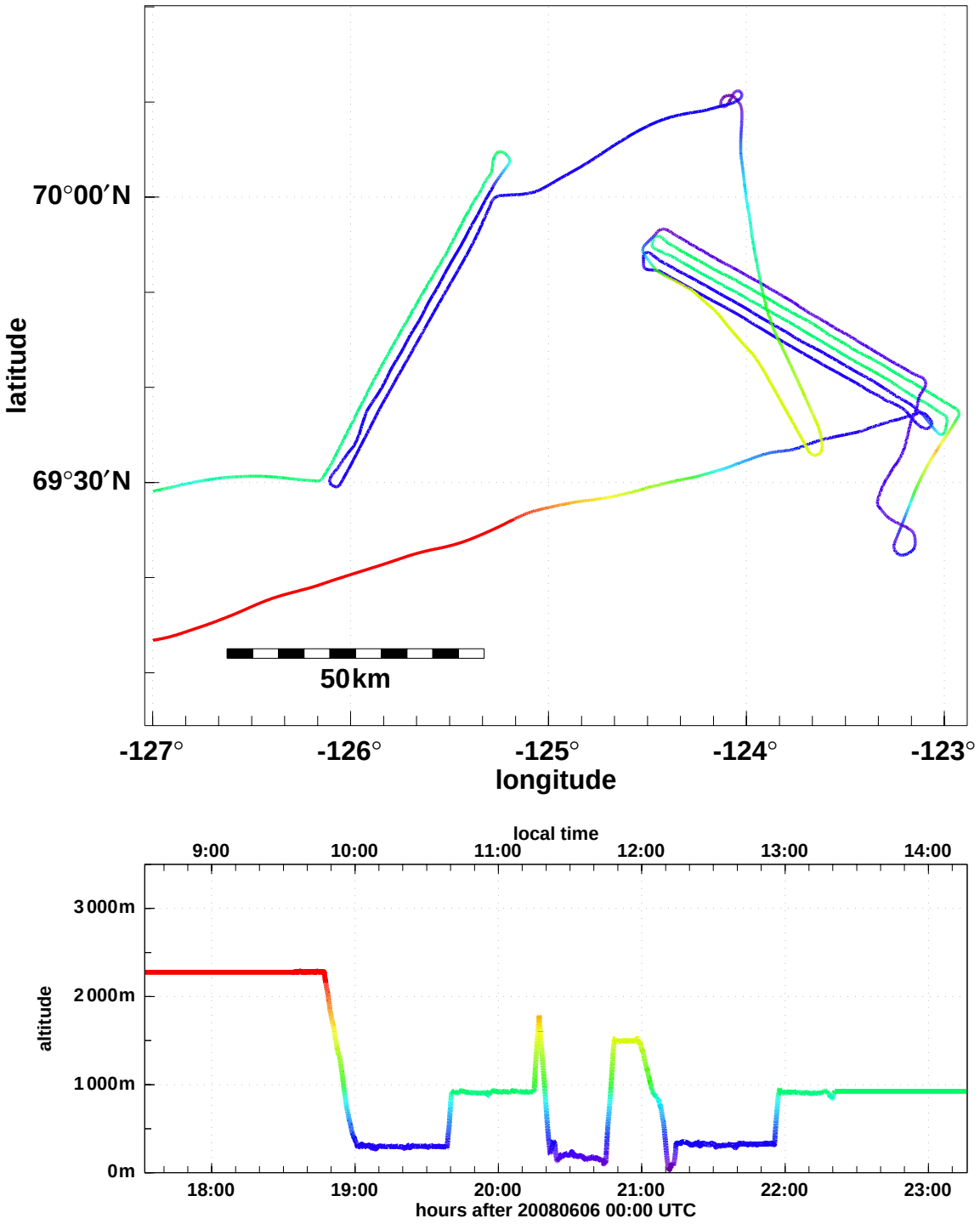

Figure 2.38: Horizontal projection of flight path (upper panel) and flight altitude as function of time (lower panel) for the mission on 06 June 2008. Violet (red) lines indicate low (high) level flight sections.

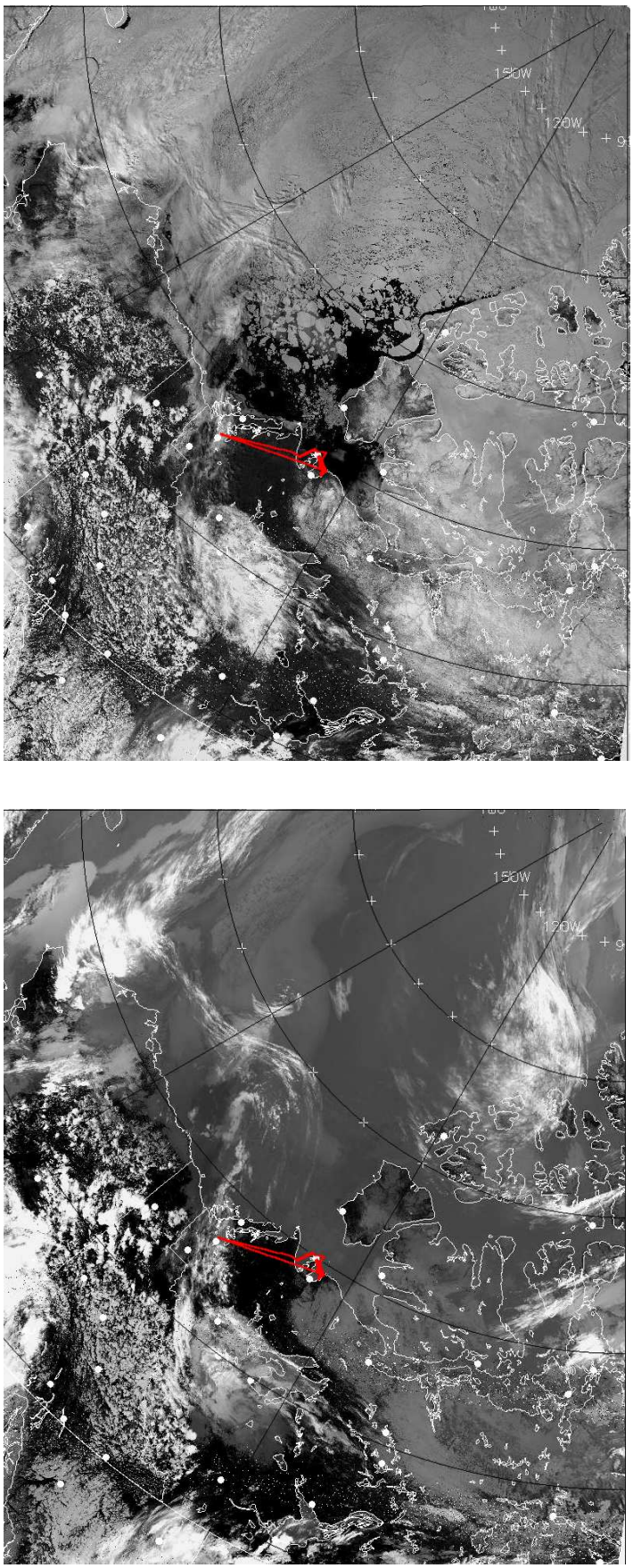

Figure 2.39: AVHRR satellite image in the visible (upper) and infrared (lower panel) range on 06 June 2008, 20:29 UTC. The flight path is marked in red.

Figure 2.40: MODIS-image showing the region of Franklin Bay, Parry Peninsula, and Darnley Bay situated in the southern Amundsen Gulf. In early June 2008, wide areas of Franklin and Darnley Bay were covered by fast ice with well-developed melt ponds. Thin black lines mark the area, where measurements took place on 06 June 2008.

Figure 2.41: Well-developed melt ponds on fast ice in Franklin Bay on 06 June 2008. The picture was taken with a hand-held camera at an altitude of appr. 330 m.

07 June 2008

Main goals of the flight

- Determination of sea ice structure in a region covered by scenes of the satellite TerraSAR-X,
- boundary-layer and surface measurements over drift ice.

Weather and ice situation

The last measurement flight was performed nearly almost under clear-sky conditions. Melt pond fraction between 72,5°N to 70°N still showed a large gradient. In the northern part, melt pond fraction on individual floes varied considerably; numerous floes in this area were still not at all covered by melt ponds. In the southern part, well-developed ponds could be observed on most of the floes.

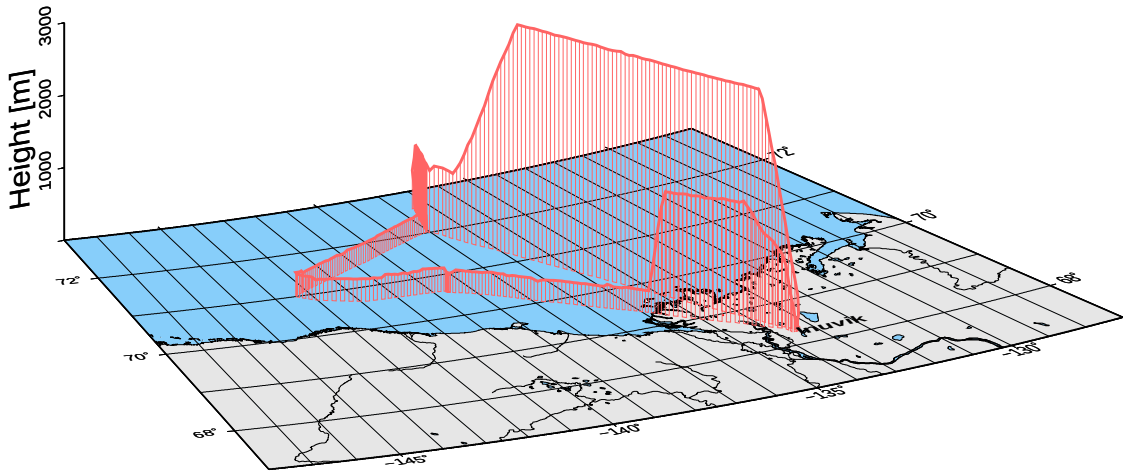

Figure 2.42: 3D-illustration of the pattern flown from Inuvik over the southern Beaufort Sea on 07 June 2008.

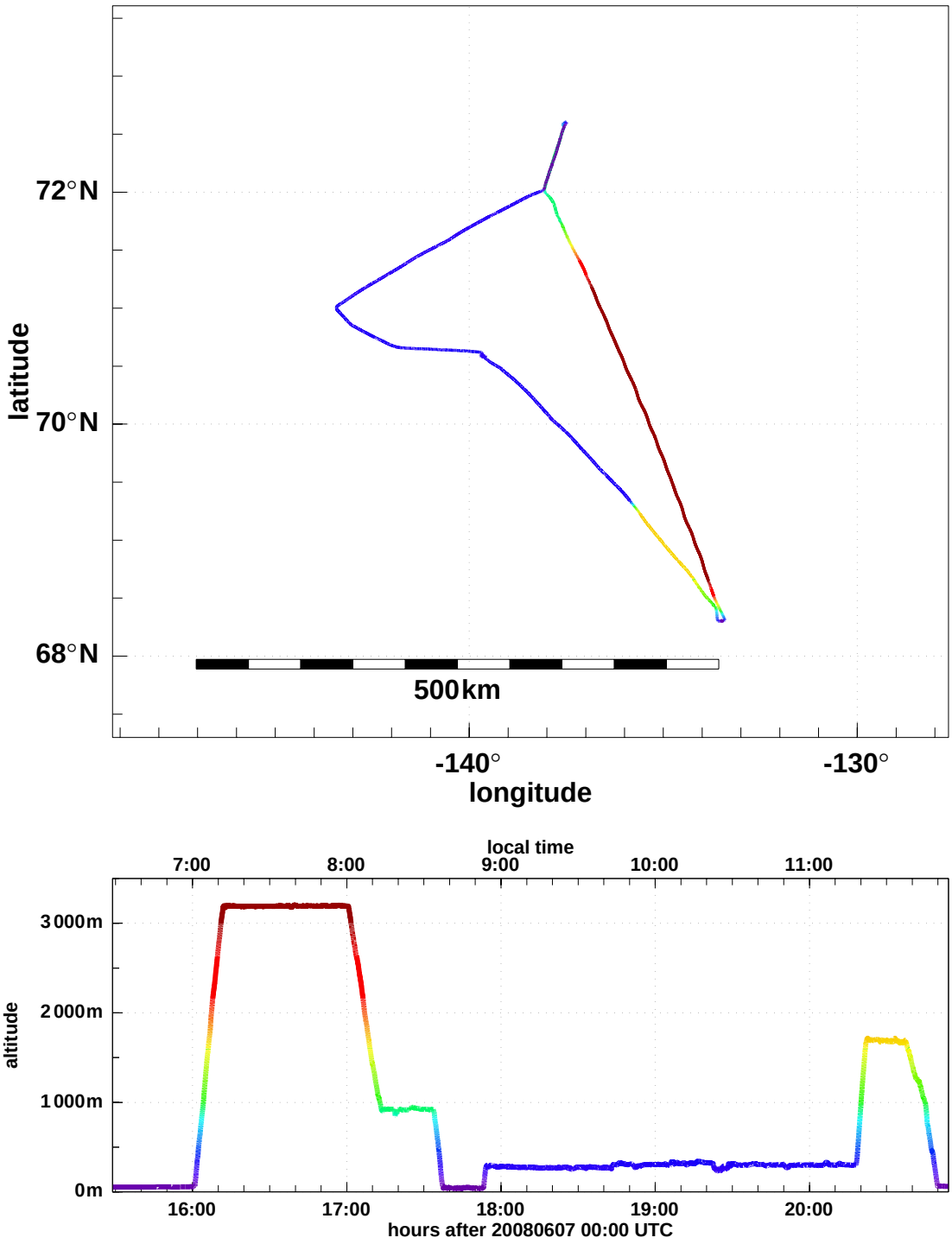

Figure 2.43: Horizontal projection of flight path (upper panel) and flight altitude as function of time (lower panel) for the mission on 07 June 2008. Violet (red) lines indicate low (high) level flight sections.

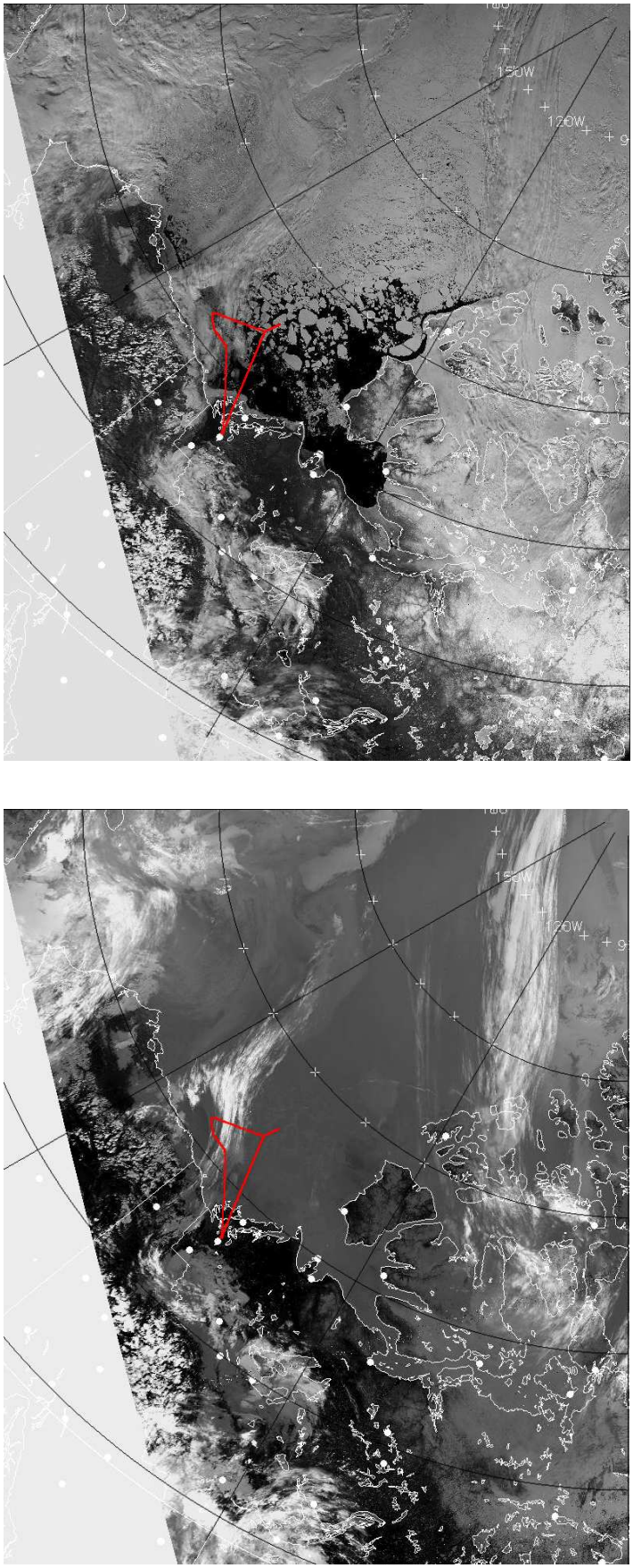

Figure 2.44: AVHRR satellite image in the visible (upper) and infrared (lower panel) range on 07 June 2008, 18:36 UTC. The flight path is marked in red.

Fig. 2.45 summarizes all tracks flown from Inuvik between 11 May 2008 and 07 June 2008.

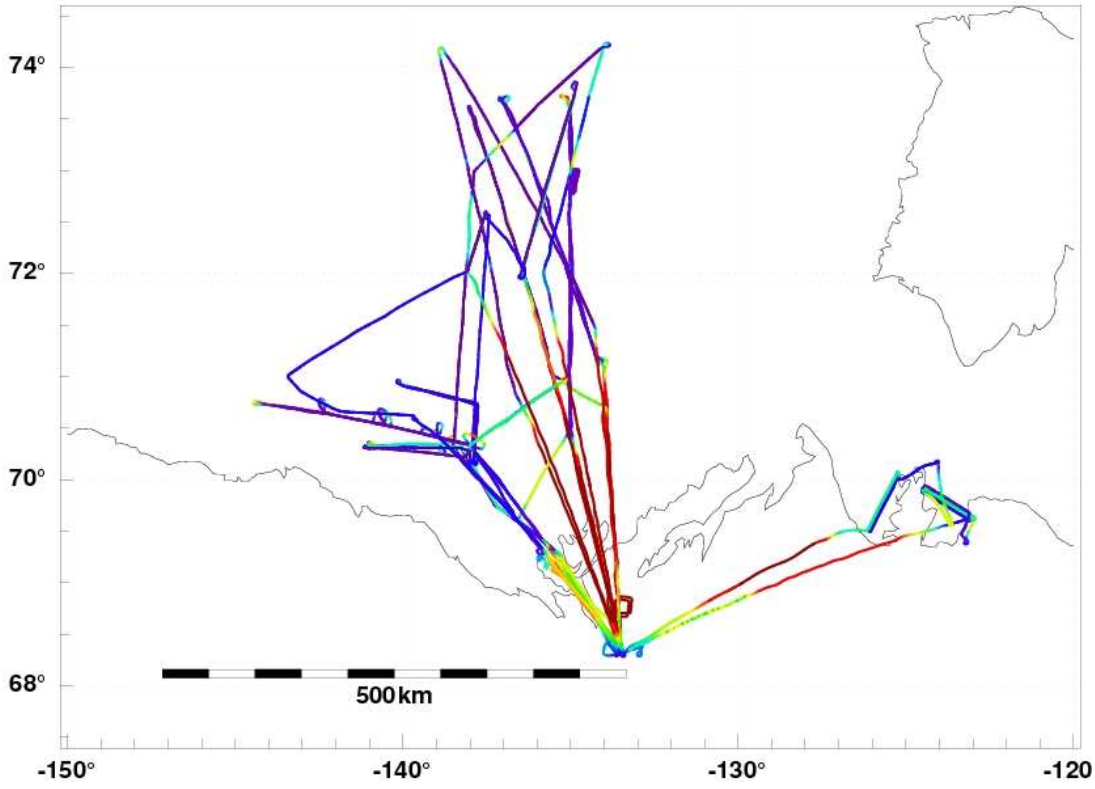

Figure 2.45: Horizontal projection of all measurement mission tracks flown from Inuvik between 11 May 2008 and 07 June 2008. Violet (red) lines indicate low (high) level flight sections.

3 Description of Weather and Ice Situation

3.1 Initial Sea Ice Conditions

The first measurement flight of the campaign MELTEX was performed on 11 May 2008. At that time the sea ice situation in the Beaufort Sea was characteristic for late winterly conditions. As already shown in Fig. 2.4 (upper panel), most parts of the Beaufort Sea were still covered by pack-ice. However, the transition to spring conditions had already started with the opening of a coastal polynya west of the Amundsen Gulf, the so-called Cape Bathurst Polynya. Compared to previous years, the polynya size was much larger than usual in the last decade. The fast opening of the Cape Bathurst Polynya in May/June was mainly caused by prevailing south-easterly winds. Another reason was the existence of wide areas covered with nilas at the northern rim of the polynya that melted during the second half of the campaign.
Figure 3.1 (upper panel) gives an impression of the sea ice situation in the region of the Cape Bathurst Polynya during the first measurement flight on 11 May 2008. Areas of open water were mixed with nilas and with small and thin first-year floes. Several tens of kilometers north of the polynya larger fields of nilas had disappeared completely. Instead, first-year floes with diameters of several hundreds of meters were overflown (see Fig. 3.1 (lower panel)). Further north, we passed even second- or multi-year floes. This visual impression is supported by a radar satellite image from 12 May 2008 (see Fig. 3.2) that is indicative of older ice north of appr. 73°N in our measurement region. During our flight up to nearly 74°N no clearly visible signs of surficial melting were observed; ice floes were covered by dry snow, whose surface temperature was partly even below -10°C.

3.2 First and Second Warming Event

Right after the first flight on 11 May 2008 we experienced the first warming event in the period of the MELTEX campaign. Figures 3.3 and 3.4 show 2m-air temperatures over the Arctic Ocean at appr. 12 Local Time on 12 May and 14 May (day of 2nd flight) as well as 17 May (3rd flight) and 19 May (4th flight). It can be seen that there was a warming trend over the Beaufort Sea in the considered period. This trend was also detected in our measurements that showed, e. g. , surface temperatures below -10°C only during the very first flight. During the following three flights they were above -5°C, occasionally reaching the melting point.

Figure 3.1: Sea ice situation characteristic for the Cape Bathurst Polynya (upper panel) and for the pack-ice region north of the polynya (lower panel) overflown during the first measurement mission on 11 May 2008. Pictures were taken with a hand-held camera at an altitude of appr. 1000 m and 30 m, respectively.

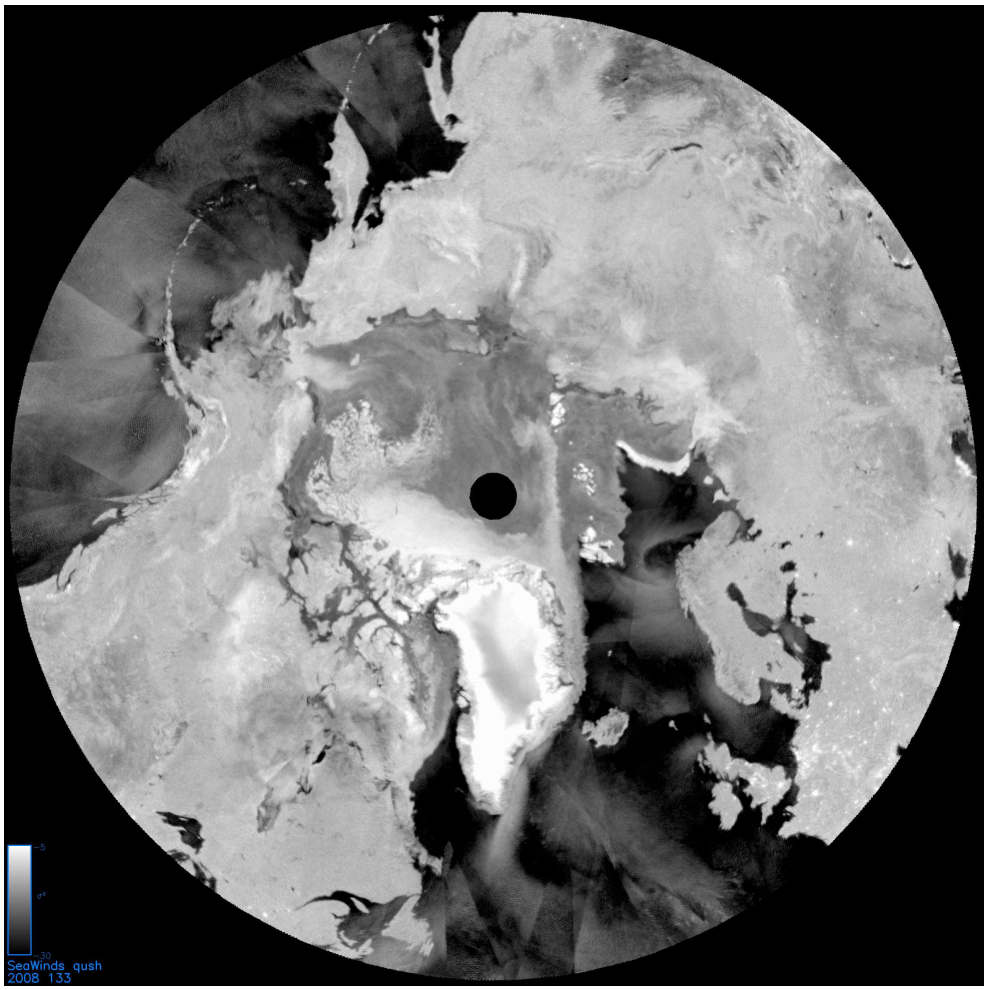

Figure 3.2: Radar intensity from QuikSCAT on 12 May 2008. Whitish colors in the Arctic Ocean indicate second- or multi-year ice whereas grayish colors indicate first-year ice.

After the 4th flight on 19 May 2008 the large-scale synoptic situation changed to conditions with cold-air advection from inner parts of the Arctic towards the coast of the Beaufort Sea. Since additional measurements planned north of Ellesmere Island could only be performed, due to logistical contraints, between 22 and 26 May 2008, we decided to transfer POLAR 5 to Eureka, where a flight was performed on 23 May 2008. On the following day POLAR 5 was transfered back to Inuvik. At the same time the large scale synoptic pattern changed again dramatically resulting in the second strongest warming event over the southern Beaufort Sea during the MELTEX campaign. This event caused the onset of melt pond formation on ice in a large band along the coast from the Cape Bathurst Polynya to Alaska. Figure 3.5 illustrates the early stage of melt pond development on sea ice overflown on 26 May 2008. Melt pond fraction was largest close to the coast, however, at about 71°N some ponds were still visible.
From 27 May to 1 June 2008, we experienced again a period with prevailing cold-air flow over the southern Beaufort Sea. As observed during the flight on 29 May 2008, this caused a refreezing of most melt ponds which were still very shallow at that time. On 2 June 2008, even a thin layer of fresh snow on the refrozen ponds was observed.

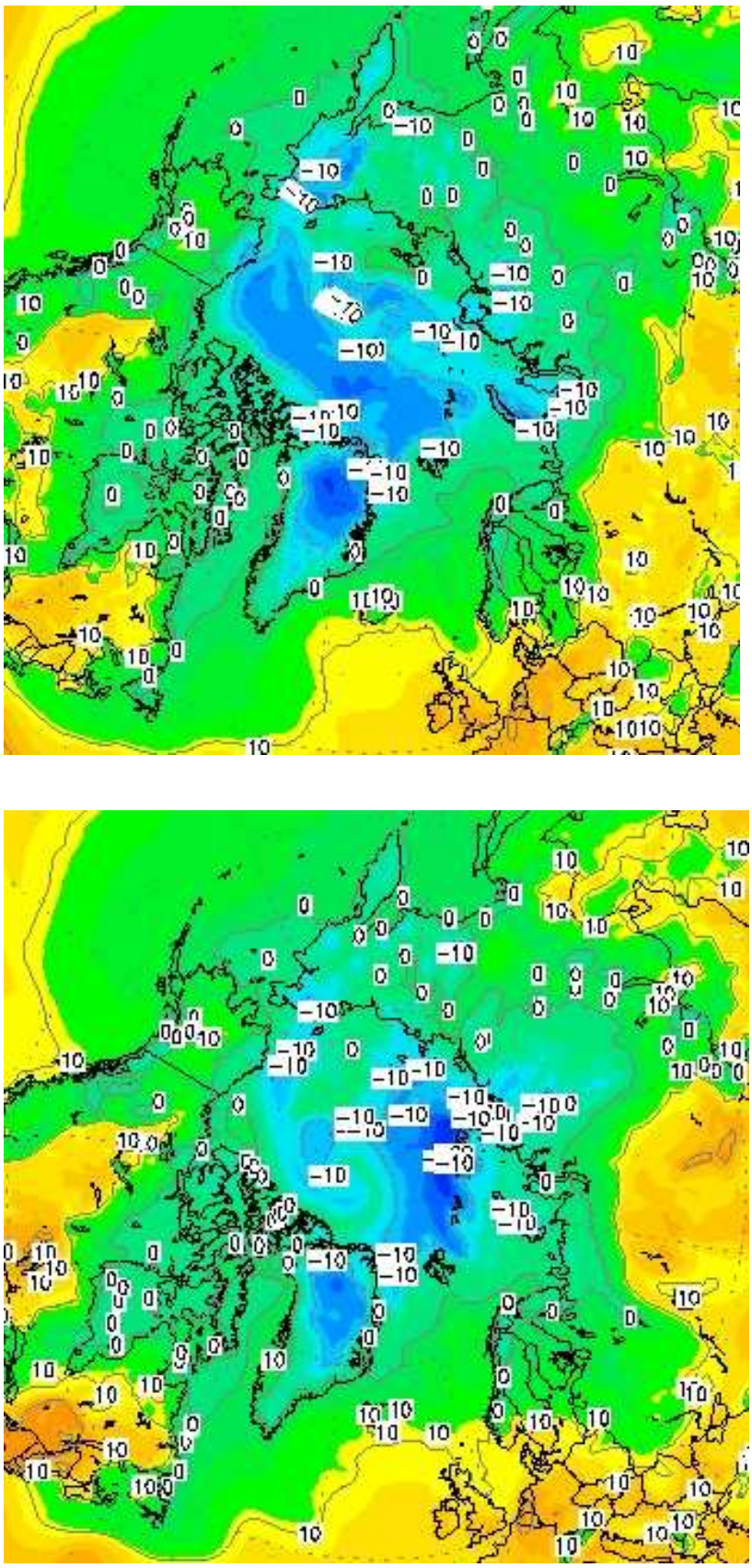

Figure 3.3: 2m-air temperature (°C) at 18 UTC (appr. 12 LT) on 12 May 2008 (upper panel) and on 14 May 2008 (lower panel). Forecasts are provided by the GFS- (Global Forecast System)-model.

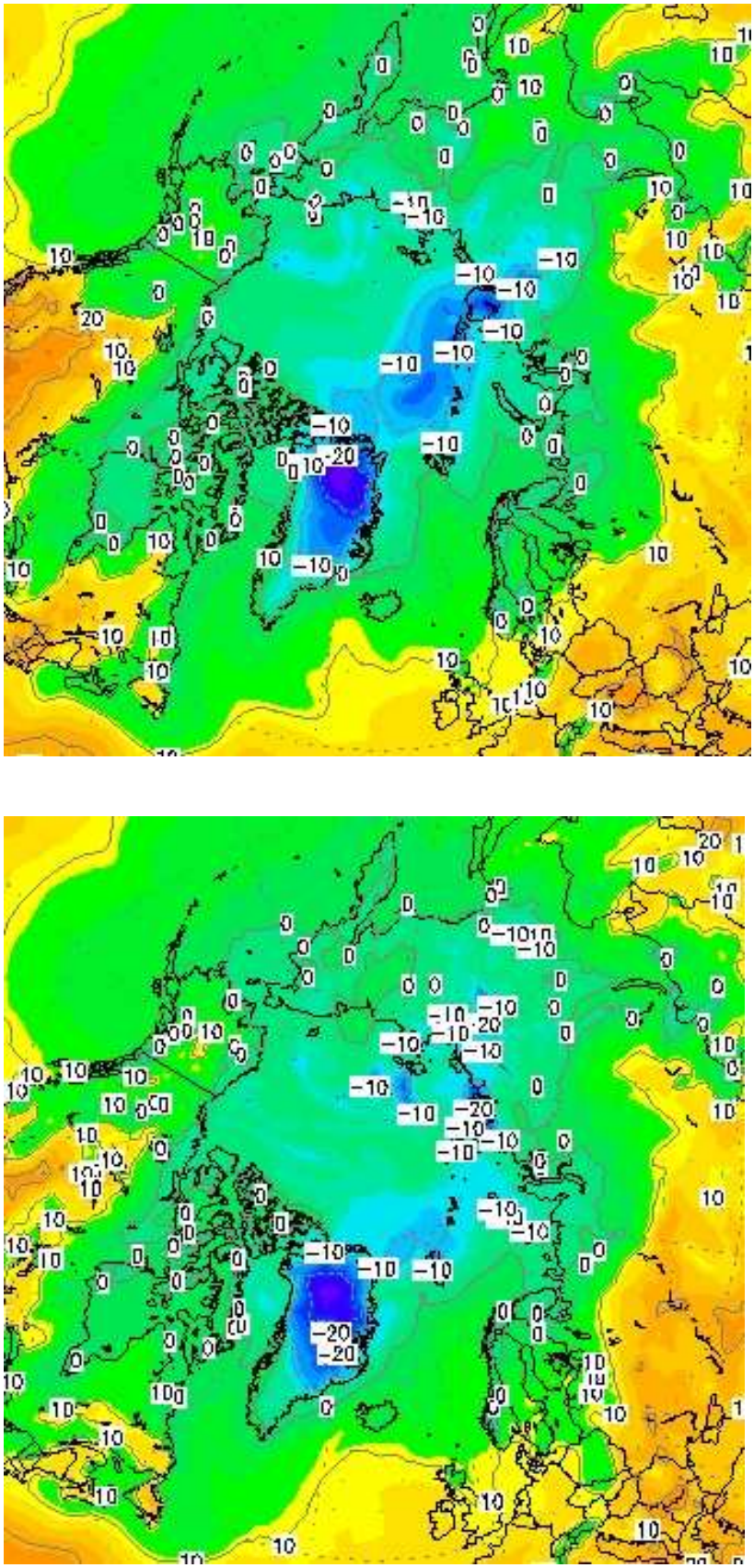

Figure 3.4: 2m-air temperature (°C) at 18 UTC (appr. 12 LT) on 17 May 2008 (upper panel) and on 19 May 2008 (lower panel). Forecasts are provided by the GFS- (Global Forecast System)-model.

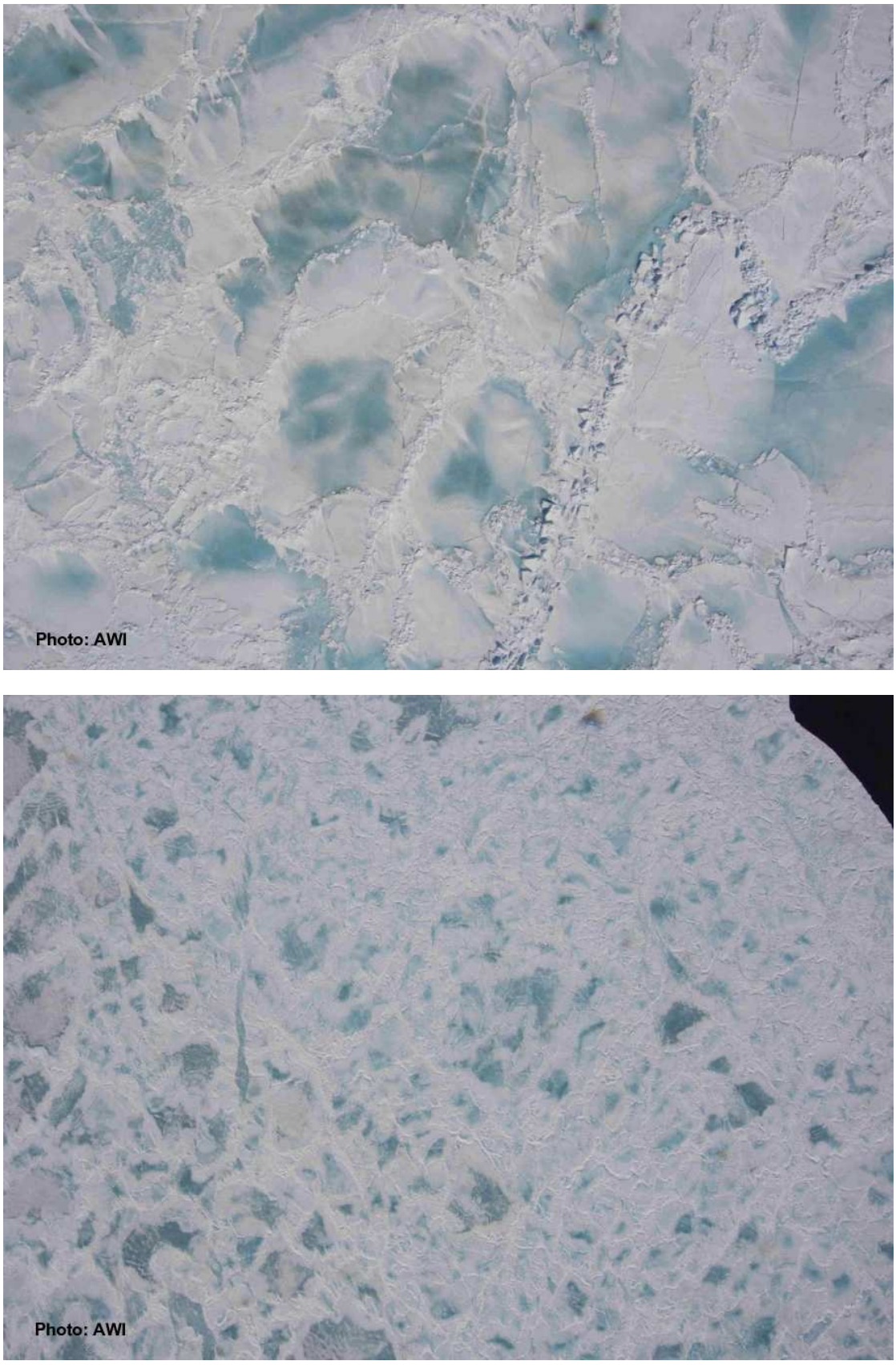

Figure 3.5: Melt ponds on sea ice overflown during the measurement mission on 26 May 2008 in the vicinity of ARGOS-buoy 28832 and west of it. Pictures were taken at an altitude of appr. 150 m and 900 m, respectively with a photo camera permanently mounted on POLAR 5.

3.3 Strongest Warming Event

During the last week of measurements from 01 to 07 June 2008, we experienced again a warming event, the strongest one during the whole MELTEX campaign. Figures 3.6 and 3.7 show a sequence of forecast maps of the 850hPa-temperature at appr. 12 Local Time from 02 to 05 June 2008. It can be clearly seen that a tongue of warm air was shifted from Alaska (Fig. 3.6) to the middle and western Beaufort Sea (Fig. 3.7). The 0°C-isotherm was pushed far over the Beaufort Sea, and it reached its largest extension in this region on 04 and 05 June 2008. This temperature distribution was caused by a low pressure system with its center at (80°N, 150°W) and a high pressure system between Banks and Ellesmere Island. A strong south easterly flow existed over most parts of the Beaufort Sea, except a band of easterly flow along the coast, which might have been caused by a channeling effect. In this area (see red line in Fig. 3.8), boundary-layer measurements were performed on 04 June 2008 to study the structure of the strongly stable ABL during this event of warm-air advection including transport processes through the capping inversion. Fig. 3.9 shows vertical temperature profiles in the boundary layer during the flight. While the ABL was well-mixed over land due to convection caused by a warm surface, a strongly stable stratification developed over sea ice, where the warm air was advected over a considerably colder surface.

Caused by this very intense warming event in the beginning of June the development of melt ponds in the measurement region was strongly forced. Fig. 3.10 gives an impression of melt-pond covered sea ice overflown on 04 June 2008.

3.4 Conclusions and Outlook

During a four-weeks period atmospheric boundary layer and surface measurements were performed in the southern Beaufort Sea. From 11 May to 07 June 2008 ice conditions changed from late winter conditions to early summer conditions with melt pond formation. However, changes in the ice cover were stronly dependend on synoptic-scale processes. The areal distribution of low and high pressure systems led to off-ice as well as on-ice flow several times. The latter was characterized by warm-air advection from land over sea ice, a process decisive for the onset of surficial melting and melt pond formation during the campaign MELTEX. Off-ice flow with cold-air advection from the inner Arctic caused an interruption of melt pond evolution and even a temporary refreezing of ponds.

During the next months, it will be investigated in detail how ice concentration and melt pond fraction changed with time, and how surface melting influenced radiation characteristics of sea ice like spectral and broadband albedo. In several case studies, the warm-air advection events experienced will be investigated to better understand the vertical heat transport in the atmospheric boundary layer during such situations.

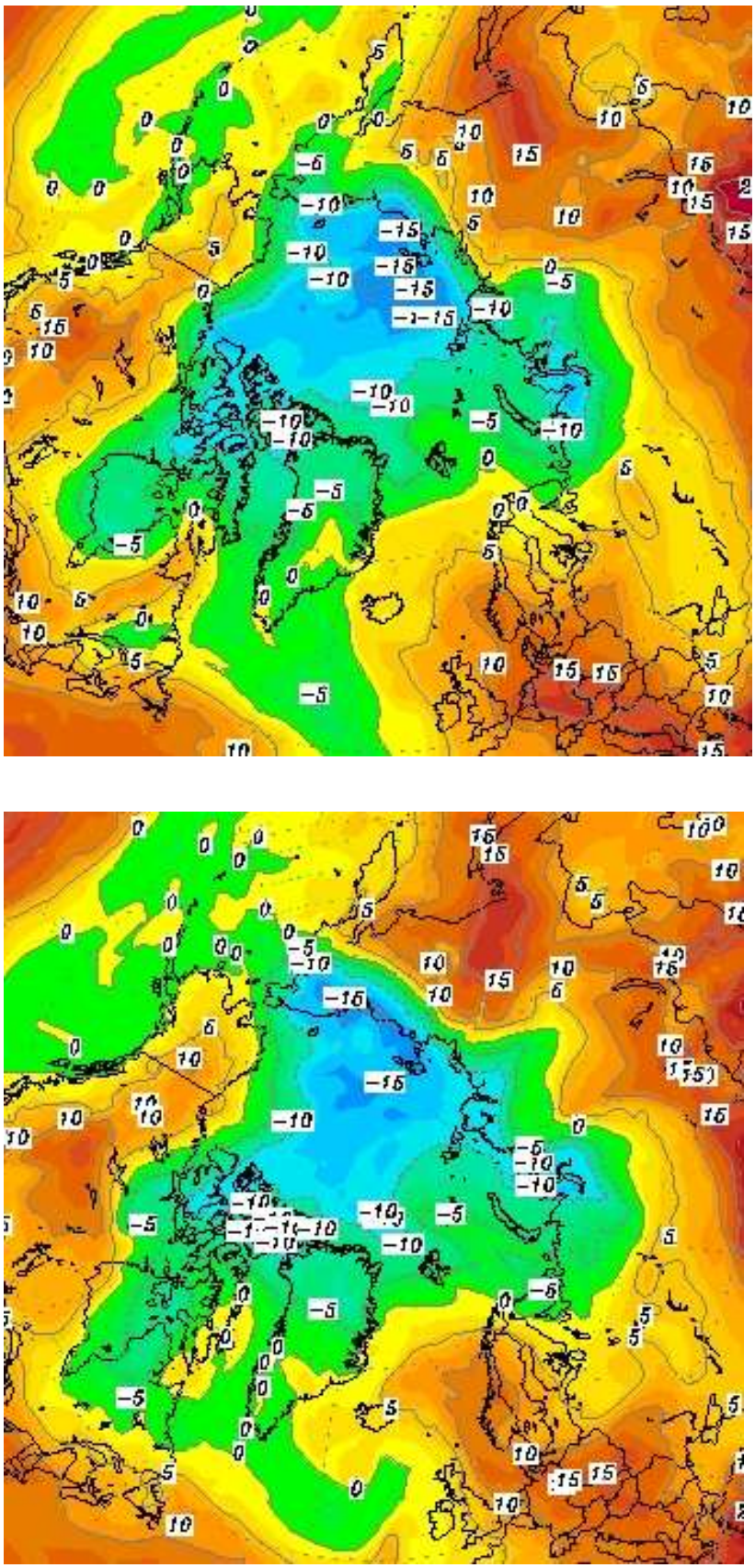

Figure 3.6: 850hPa-temperature (°C) at 18 UTC (appr. 12 LT) on 02 June 2008 (upper panel) and on 03 June 2008 (lower panel). Forecasts are provided by the GFS- (Global Forecast System)-model.

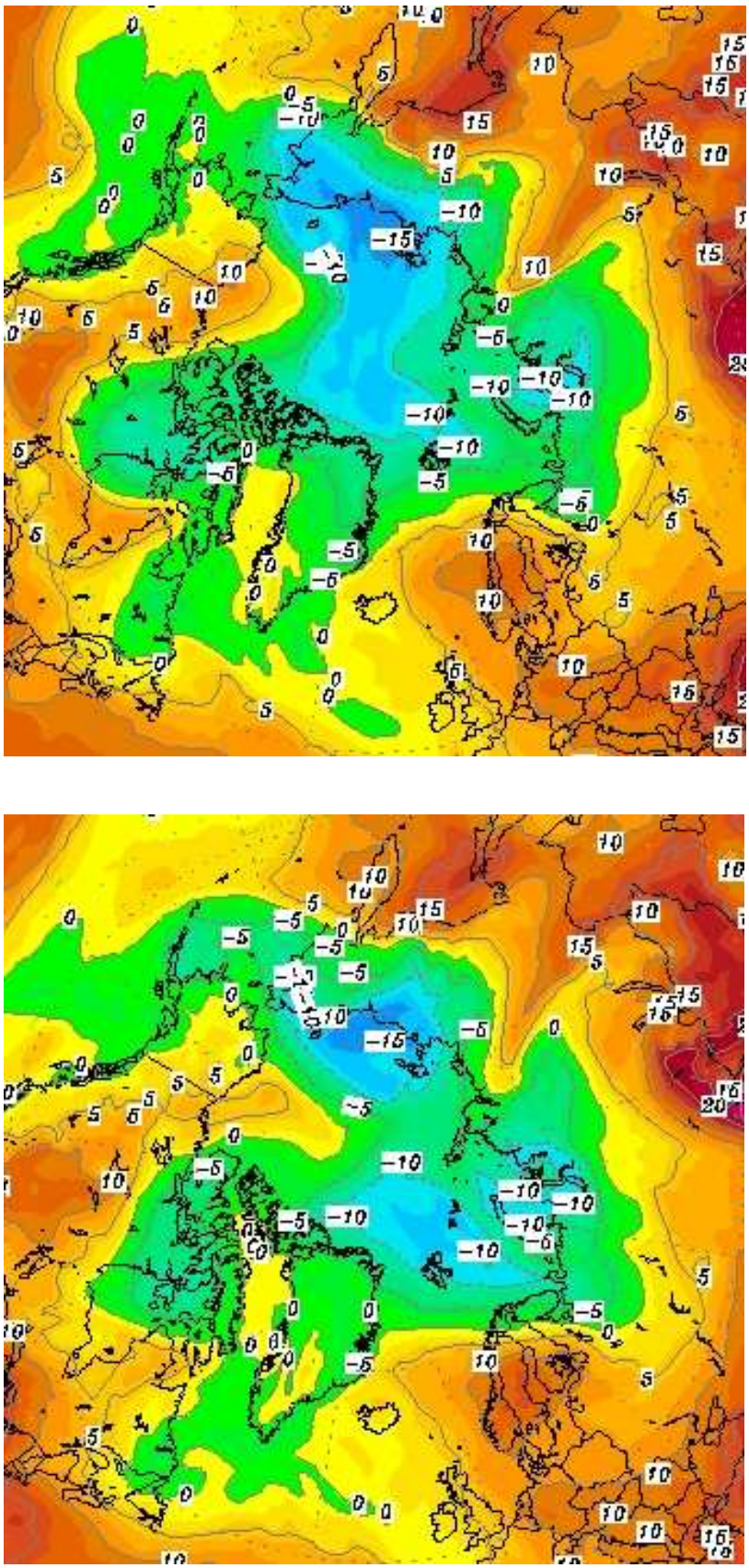

Figure 3.7: 850hPa-temperature (°C) at 18 UTC (appr. 12 LT) on 04 June 2008 (upper panel) and on 05 June 2008 (lower panel). Forecasts are provided by the GFS- (Global Forecast System)-model.

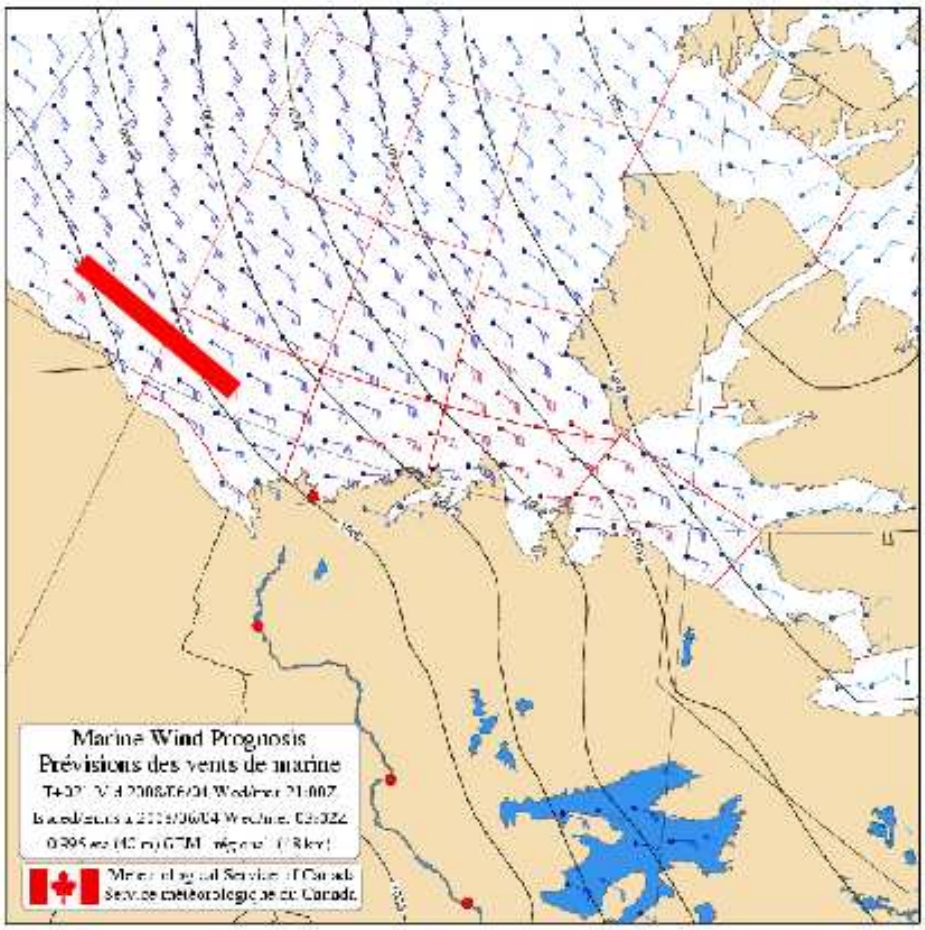

Figure 3.8: Near-surface wind at 21 UTC (appr. 15 LT) on 04 June 2008. The Forecast was provided by the Meteorological Service of Canada. The thick red line indicate a section of the flight path on 04 June 2008, where primarily boundary layer measurements were performed.

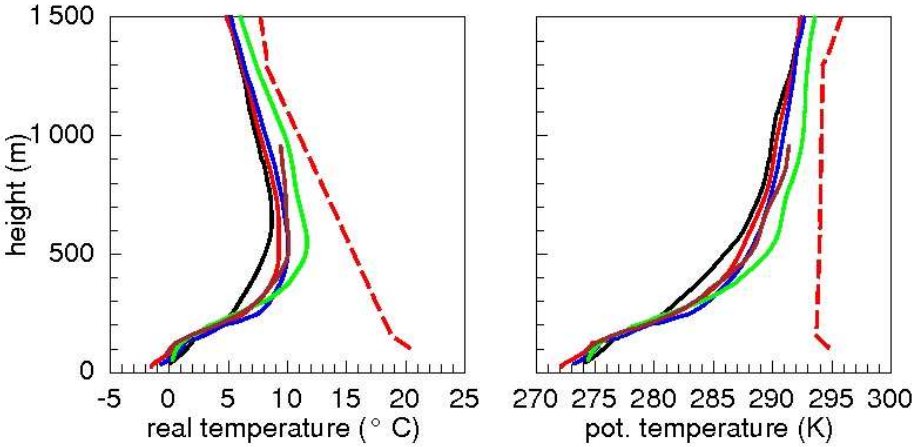

Figure 3.9: Vertical profiles of real temperature (°C) (left panel) and potential temperature (K) (right panel) measured during the flight on 04 June 2008. The dashed red line represents data from the daily routine radiosonde observations in Inuvik. The full lines represent data taken during ascents and descents over sea ice downstream the coast along the red line in Fig. 3.8.

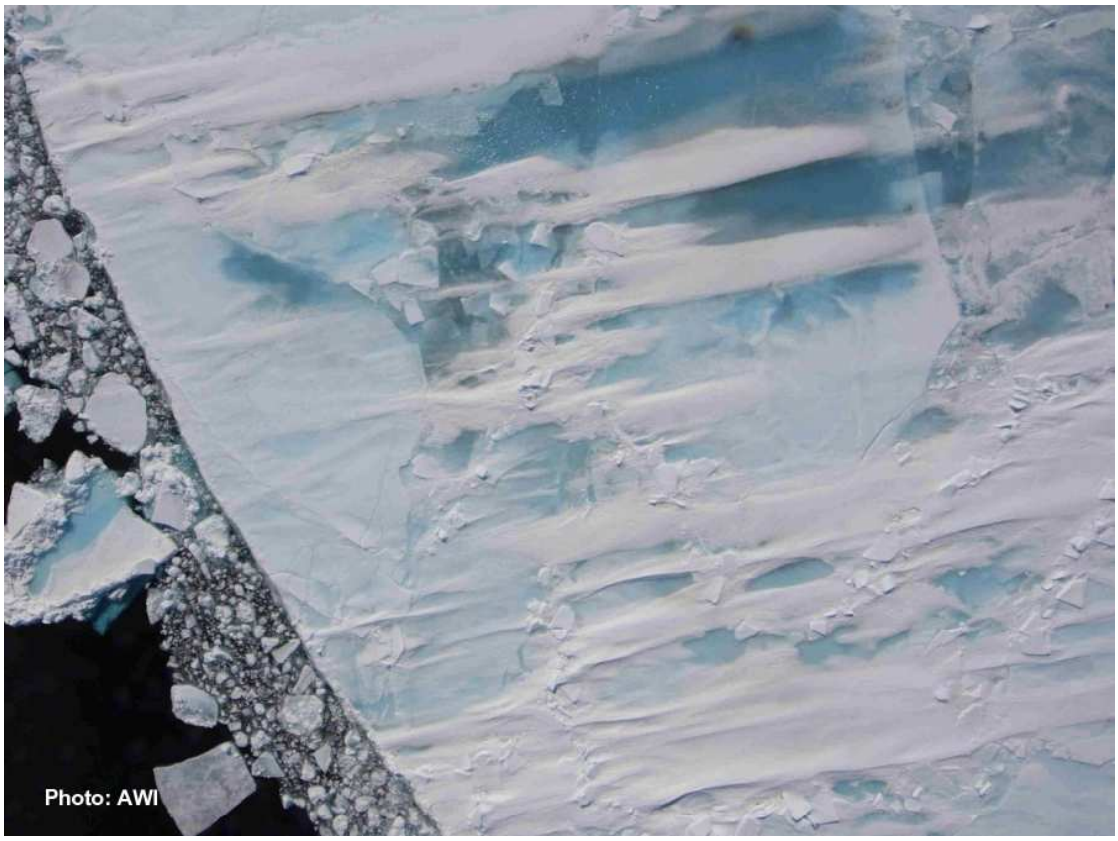

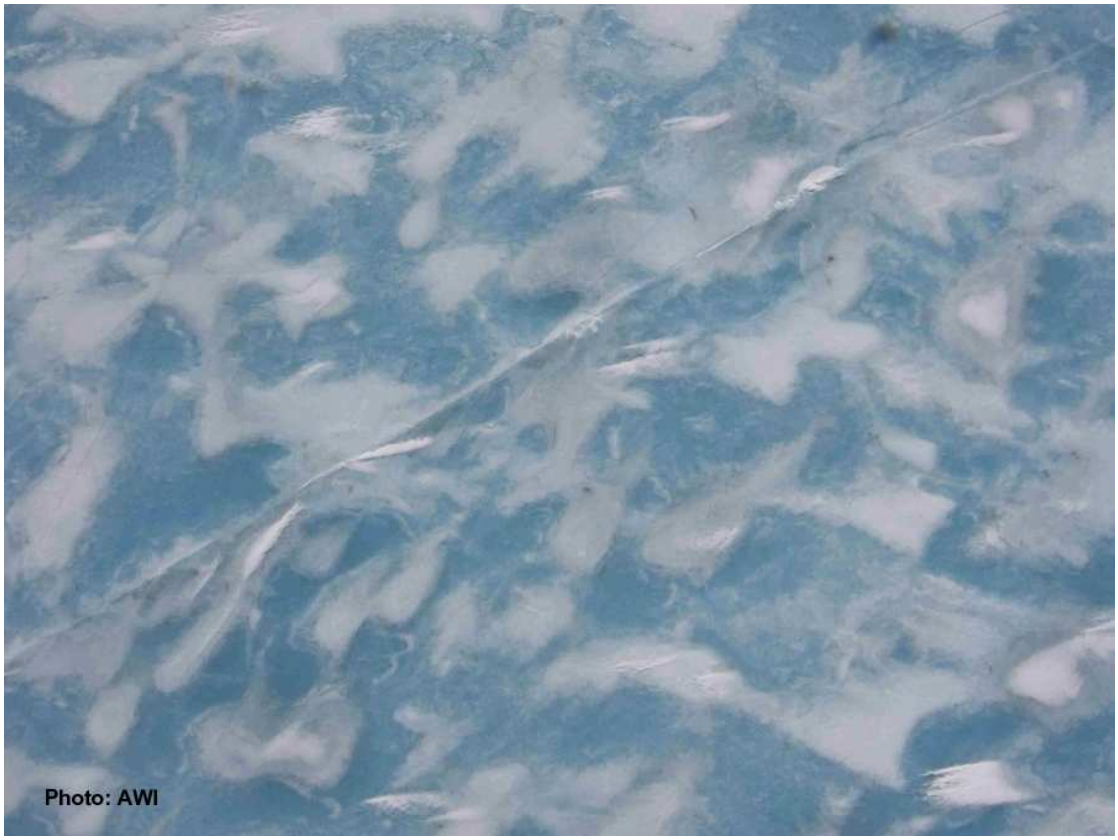

Figure 3.10: Melt ponds on sea ice overflown during the measurement mission on 04 June 2008 in the vicinity of ARGOS-buoy 28832 and west of it. Pictures were taken at an altitude of appr. 70 m and 75 m, respectively with a photo camera permanently mounted on POLAR 5.

4 Satellite Remote Sensing

4.1 Motivation of the Remote Sensing Study

For MELTEX it was important to gather information about the ice conditions. This was achieved during the measurement flights by using optical scanner systems, aerial photography, and hand-held photo cameras. Hence it was obvious to employ the collected data for the interpretation of satellite radar imagery acquired over the same sea ice region. Recently, new satellites were launched into space carrying radar systems: ALOS in January 2006 (with the Phased-Array type L-band Synthetic Aperture Radar, PALSAR), TerraSAR-X in October 2006, and Radarsat-2 in December 2007. Together with the Advanced Synthetic Aperture Radar (ASAR) of the ENVISAT, a hitherto unprecedented opportunity arose for collecting data at various image modes. Differences occur in radar frequency (ALOS: L-band, 1.27 GHz; TerraSAR-X: X-band, 9.65 GHz; Radarsat-2: C-band, 5.405 GHz, Envisat: C-band, 5.331GHz) and the availability of different imaging alternatives such as wide swath mode (covering a large area with low spatial resolution) and high-resolution mode (narrow imaging strip, fine spatial resolution), single- and multiple-polarization operation, and different radar incidence angle ranges. Since the appearance of sea ice in a radar image depends on the frequency, polarization, and incidence angle, ambiguities in the interpretation can be alleviated by combining the products of different satellite systems. In particular the high-resolution satellite modes make it easier to identify small or narrow ice structures that otherwise can only be observed during measurement flights and in airborne images.

4.2 Objectives of the Satellite Data Analysis

The following goals and questions were defined for the study of satellite images in combination with airborne data acquired during MELTEX:

- Comparison of different radar images: What are the effects of frequency, polarization, and incidence angle on the ice type discrimination and structure recognition? For data analysis, images are available from ENVISAT ASAR, ALOS PALSAR, TerraSAR-X, and Radarsat-2.
- Use of high-resolution radar images (<10m spatial resolution) for detailed studies in comparison to measurements from POLAR 5: are such satellite data an alternative to airborne SAR imaging? For our study, we received high-resolution images from TerraSAR-X (StripMap) and Radarsat-2 (FineQuadPol).
- What is the influence of melting conditions on ice type discrimination in radar images?

- How well can we determine the timing of melt onset using radar images?
- Is it possible to detect melt ponds in the high-resolution imagery?

Since the onset of strong melt occurred not before the last days of the MELTEX-campaign, it remains to be seen whether the available data are sufficient for a detailed study focusing on the last three items.

4.3 Ordering and Types of Satellite Data

Prior to the campaign, radar images of the satellite missions mentioned above were ordered for the measurement area between 72°N and 75°N and between 130°W and 140°W, using the multi-mission catalogue service EOLISA of the European Space Agency (ESA) for Envisat ASAR and ALOS PALSAR , EOWEB (Earth Observation on the Web) of the German Aerospace Center (DLR) for TerraSAR-X , and AUIG (ALOS User Interface Gateway) of the Japan Aerospace Exploration Agency (JAXA) for ALOS PALSAR. The Radarsat-2 images were ordered via MacDonald, Dettwiler and Associates Ltd. (MDA) Geospatial Services, Canada.
Data could be obtained as part of accepted proposals for data utilisation: ENVISAT and ALOS images through AOALO.3545 (ALOS Announcement of Opportunity, ESA and JAXA), TerraSAR-X images through OCE0078 (TerraSAR-X pre-launch announcement of opportunity) and Radarsat-2 through project 802 of the SOAR-program (Science and Operational Applications Research for Radarsat-2).

Since it is possible to select between different imaging modes of a radar system, as mentioned above, criterions are needed for possible imaging strategies. For MELTEX, the following criterions were used, in decreasing order of priority:

- distance between base airport in Inuvik and the sea ice area covered during satellite data acquisition,
- spatial and temporal overlap between different satellite systems, and
- coverage in north-south direction.

In the Polar Regions, field campaigns are relatively rare occasions for combining satellite imagery with complementary images or other data from airborne and/or ground-based sensors. Hence, a number of high resolution images that were within the flight distance of POLAR 5 were ordered prior to the campaign start for as many days within a two-weeks window as possible, taking into account the highly variable weather conditions in the Arctic during spring. In fact, geographical overlaps between flight tracks and satellite images with short time gaps of about one hour or less could be realized only three times during MELTEX (on 29 May, 3 June, 6 June, all with TerraSAR-X, in one case additionally with Radarsat-2). Overlaps between different satellite systems were chosen such that imaging modes were different. In such cases, the effect of, e.g., different frequencies and polarizations, incidence angles, and spatial resolutions on the appearance of the sea ice cover in a radar image can be studied directly. Time intervals between overlapping scenes are between a few minutes and several hours. In the latter case, changes of the sea ice cover

Date	Time	Satellite, Sensor	Mode
27 May 2008	161423	TerraSAR-X	Stripmap HH, VV
	161444	TerraSAR-X	Stripmap HH, VV
	161504	TerraSAR-X	Stripmap HH, VV
	201621	Envisat ASAR	Altern. Pol. HH, VV
	201642	Envisat ASAR	Altern. Pol. HH, VV
	201705	Envisat ASAR	Altern. Pol. HH, VV
28 May 2008	155713	TerraSAR-X	Stripmap HH, HV
	155733	TerraSAR-X	Stripmap HH, HV
	155753	TerraSAR-X	Stripmap HH, HV
	194439	Envisat ASAR	Altern. Pol. HH, VV
	194514	Envisat ASAR	Altern. Pol. HH, VV
29 May 2008	154001	TerraSAR-X	Stripmap VV, VH
	154021	TerraSAR-X	Stripmap VV, VH
	154041	TerraSAR-X	Stripmap VV, VH
	1530-1640	Polar 5	
30 May 2008	155942	Radarsat-2	Fine-Quad
	202157	Envisat ASAR	Wide Swath HH

Table 4.1: Received satellite images for MELTEX during May (status 15 January 2009).

due to ice drift and deformation have to be considered. The idea of acquiring images along a relatively large distance in north-south direction was to cover areas of different stages of melting, with higher temperatures closer to the coast.

Not all images that were ordered prior to MELTEX were finally acquired. This was due to conflicts with other studies focusing on the same region at the same time. In such cases we obtained images in other modes than what we ordered, or our area was not covered at all. This was valid for many ENVISAT and all ALOS scenes. However, all TerraSAR-X and Radarsat-2 images that were ordered for MELTEX were acquired and delivered.
In the months following the campaign, the image archives were checked in order to find out, whether imagery acquired for the other studies were usable for the MELTEX data analysis. This was the case in particular for ALOS but also for ENVISAT. In Tables 4.1 and 4.2, scenes are listed that were delivered already (status 15 January 2009). Details of the different imaging modes ordered for MELTEX are provided in Table 4.3. Additional images were or will be ordered (in particular ALOS ScanSAR mode images which cover a strip width of 250-350 km).

Date	Time	Satellite, Sensor	Mode
01 June 2008	053957	Envisat ASAR	Glob. Monitoring
	054529	Envisat ASAR	Altern. Pol. HH, VV
	054550	Envisat ASAR	Altern. Pol. HH, VV
	062358	ALOS PALSAR	Polarimetry
	062406	ALOS PALSAR	Polarimetry
	062414	ALOS PALSAR	Polarimetry
	062422	ALOS PALSAR	Polarimetry
	162320	TerraSAR-X	Stripmap HH, VV
	162339	TerraSAR-X	Stripmap HH, VV
	192024	Envisat ASAR	Altern. Pol. HH, VV
02 June 2008	160609	TerraSAR-X	Stripmap HH, HV
	160629	TerraSAR-X	Stripmap HH, HV
	202740	Envisat ASAR	Wide Swath HH
	1900-2130	POLAR 5	
03 June 2008	154243	Radarsat-2	Fine-Quad
	155245	Radarsat-2	Fine-Quad
	154858	TerraSAR-X	Stripmap VV, VH
	154918	TerraSAR-X	Stripmap VV, VH
	1550-1615	Polar 5	
04 June 2008	064722	ALOS PALSAR	Fine Resolution HH
	064730	ALOS PALSAR	Fine Resolution HH
	064739	ALOS PALSAR	Fine Resolution HH
	064755	ALOS PALSAR	Fine Resolution HH
	064803	ALOS PALSAR	Fine Resolution HH
	064828	ALOS PALSAR	Fine Resolution HH
	153205	TerraSAR-X	Stripmap HH, HV
	192449	Envisat ASAR	Altern. Pol. HH, VV
	192509	Envisat ASAR	Altern. Pol. HH, VV
	192608	Envisat ASAR	Altern. Pol. HH, VV
	2200-2315	POLAR 5	
05 June 2008	203324	Envisat ASAR	Wide Swath HH
07 June 2008	161503	TerraSAR-X	Stripmap VV, VH
	1720-1750	POLAR 5	

Table 4.2: Received satellite images for MELTEX during June (status 15 January 2009).

Imaging Mode	Properties
TerraSAR-X Stripmap, Dual-Polarization	swath width 15 km, pixel spacing 3 m polarization VV+VH or HH+HV or VV+HH incidence angles in the interval 25 - 45 deg across-track angle change in a given scene: 1 - 1.5 deg effective number of looks: 1.2-1.8 effective spatial resolution 6.6-7.7 m
Envisat ASAR Global Monitoring	swath width 400 km, pixel spacing 500 m polarization HH or VV incidence angle variation across-track: 19-43 deg effective number of looks: 7-9 effective spatial resolution: 1 km noise equivalent sigma zero: -31.5 dB to -35 dB
Envisat ASAR Wide Swath Medium Resolution	swath width 400 km, pixel spacing 75 m polarization HH or VV incidence angle variation across-track: 19-43 deg effective number of looks: 11.5 effective spatial resolution: 150 m noise equivalent sigma zero: -20.8 dB to -26.2 dB
Envisat ASAR Image mode Alternating Polarization Precision Image	swath width 56-105 km, pixel spacing 12.5 m polarization VV+VH or HH+HV or VV+HH incidence angles in the interval 15 - 45 deg across-track angle change in a given scene: 3 - 8 deg effective number of looks: > 1.8 effective spatial resolution: 30 m noise equivalent sigma zero: -19.4 dB to -22 dB
ALOS PALSAR Fine Resolution Single-Polarization	swath width 40-70 km spatial resolution 7-44 m (ra) polarization HH or VV incidence angles in the interval 8 - 60 deg noise equivalent sigma zero: -23 dB to -25 dB
ALOS PALSAR Polarimetric Mode	swath width 20-65 km spatial resolution 20-89m (ra), 30m at 24deg polarization VV+VH+HH+HV incidence angles in the interval 8 - 30 deg noise equivalent sigma zero: -19 dB
Radarsat-2 Fine-Quad-Polarization	swath width 25 km, pixel spacing 4.7m (ra) x 5.1m (az) (SLC) polarization VV+VH+HH+HV incidence angles in the interval 20 - 41 deg effective number of looks: 1

Table 4.3: Image mode properties (details provided by the space agencies). SLC=single-look complex, az=azimuth, ra=range

On the basis of images that we have archived already (status 15 January 2009), there are a number of occasions for which the combination of different data is possible (see also Figs. 4.1 - 4.8). Of large interest are satellite data acquisitions almost in parallel to our measurement flights:

- 29 May - overlap between TerraSAR-X and POLAR 5 flight, less than one hour time difference.
- 3 June - overlap between TerraSAR-X and Radarsat-2 (acquisitions at an interval of five minutes) and between both satellites and POLAR 5 (up to half an hour time difference).
- 7 June - overlap between TerraSAR-X and POLAR 5 (time difference less than hundred minutes).

The following data sets are useful to investigate differences between X-and C-band and between high, moderate and coarse spatial resolution:

- 27 May - overlap between TerraSAR-X and ENVISAT images, 4 hours difference.
- 28 May - same situation as on 27 May (spatial gaps between ENVISAT and TerraSAR-X scenes can be closed by ordering the corresponding archived data).
- 30 May - overlap between a Radarsat-2 high-resolution and an ENVISAT low resolution image, 4.5hours difference.
- 2 June - TerraSAR-Xscenes in a wide-swath image of ENVISAT with a time difference of 4.5 hours. POLAR 5 did not enter this region. However, from archived data, images covering the POLAR 5 track may be available.

A comparison between ALOS and ENVISAT is possible with data from the following two days:

- 1 June - A small area is covered by ENVISAT (ASAR image mode) and ALOS (PALSAR polarimetric mode) with a time gap of about 13 hours. This area and additional ALOS scenes are covered by an ENVISAT overpass in global monitoring mode (one hour earlier than the ALOS images).
- 4 June - a similar situation as on 1 June (combination of ALOS and ENVISAT data over a small area) and the possibility to combine POLAR 5 data with ALOS images (by ordering additional ALOS scenes) with, however, a time difference of 8 to 9 hours.

By ordering more satellite data from the archives, in particular from ALOS, further combinations of L-band with C- and X-band may be available for detailed studies.

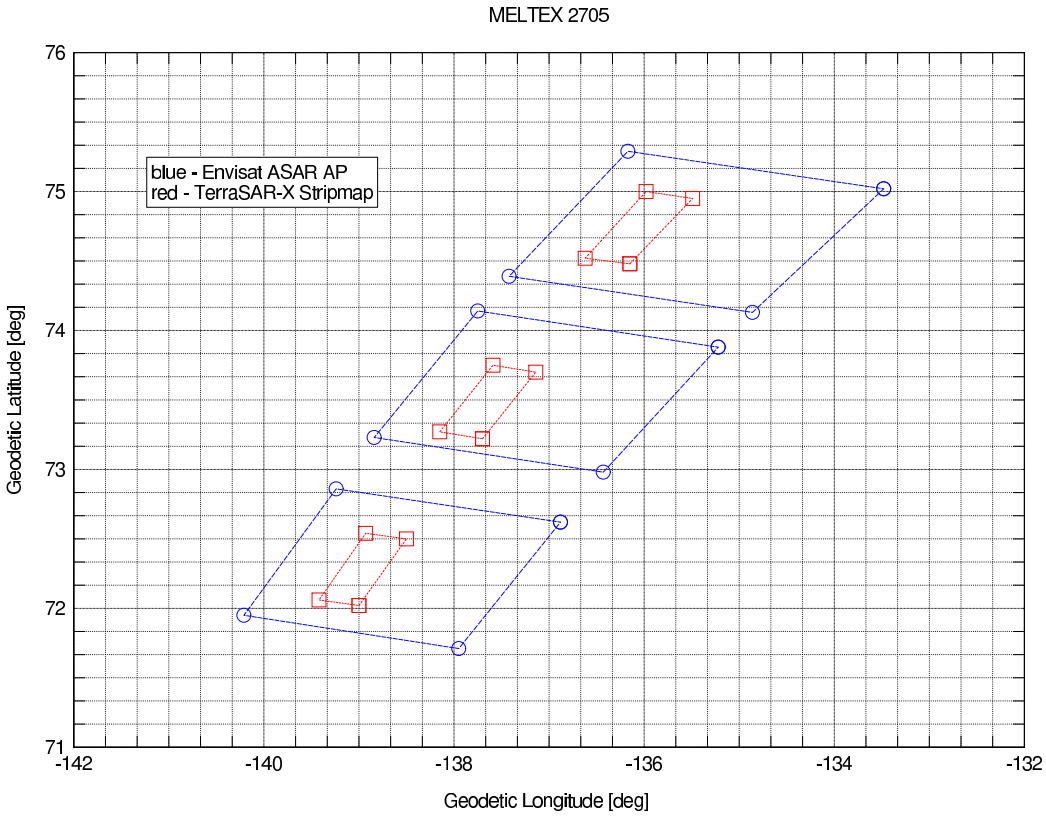

Figure 4.1: Satellite image coverage for 27 May.

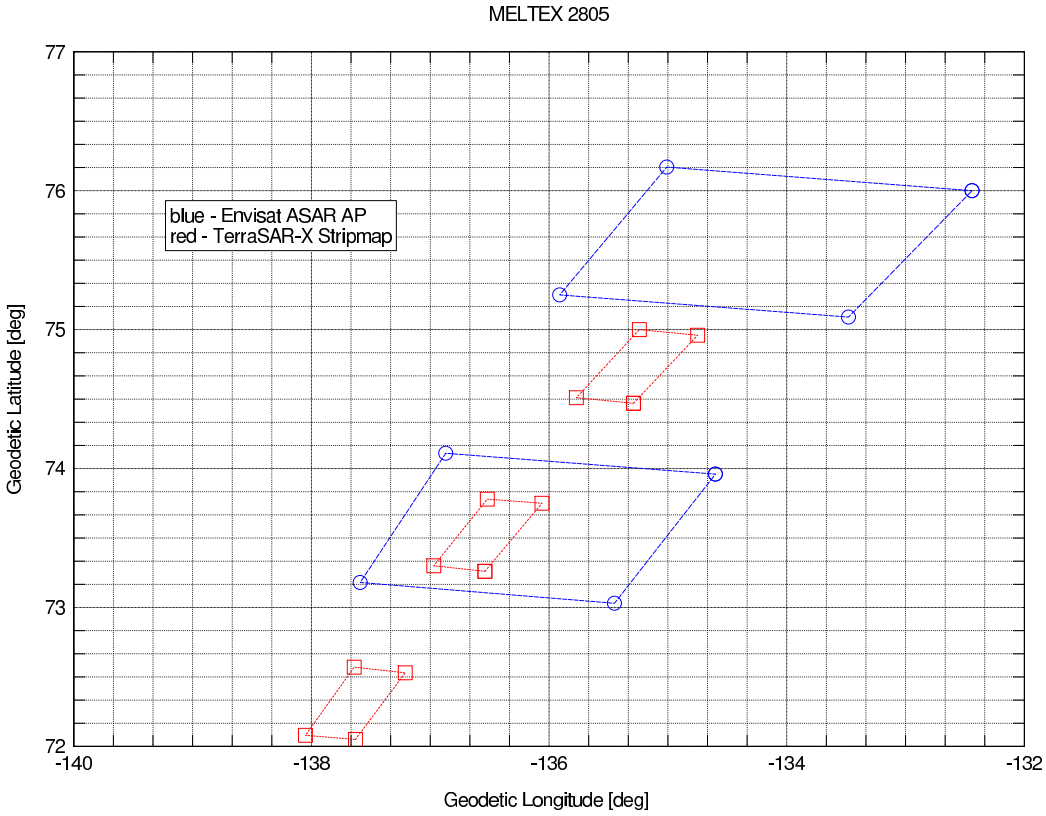

Figure 4.2: Satellite image coverage for 28 May.

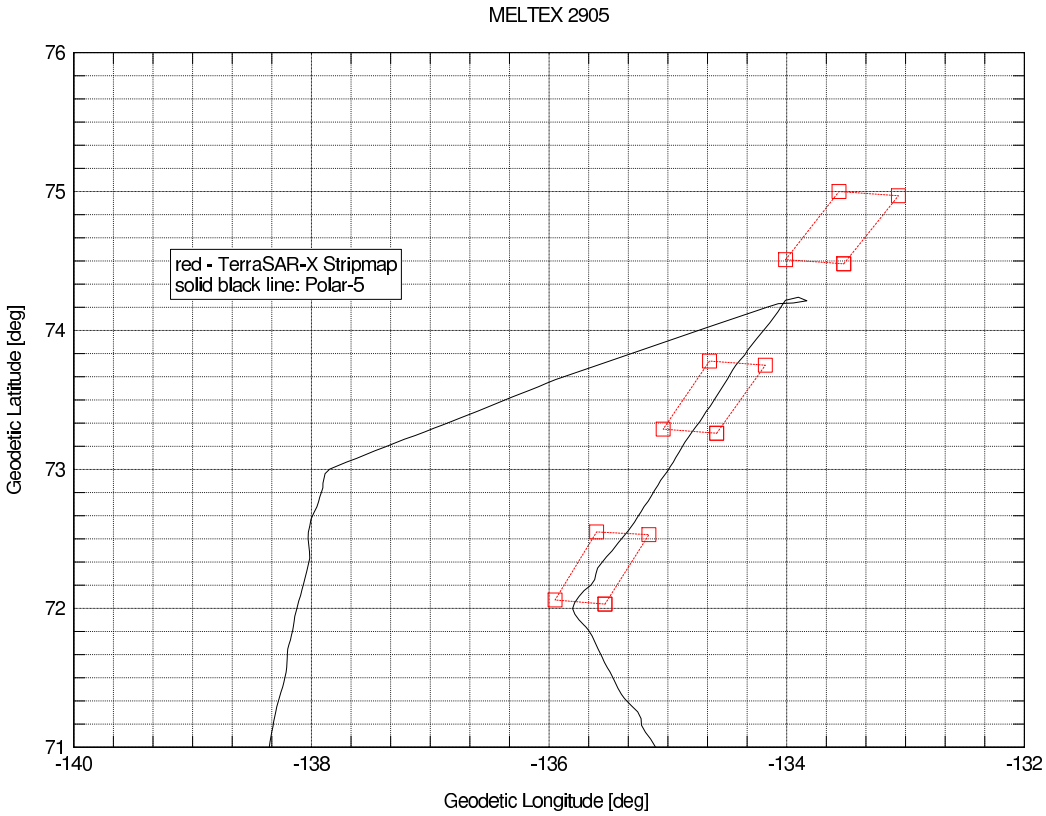

Figure 4.3: Satellite image coverage and flight track of POLAR 5 for 29 May.

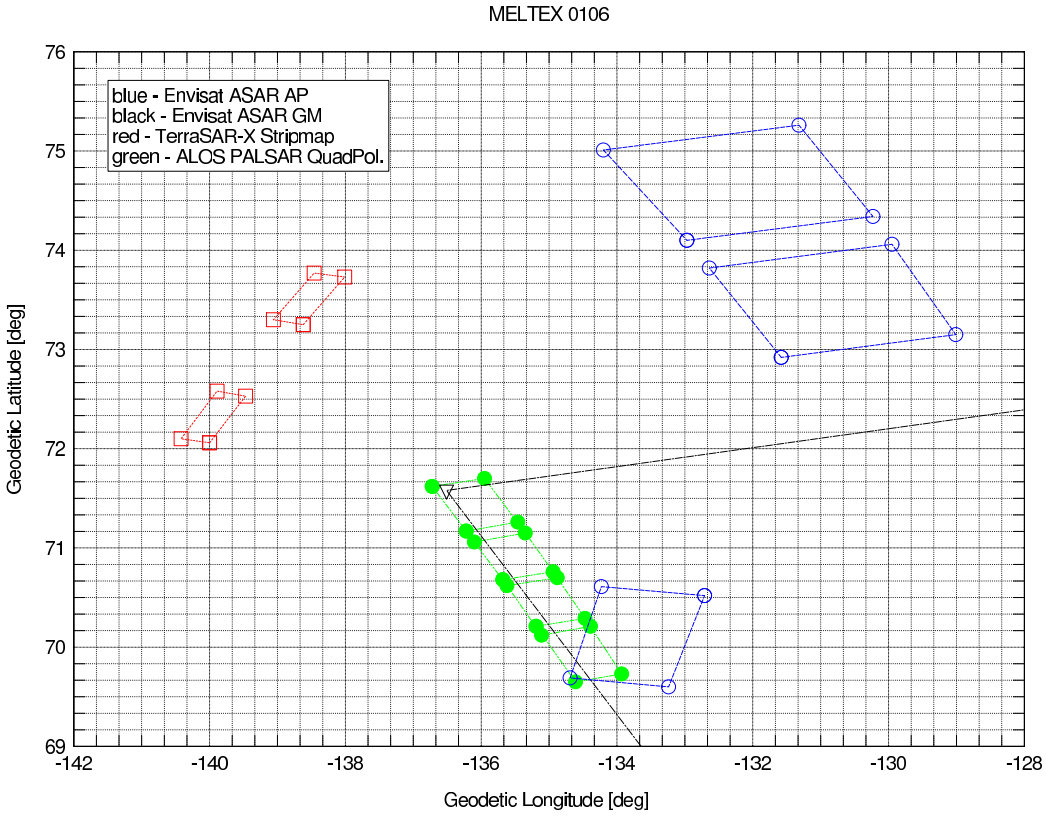

Figure 4.4: Satellite image coverage for 1 June.

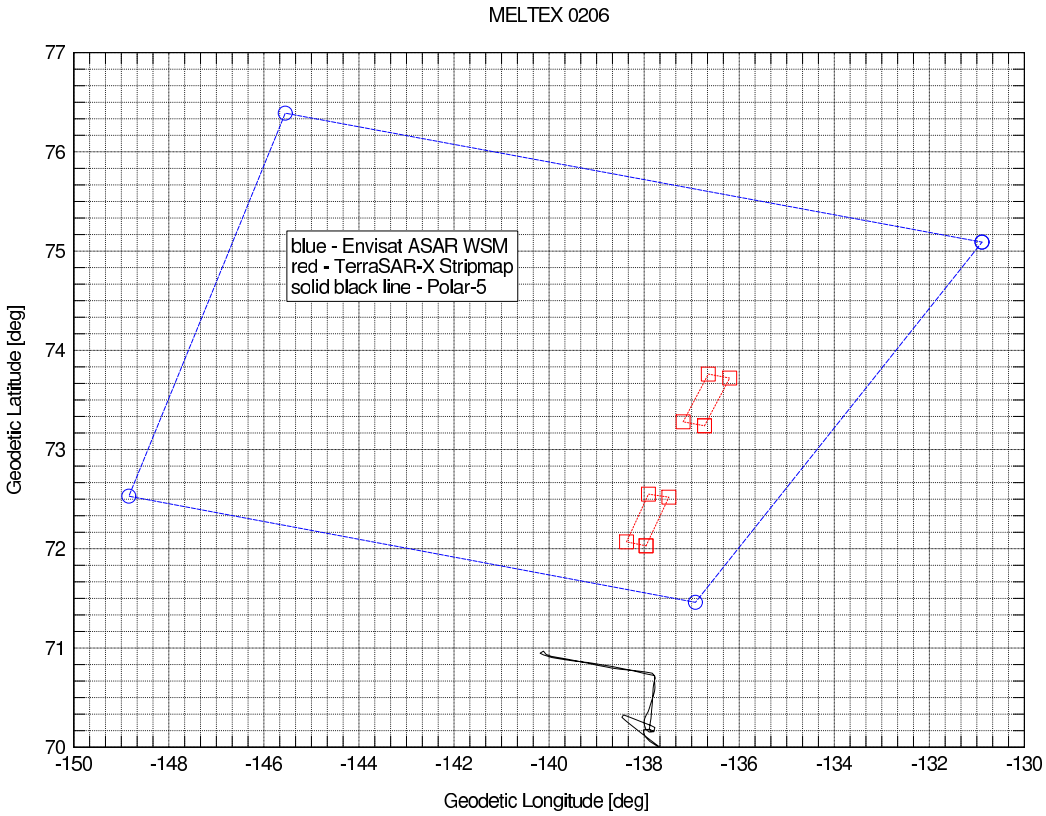

Figure 4.5: Satellite image coverage and flight track of POLAR 5 for 2 June.

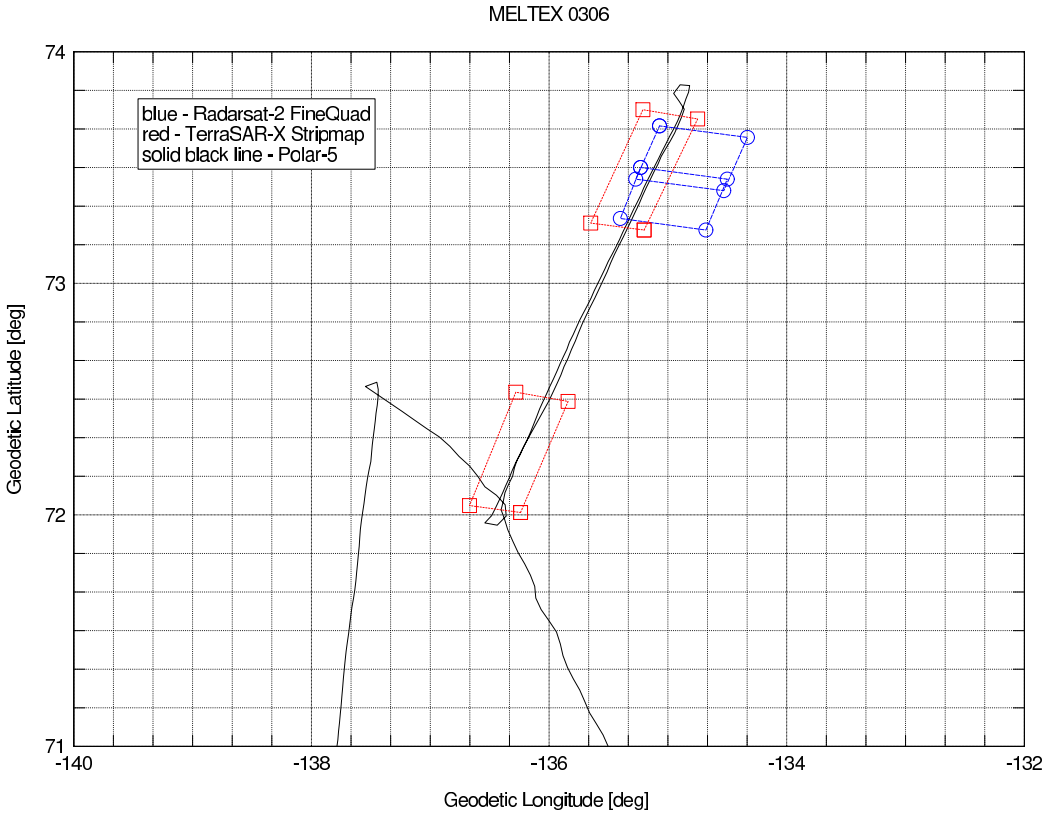

Figure 4.6: Satellite image coverage and flight track of POLAR 5 for 3 June.

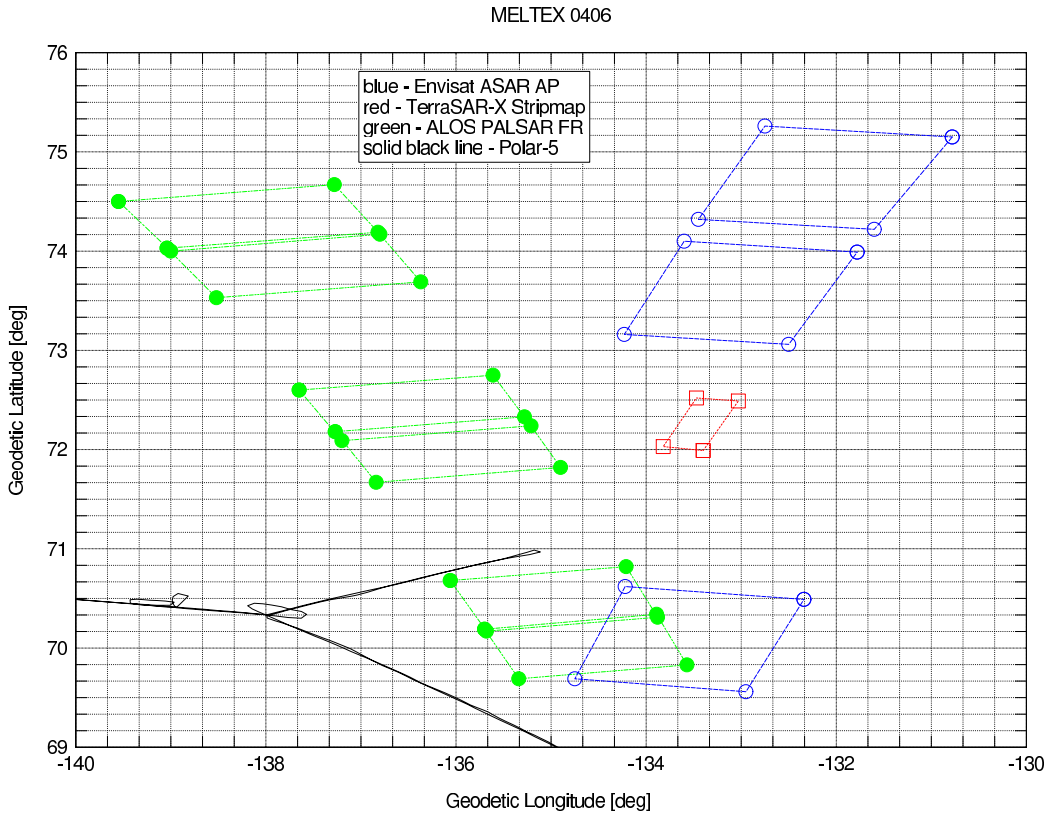

Figure 4.7: Satellite image coverage and flight track of POLAR 5 for 4 June. The swath of the ENVISAT ASAR was switched from IS7 to IS6 at the lowermost frame.

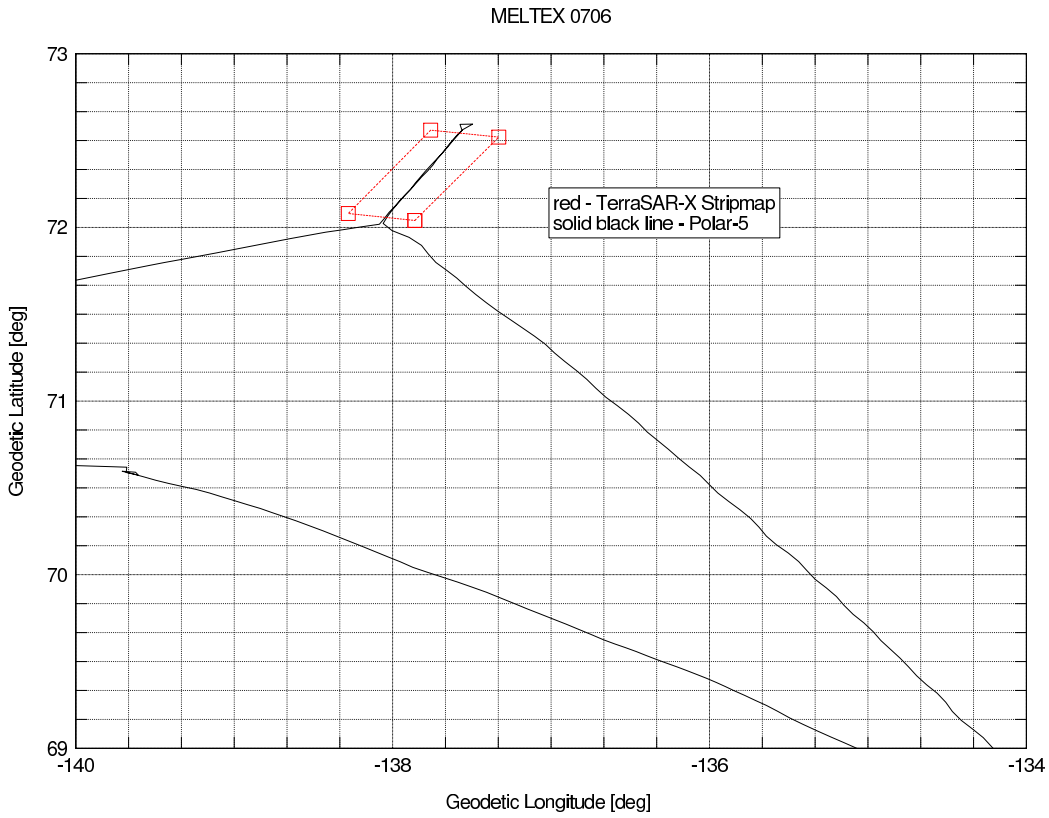

Figure 4.8: Satellite image coverage and flight track of POLAR 5 for 7 June.

4.4 Examples of Satellite Images

In this section, a few examples of images are shown and discussed. The examples are not absolutely calibrated, and the color stretch was carried out separately for each image according to the standard setting of the ENVI software package, which was utilized for image preparation. Except the Radarsat-2 images, which are in slant-range format, all imagery is inground-range, i. e. corresponds to the nadir view from the airplane. The aerial photos and scanner data acquired from POLAR 5 were not available at the time when this report was written.

The first example (Fig. 4.9) is from May 27 and shows ENVISAT ASAR data acquired at Alternating-Polarization (AP) mode with a pixel size of 12.5 m in comparison to TerraSAR-X Stripmap data with a pixel spacing of three meters (see also Table 4.3 for details of the respective image products). In both cases, dual-polarization data are available (HH- and VV). The incidence angle range is 26-31.4° for the ENVISAT image, and 31-32.3° for the TerraSAR-X scene. The appearance of the sea ice cover is very similar in both images, indicating that the radar signature does not change significantly when changing from C- to X-band.

In Fig. 4.10, TerraSAR-X Stripmap images are depicted which were taken on 27 May at air temperatures below freezing point and on 7 June at a stage of significant melting (see Fig. 4.11). It seems that the ice structure is less visible in the later scene which is a consequence of the moist snow cover by which the penetration depth of the radar signal is significantly reduced compared to the dry snow case. The bright areas in the TerraSAR-X scene from 7 June, indicated by the letter "A", are presumably from rougher sea ice such as shown on the photo marked by "A" in Fig. 4.11. This, however, has still to be checked with the airborne scanner data and aerial photography.

The next example are two wide swath images from the ENVISAT ASAR which cover an area of 400 km x 400 km (Fig. 4.12). The first one was acquired on 2 June, the second on 5 June. It is obvious that structures of the ice cover clearly visible in the former are much more difficult to identify in the latter. This can be attributed to a larger snow wetness which "hides" the rougher ice surface so that the backscattered radar signal intensity is lower. Also QuikSCAT data reveal a drop of the radar intensity between 4 June and 6 June (Fig. 4.13).

In the last example, two Radarsat-2 images overlap with a TerraSAR-X strip (Fig. 4.14). Note that the Radarsat-2 images are still in slant-range format. In ground-range projection, the corresponding image width is 15 km. Again, it is noted that the radar signature difference between C- and X-band is only small. The corresponding ice situation as observed during a POLAR 5 flight is shown in Fig. 4.15.

Many details can be recognized in the high-resolution radar images in Fig. 4.14, hence they are an acceptable substitute for airborne radar imagery in field studies. The major disadvantage is that their acquisition is fixed to a certain area at a certain time, the advantage is the difference of the incidence angle between near- and far range edge of the image, which is much smaller than in the airborne case. In comparison to optical data, radar images show ice structures hidden under the snow, provided that the snow is dry.

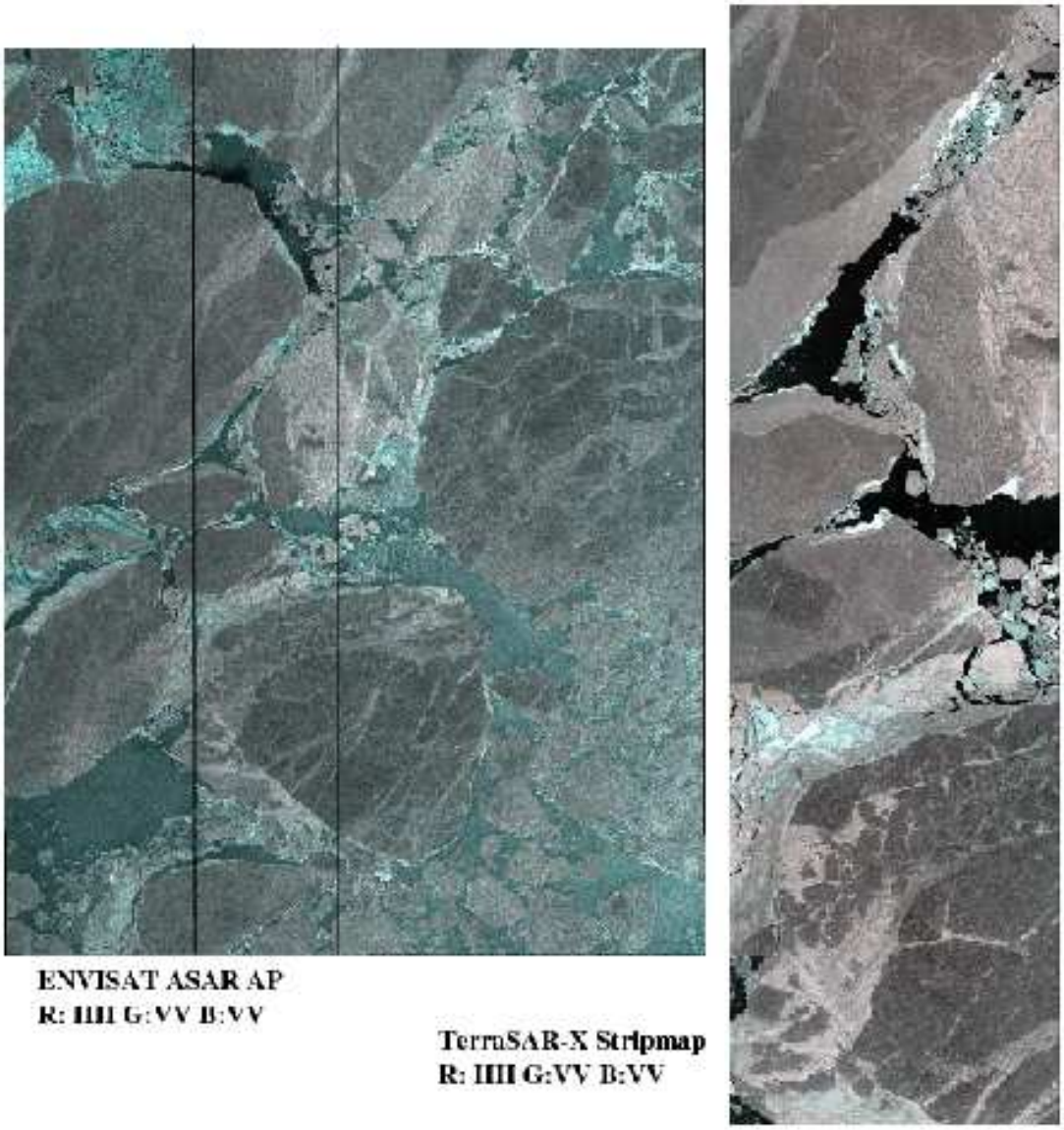

Figure 4.9: ENVISAT ASAR (left) and TerraSAR-X (right panel) images acquired on 27 May over the Beaufort Sea. In Fig. 4.1, their geographical position is indicated by the southernmost pair of frames. The two black lines in the ENVISAT image indicate the left and right border of the TerraSAR-X strip. The time difference between the images is four hours.

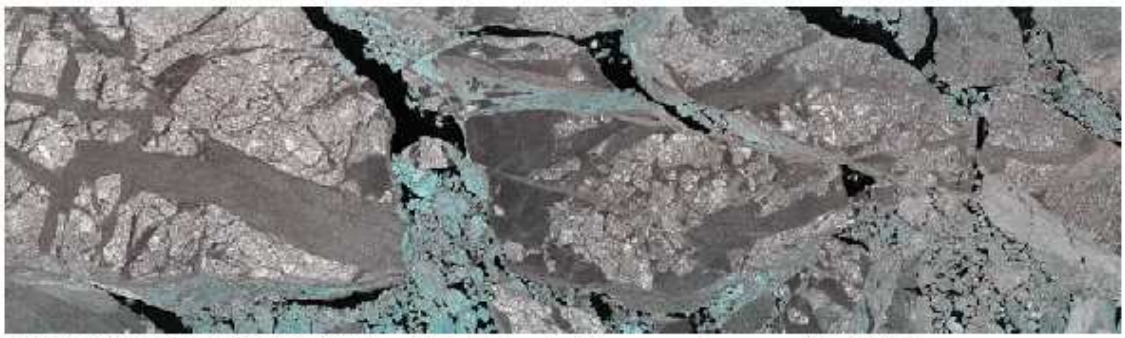

27-05-2008, R:HH G:VV B:VV, width 15 km, incidence angle range 31-32.3 deg

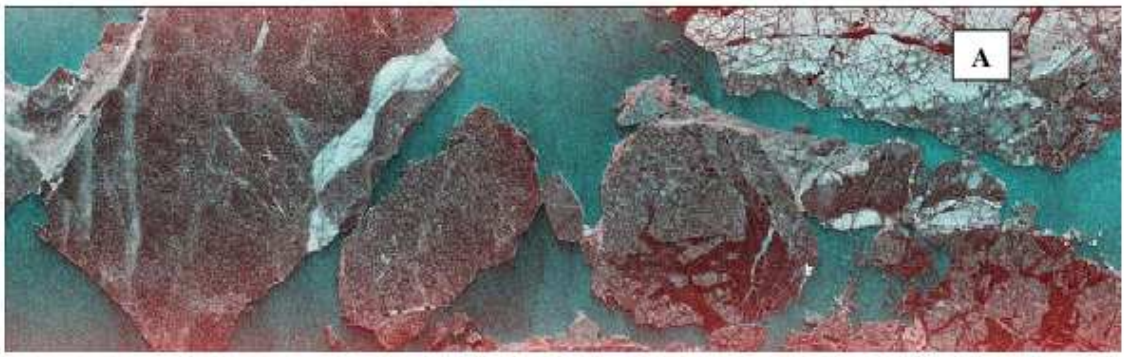

07-06-2008, R:VH G:VV B:VV, width 15 km, incidence angle range 27.5-29 deg

Figure 4.10: Two TerraSAR-X scenes from the beginning and the end of the two-weeks period for combined satellite-airborne data acquistions during MELTEX.

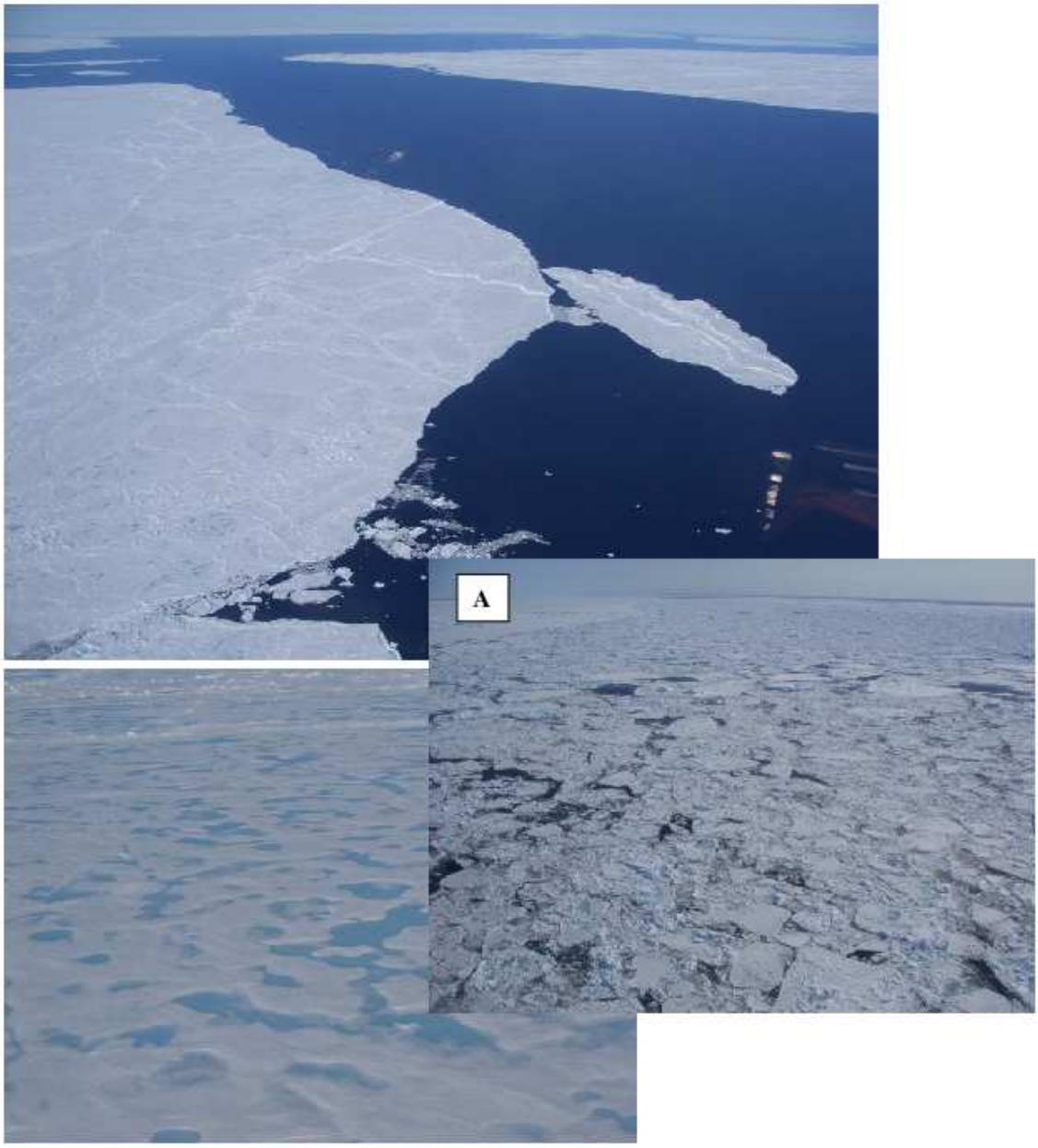

Figure 4.11: Airborne hand-held photography from 7 June. The uppermost photo was taken from an altitude of 1000 m, the two other ones from 30-50 m height.

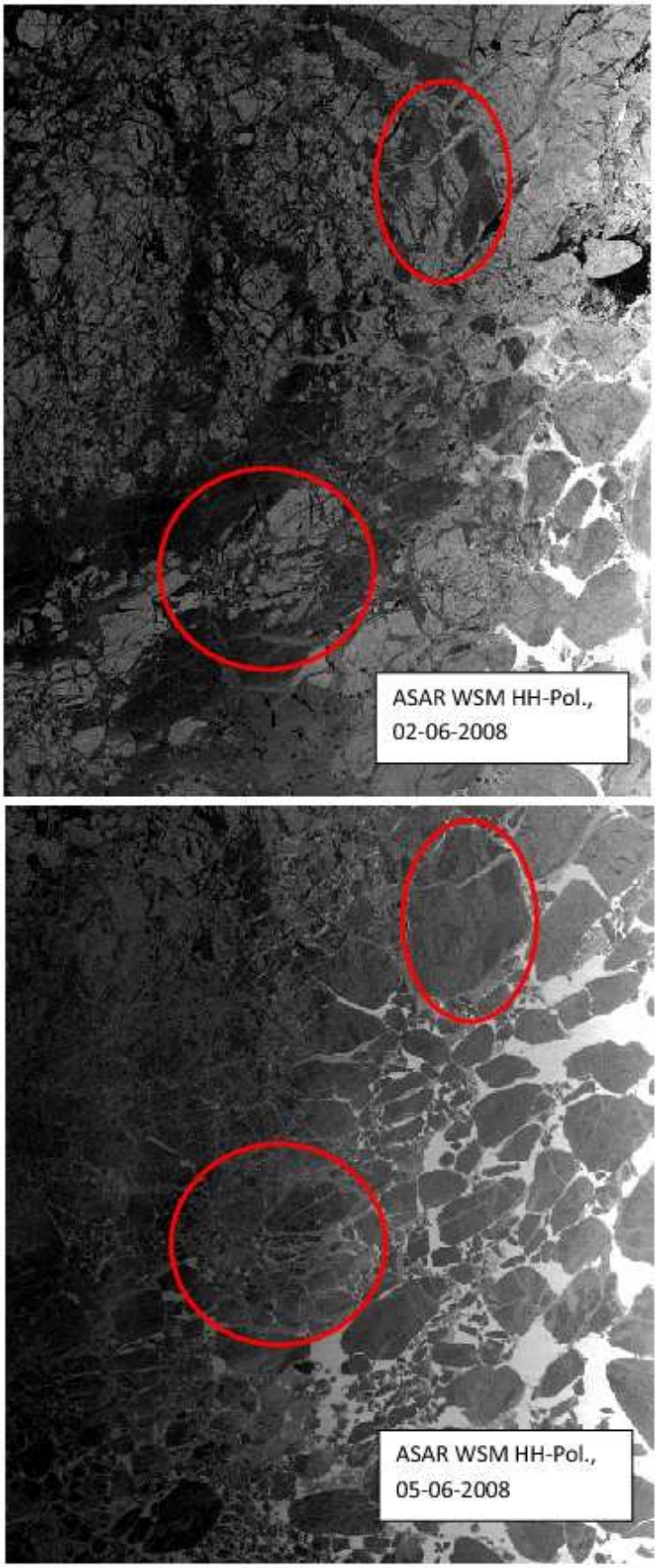

Figure 4.12: ENVISAT ASAR wide swath mode images acquired prior and during melting conditions. The red ellipses indicate particular areas for comparison.

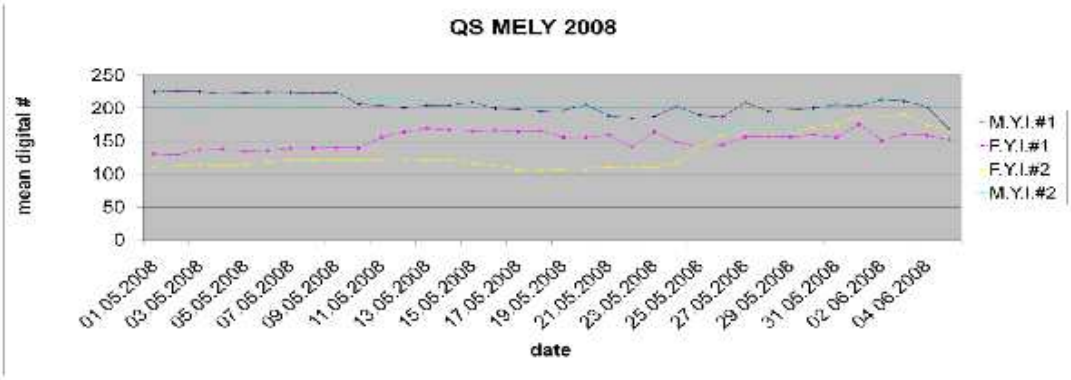

Figure 4.13: Radar intensity from QuikSCAT data as a function of time at four different locations. A significant decrease can be observed at position M.Y.I1 between 4 June and 6 June. This figure was kindly provided by the Canadian Ice Service.

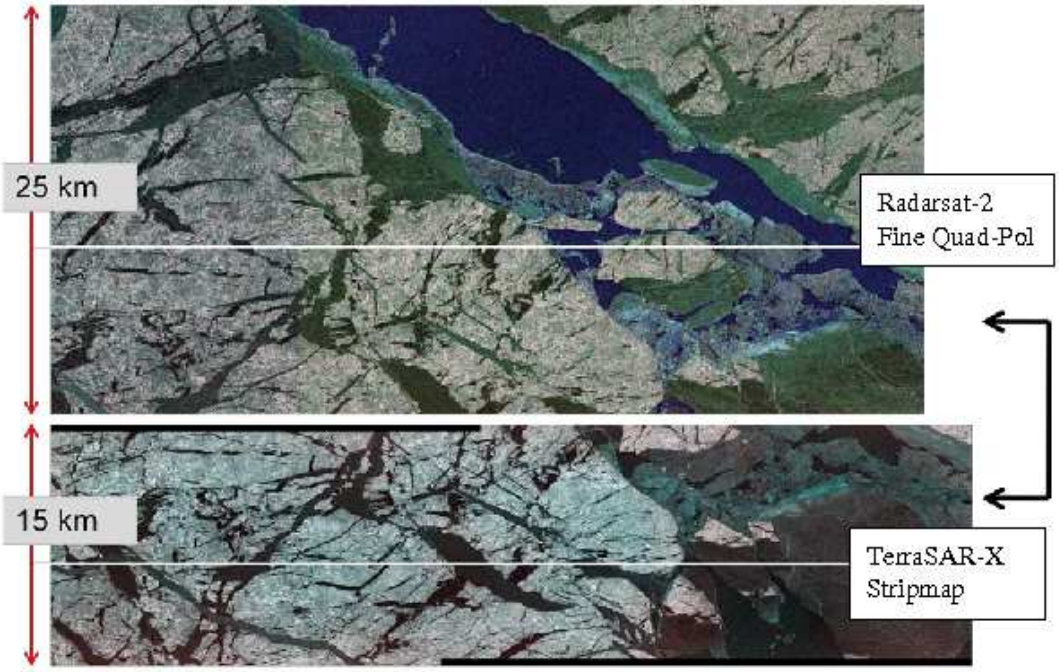

Figure 4.14: TerraSAR-X image (below) and a Radarsat-2 strip composed of two scenes (above), acquired on 3 June. The color layer scheme is R-VH G-VV B-VV for the TerraSAR-X scene and R-HV G-HH B-VV for the Radarsat-2 scene. The area in common is indicated by the arrow on the right side.

Figure 4.15: Ice situation in the area covered by the satellite images shown in Fig. 4.14. The photo was taken from POLAR 5 at an altitude of 1000 m.

4.5 Conclusions and Outlook

During a two-weeks interval of the MELTEX campaign, data were acquired from various satellite radar systems (ENVISAT, ALOS, Radarsat-2, TerraSAR-X) over sea ice in the Beaufort Sea. Single legs of flights with POLAR 5 were carried out over areas covered by satellite imagery. From the airplane, optical scanner data and aerial and hand-held photos were taken which will be used in the analysis of radar images. For ENVISAT and ALOS, many scenes that were ordered prior to the MELTEX campaign were not acquired due to demands from other working groups focusing on research in the Beaufort Sea at the same time. However, a number of images acquired for other groups are available from the ESA and JAXA archives that are useful for MELTEX.

The status of the MELTEX remote sensing part is as follows:

- Spatial overlaps between images of TerraSAR-X and Radarsat-2 and almost simultaneous aircraft flights with only small time differences could be carried out on three days during the campaign.
- Between different satellites, the time gap was in general much larger (a few to several hours) because of orbit configurations and timing.
- Melting conditions occurred mainly towards the end of the two-weeks period. ENVISAT ASAR wide swath mode images from two days in June show significant

changes in the radar signature indicating the onset of melt.

- The high-resolution satellite images can be used as an acceptable substitute for airborne radar images, considering specific pros and cons (discussed above).

During the next months, it will be investigated how the sensor configuration affects the separation of sea ice types in radar images. Changes of the radar signatures during the onset of melt will be studied. Another item of interest is the identification of melt ponds in high-resolution radar imagery. Radar signatures will also be compared to the measured albedo data.

References

Curry, J.A., J.L. Schramm, D.K. Perovich and J.O. Pinto (2001), Application of SHEBA/FIRE data to evaluation of snow/ice albedo parameterizations, J. Geophys. Res., 106(D14), 15345-15355.

Ehrlich, A., E. Bierwirth, M. Wendisch, J.-F. Gayet, G. Mioche, A. Lampert and J. Heintzenberg (2008), Cloud phase identification of arctic boundary-layer clouds from airborne spectral reflection measurements: Test of three approaches, Atmos. Chem. Phys., 8, 7493-7505.

Eicken, H., T.C. Grenfell, D.K. Perovich, J.A. Richter-Menge and K. Frey (2004), Hydraulic controls of summer Arctic pack ice albedo, J. Geophys. Res., 109, C08007, doi:10.1029/2003JC001989.

Fetterer, F. and N. Untersteiner (1998), Observations of melt ponds on Arctic sea ice, J. Geophys. Res., 103(C11), 24821-24835.

IPCC, 2007: Climate Change 2007: The Physical Science Basis. Contribution of Working Group I to the Fourth Assessment Report of the Intergovernmental Panel on Climate Change [Solomon, S., D. Qin, M. Manning, Z. Chen, M. Marquis, K.B. Averyt, M. Tignor and H.L. Miller (eds.)]. Cambridge University Press, Cambridge, United Kingdom and New York, NY, USA, 996 pp.

Køltzow, M. (2007), The effect of a new snow and sea ice albedo scheme on regional climate model simulations, J. Geophys. Res., 112, D07110, doi: 10.1029/2006JD007693.

McElroy, C.T. (1995), A spectroradiometer for the measurement of direct and scattered solar irradiance from on-board the NASA ER-2 high-altitude research aircraft, Geophys. Res. Lett., 22(11), 1361-1364.

Perovich, D.K., C.S. Roesler and W.S. Pegau (1998), Variability in Arctic sea ice optical properties, J. Geophys. Res., 103(C1), 1193-1208.

Rinke, A., K. Dethloff, J. Cassano, J.H. Christensen, J.A. Curry, J.E. Haugen, D. Jacob, C. Jones, M. Køltzow, A.H. Lynch, S. Pfeifer, M.C. Serreze, M.J. Shaw, M. Tjernström, K. Wyser, M. Zagar (2006): Evaluation of an ensemble of Arctic regional climate models: Spatiotemporal fields during the SHEBA year, Climate dynamics, 26, 459-472, doi:10.1007/s00382-005-0095-3.

Tjernström, M., M. Zagar, G. Svensson, J. Cassano, S. Pfeifer, A. Rinke, K. Wyser, K. Dethloff, C. Jones, T. Semmler, M. Shaw (2005): Modelling the arctic boundary layer: An evaluation of six arcmip regional-scale models using data from the Sheba project, Boundary-Layer Meteorol.,117(2), 337-381.

Tschudi, M.A., J.A. Curry and J.A. Maslanik (2001), Airborne observations of summertime surface features and their effect on surface albedo during FIRE/SHEBA, J. Geophys. Res., 106(D14), 15335-15344.

Uttal, T. and co-authors (2002), Surface energy budget of the Arctic ocean, Bull. Am. Meteorol. Soc., 83, 255-275.

Acknowledgements

Our special thanks go to the aircraft crew. We thank the pilots, J. Janssen and A. Jenkins, for their very careful operations, and we thank the mechanic, D. Woudsma, for his creative solution of technical problems and his help in repairing measurement instruments.

We thank Dr. C. Th. McElroy, the responsible scientist for the CPFM-pod, for the fruitful cooperation during the campaign.

Furthermore, we acknowledge the support and the availability of facilities of the Aurora Research Institute in Inuvik and of the High Arctic Weather Station in Eureka, Canada.

Our thanks go also to Dr. W. Strapp and further scientists of Environment Canada for their great help in preparing the campaign MELTEX.

We thank the Canadian Weather and Ice Service for providing us with useful operational forecasts for the Canadian Arctic.

The opportunity to obtain satellite images through projects AOALO.3545 (ESA and JAXA), OCE0078 (TerraSAR-X) SOAR project 802 (Radarsat-2) is gratefully acknowledged too.

The campaign MELTEX was a contribution to EU project DAMOCLES and to the International Polar Year 2007/2008.

Die "Berichte zur Polar- und Meeresforschung" (ISSN 1866-3192) werden beginnend mit dem Heft Nr. 569 (2008) ausschließlich elektronisch als Open-Access-Publikation herausgegeben. Ein Verzeichnis aller Hefte einschließlich der Druckausgaben (Heft 377-568) sowie der früheren **"Berichte zur Polarforschung** (Heft 1-376, von 1982 bis 2000) befindet sich im Internet in der Ablage des electronic Information Center des AWI (**ePIC**) unter der URL http://epic.awi.de. Durch Auswahl "Reports on Polar- and Marine Research" auf der rechten Seite des Fensters wird eine Liste der Publikationen in alphabetischer Reihenfolge (nach Autoren) innerhalb der absteigenden chronologischen Reihenfolge der Jahrgänge erzeugt.

To generate a list of all Reports past issues, use the following URL: http://epic.awi.de and select the right frame to browse "Reports on Polar and Marine Research". A chronological list in declining order, author names alphabetical, will be produced, and pdf-icons shown for open access download.

Verzeichnis der zuletzt erschienenen Hefte:

Heft-Nr. 580/2008 — "The Expedition ANTARKTIS-XXIII/6 of the Research Vessel 'Polarstern' in 2006", edited by Ulrich Bathmann

Heft-Nr. 581/2008 — "The Expedition of the Research Vessel 'Polarstern' to the Antarctic in 2003 (ANT-XX/3)", edited by Otto Schrems

Heft-Nr. 582/2008 — "Automated passive acoustic detection, localization and identification of leopard seals: from hydro-acoustic technology to leopard seal ecology", by Holger Klinck

Heft-Nr. 583/2008 — "The Expedition of the Research Vessel 'Polarstern' to the Antarctic in 2007 (ANT-XXIII/9)", edited by Hans-Wolfgang Hubberten

Heft-Nr. 584/2008 — "Russian-German Cooperation SYSTEM LAPTEV SEA: The Expedition Lena - New Siberian Islands 2007 during the International Polar Year 2007/2008", edited by Julia Boike, Dmitry Yu. Bolshiyanov, Lutz Schirrmeister and Sebastian Wetterich

Heft-Nr. 585/2009 — "Population dynamics of the surf clams *Donax hanleyanus* and *Mesodesma mactroides* from open-Atlantic beaches off Argentina", by Marko Herrmann

Heft-Nr. 586/2009 — "The Expedition of the Research Vessel 'Polarstern' to the Antarctic in 2006 (ANT-XXIII/7)", edited by Peter Lemke

Heft-Nr. 587/2009 — "The Expedition of the Research Vessel 'Maria S. Merian' to the Davis Strait and Baffin Bay in 2008 (MSM09/3), edited by Karsten Gohl, Bernd Schreckenberger, and Thomas Funck

Heft-Nr. 588/2009 — "Selected Contributions on Results of Climate Research in East Germany (the former GDR)", edited by Peter Hupfer and Klaus Dethloff

Heft-Nr. 589/2009 — "The Expedition of the Research Vessel 'Polarstern' to the Arctic in 2008 (ARK-XXIII/1)", edited by Gereon Budéus

Heft-Nr. 590/2009 — "The Expedition of the Research Vessel 'Polarstern' to the Arctic in 2008 (ARK-XXIII/2)", edited by Gerhard Kattner

Heft-Nr. 591/2009 — "The Expedition of the Research Vessel 'Polarstern' to the Antarctic in 2008 (ANT-XXIV/4)", edited by Andreas Macke

Heft-Nr. 592/2009 — "The Expedition of the Research Vessel 'Polarstern' to the Antarctic in 2007 (ANT-XXIV/1)", edited by Sigrid Schiel

Heft-Nr. 593/2009 — " The Campaign MELTEX with Research Aircraft 'POLAR 5' in the Arctic in 2008", edited by Gerit Birnbaum, Wolfgang Dierking, Jörg Hartmann, Christof Lüpkes, André Ehrlich, Thomas Garbrecht, and Manuel Sellmann